
QUASI

The Assembly of Mass-Produced Components

Final report

Lappeenranta 16.5.2006

Saara Kouvo	Lappeenranta University of Technology
Anssi Jansson	VTT Industrial Systems (until 20.3.2006)
Martti Verho	VTT Industrial Systems
Hannu Minkkinen	VTT Processes
Veli Kujanpää	VTT / Lappeenranta University of Technology

Table of contents

1. Introduction	3
2. Laser welding of plastics	3
2.1. Light – matter interaction	4
2.2. Laser welding processes	4
2.3. Laser transmission welding techniques	5
2.3.1. Contour welding	5
2.3.2. Quasi-simultaneous welding	6
2.3.3. Simultaneous welding	7
2.3.4. Mask welding	8
2.4. The effect of material properties	8
2.4.1. Optical properties of plastics	8
2.4.2. Thermal behaviour of plastics	12
3. Experimental setup	13
3.1. Equipment	13
3.1.1. Diode laser	13
3.1.2. Nd:YAG laser	16
3.1.3. Fiber laser	16
3.1.4. Clamping devices	16
3.2. Welding tests	17
3.2.1. The effect of process parameters to welding of PP and PC	17
3.2.2. Elastomers	21
3.2.3. Transmission measurements	22
3.2.4. Clearweld welding tests	22
3.2.5. T-joint welding tests	24
3.2.6. 3D welding tests	24
3.3. Tensile tests	26
3.3.1. Lap joint	26
3.3.2. T-joint	27
3.4. Thermodynamic modelling	27
3.4.1. Modelling approach	27
3.4.2. Material properties	30
4. Results and discussion	31
4.1. The effect of process parameters on welding of PP and PC	31
4.1.1. The effect of welding speed	31
4.1.2. The effect of number of scans	35

4.1.3.	The effect of pigment concentration	38
4.1.4.	The effect of fiber glass	39
4.1.5.	The effect of air gap	41
4.1.6.	The effect of welding time	44
4.1.7.	Welding time of 0.5 s – 4 s	46
4.2.	Elastomers	49
4.3.	Transmission measurements	50
4.4.	Clearweld welding tests	59
4.4.1.	Clearweld tests 1	59
4.4.2.	Clearweld tests 2	62
4.5.	T-joint welding tests	69
4.6.	3D-welding tests	72
4.7.	Thermodynamic modelling	73
5.	Conclusions	76
6.	References	77

1. Introduction

The aim of this project “The Assembly of Mass-Produced Components” was to develop the laser welding of plastics by studying the weldability of the materials and the effect of welding parameters. The effect of different material properties like pigments and additives were also studied. The weldability of different plastics was trying to improve by using different laser absorbers and laser transmissive additives and dyes. These studies were oriented to resolve the problems in mass-production and to carry out the real-time quality monitoring system. Welding of 3D geometries in mass production was also clear up in theory and also with some tests.

This project was funded by TEKES, VTT and industrial partners. The duration of the project was 1.6.2003 – 31.12.2005. Research partners of this project were VTT Industrial Systems, VTT Processes and Lappeenranta University of Technology. Companies involved in this project were Audel Oy, Elcoteq Oyj, Foxconn Oy, Gentex Corporation, Nokia Oyj, Perlos Oyj and Salcomp Oy. Leader of this project was VTT Industrial systems.

2. Laser welding of plastics

In the past years different laser types have been used for welding of plastics. The CO₂ laser was used when laser welding of polymers was first demonstrated in the 1970's [1]. Laser transmission welding of polymers with the Nd:YAG laser was first described in 1985 for welding automotive components [2]. At first, the growth of the market of laser welding of plastics was slow due to high operating and investment costs and the big size of the CO₂ and Nd:YAG laser systems. Since high power diode lasers came to the market, the number of applications has grown rapidly and the process has obtained higher interest in the industry. The compact size, low running costs and competitive price of the diode lasers have increased commercial interest towards laser welding of plastics.

Laser transmission welding of plastics has gained interest in the different fields of industry as in the automotive, mechanical and electronics industry. This technique has several advantages compared to conventional techniques like good visual properties of the weld, minimal thermal, mechanical and electrical effect to the product, possibility to weld hermetic 3D welds and thermoplastics elastomers [3]. Laser transmission welding with diode lasers has become the most used laser welding technique to weld plastics. Several different laser transmission welding techniques have been demonstrated in the past few years. These techniques are quasi-simultaneous welding, contour welding, simultaneous welding and mask welding. Quasi-simultaneous laser welding has gained interest in mass-production applications, because it's a flexible and fast technique, which is an advantage in mass-production, where the welding times needed are often only a few seconds.

The applications of a welding process are typically defined by welding costs, weld quality and properties possible for the process. In laser welding of polymers, the high weld quality is restricted by too low heat input leading to insufficient weld strength and too high heat input causing decomposition of the material. Strength and the decomposition of the material are strongly dependent on the process parameters and temperature distribution inside the weld seam. The most important process parameters are laser power, welding speed, size of the laser beam on the work piece, clamping pressure and in quasi-simultaneous welding the number of scans. Material properties and the size of the air gap also have a significant affect on the weld quality. The temperature field inside the weld during welding can be controlled with these process parameters. [4]

2.1. Light – matter interaction

When laser light is incident to a materials surface four different effects can be observed (Figure 1). Laser light can be reflected from the surface of material (R). Remaining part of the light is penetrating into the material and can be absorbed to the material and transferred to the heat (A) or light can be scattered to different directions (R'). That part of the light, which is not influenced with the material, is transmitted (T). The absorption of material is depending on the material properties, wavelength and intensity of laser light. Many thermoplastics are not homogenous, because of their crystalline nature or the additives inside of the material. Because of the materials inhomogeneous nature laser light is reflected and scattered inside the material and theoretical description of the absorption properties is very complex. When used overall description of the process Lambert-Beer's law can be used. According to the Lambert-Beer's law, $I(x) = I_0 e^{-\alpha x}$, where I denotes the intensity of the light and α represents the absorption coefficient, which can also be dependent on the material, the wavelength of laser, temperature and other parameters. Absorption of laser light can be a surface absorption or a volume absorption. The additives inside of material and their concentration determinate the penetration depth. [5]

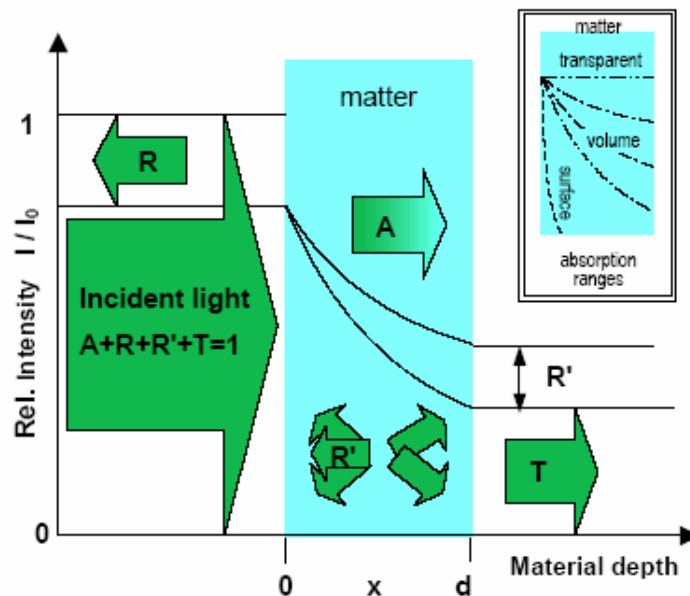


Figure 1. Light – matter interaction and intensity curve for transparent (—), volume absorbing (---) and surface absorbing material (---). [5]

2.2. Laser welding processes

Butt welding configuration is difficult to control for laser welding of plastics, as a consequence of the special properties of the material. Contrary to metals, heat conductivity is very small for polymers. The polymer can only be melted over its entire depth, if almost uniform absorption is realized over the thickness of the material (Figure 2). If we use a material which has a high absorption laser light generates a high temperature at the surface of plastic. If the material has a low absorption the laser light reaches the whole welding area. In this case a large amount of laser power is needed to form a weld. A problem also arises from the high viscosity of the molten polymer. Even if the material has been softened it does not necessarily flow together deliberately. That's why butt welding is not an optimal configuration for laser welding of plastics. [5]

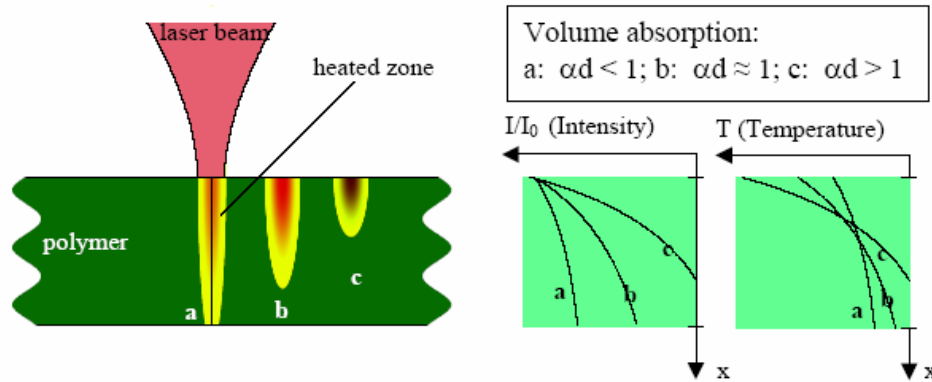


Figure 2. A schematic presentation of a butt welding configuration (intensity and temperature profile). [5]

More suitable configuration for laser welding of plastics is overlap joint. Overlap welding is much easier to handle and to control than the butt welding. In overlap welding a special configuration is necessary (Figure 3). The top plastic should have low absorption and reflection to the laser wavelength in the near infrared region so that the laser beam could penetrate through the first plastic. The laser beam is absorbed by the surface layer of the bottom plastic, which has good absorption properties. The second part is heated and when both parts are clamped together during welding, the heat is transferred to the first polymer and the surface layers of both parts are melted. After cooling and solidification of the molten material the weld is formed. This method is called laser transmission welding. [3], [5]

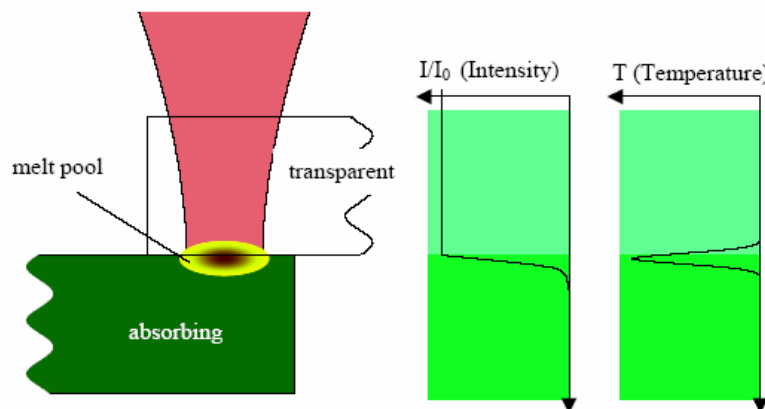


Figure 3. A schematic presentation of an overlap welding configuration (intensity and temperature profile). [5]

2.3. Laser transmission welding techniques

Special properties of plastics and the laser technology, especially the properties of diode lasers have made possible to use different laser transmission welding techniques. These different techniques are contour welding, quasi-simultaneous welding, simultaneous welding and mask welding.

2.3.1. Contour welding

Common plastic welding technique is the so called contour welding (Figure 4). In this technique the focused laser beam is moved over the materials surface, following the weld seam geometry. Two different methods can be used. The component moves and the laser is stationary or the component is stationary and the laser moves. In the first technique the component can be moved with 2-axis table or the components can be moved continuously on production line under the laser. In the second technique the laser can be moved with a

robot or with a gantry workstation. Typically the laser power is in the range of 10 to 100 W and the welding speeds are in the range of 2 to 5 m/min, in some cases up to 20 m/min. This method provides a simple, very flexible, easy controllable and cost efficient method for laser welding of polymers. The change of welding path requires only change of the program of the robot. Because of that the small series can be welded without change of any hard tooling, only by changing the program. With contour welding any size of parts can be welded. Only limit for the size of the part is the size of robots working volume. When robot is used the three dimensional welding is possible. Even if this technique has many advantages it has also some drawbacks. One limit is the welding speed when the laser beam is guided with an industrial robot. Typical processing speed of industrial robot is below 10 m/min. For example in mass-production applications the industrial robots are not fast enough to achieve welding times needed. When industrial robot is used at high speeds some problems will arise i.e. the accuracy of robot is diminished due to the fact that they tend to cut corners and wobble. The most difficult contour for industrial robots is when welding around a 90 degree corners. The axes have to move very fast to maintain the required welding speed and this usually results in bad welds or vice versa in too slow a welding speed. Most examples for polymer welding, which are known so far, have been performed according to this method. [6], [5], [7]

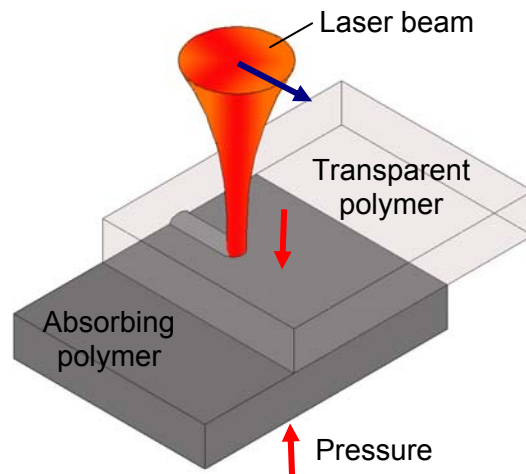


Figure 4. The principle of contour welding of plastics.

2.3.2. Quasi-simultaneous welding

In quasi-simultaneous laser welding (Figure 5) the laser head and the component don't move. The laser beam is scanned several times around or across the weld path very fast with a galvo mirror system. Because of the low thermal conductivity of polymers, the welding path heats up gradually and approximately evenly, such that a quasi-simultaneous melting of the entire welding track occurs. [8] In general quasi-simultaneous welding is a fast and flexible technique and that's why it has gained interest in mass-production. With today's scanner system as fast as 10 m/s welding speed can be achieved. Short welding time can be achieved with different combinations of parameters, welding speed, number of scans and laser power and that's why there is a better possibility to find suitable parameters for each case. In quasi-simultaneous welding the change of the welding path can be done by changing only the program for the scanner. Thus the system can be used both for flexible welding of the small series and the mass-production with short through put time. The quasi-simultaneous welding showed also great potential in bridging air gaps. When quasi-simultaneous welding and contour welding was compared it was noticed that quasi-simultaneous welding can bridge wider air gaps than contour welding [9]. Three dimensional welding is also possible with quasi-simultaneous welding. Although a using of scanners makes development of three dimensional welding techniques quite a challenging job. There are few techniques to weld 3D joints with quasi-simultaneous welding, 3D scanners, multiple

scanners and scanners + mirrors can be used [6]. There are also some drawbacks in quasi-simultaneous welding. The scanner technique limits the size of the welding area. The size of the welding area depends on the used laser type and the optics. With diode lasers the working area achieved with same focal spot size is smaller than with Nd:YAG lasers. A larger welding area can be obtained only with a larger focal spot size. For example with a diode laser the working area of 100 mm x 100 mm can be achieved with 1 mm spot size and working area of 260 mm x 260 mm with spot size of 2.6 mm respectively [10]. The other drawback of the high welding speed is the required laser power. In general quasi-simultaneous welding requires higher laser powers than the contour welding. The maximum laser power needed is ca. 200 W for quasi-simultaneous welding.

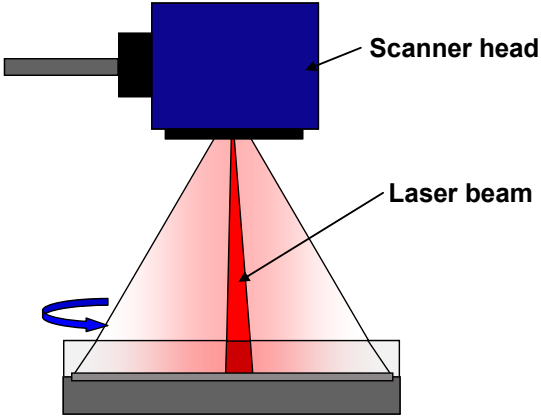


Figure 5. The principle of quasi-simultaneous welding of plastics.

2.3.3. Simultaneous welding

In simultaneous welding technique the work piece is stationary and several fixed diode lasers are mounted on the shape of the weld joint (Figure 6). The joint is irradiated with all the diode lasers at same time for a given time. The material is melted simultaneous. There are different strategies to carry out the technique, such as direct irradiation of the weld seam contour, using classic optical components, employing mask technology or application of fibre bundles. At the moment direct irradiation with the single high power diode laser modules is the most common method. The advantages of the simultaneous welding are short cycle times, no dynamic motion system guiding the laser beam required, longer interaction times than in contour welding and a marked gap bridging capability. Of course there are some drawbacks like higher total laser power than in contour welding, less flexibility than in contour and quasi-simultaneous welding and marked expenditure for special beam shaping components if complex, round shaped parts are considered. [5]

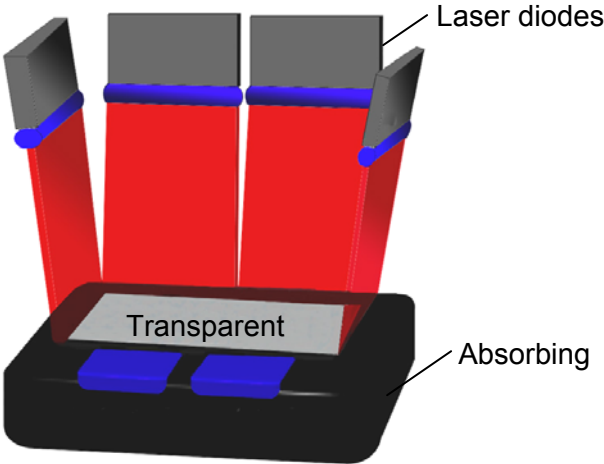


Figure 6. The principle of simultaneous welding of plastics. [5]

2.3.4. Mask welding

In the mask welding technique the mask is put between the laser and the work piece (Figure 7). The mask has the same geometry as the weld has. So those places, which shall not be in contact with laser light, are covered with the mask. The laser could be moved with any above described techniques (contour, simultaneous or quasi-simultaneous welding). With this technique accurate and small welds can be done. Technique is suitable only for flat surfaces.

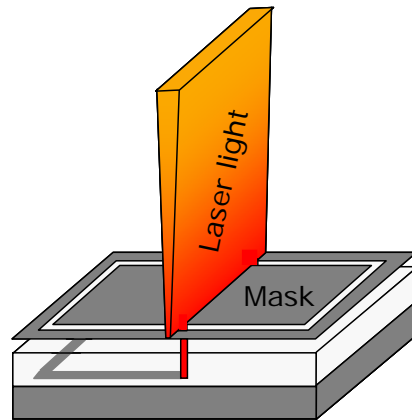


Figure 7. The principle of mask welding.

2.4. The effect of material properties

Material properties of plastics are important for the success and the understanding of the laser welding process. Optical properties of plastics have the most important effect to the welding process but other properties like thermal and mechanical properties are also very important.

2.4.1. Optical properties of plastics

Optical properties of plastic have a great influence on the laser transmission welding process. The top plastic has to be transparent and the bottom plastic has to be absorbing for the laser light. Most plastics are almost not absorbing for the near infra red radiation, like diode laser and Nd:YAG laser light in their natural state (Figure 8). Low absorption does not always mean high transmission. Laser light could reflect at the surface of plastic or inside of the plastic from some scattering effects. If the material is crystalline the incoming radiation can easily be deflected by scattering effects in the bulk material. This could increase the laser spot diameter and reduce the power density in the contact area of materials (Figure 9). [5]

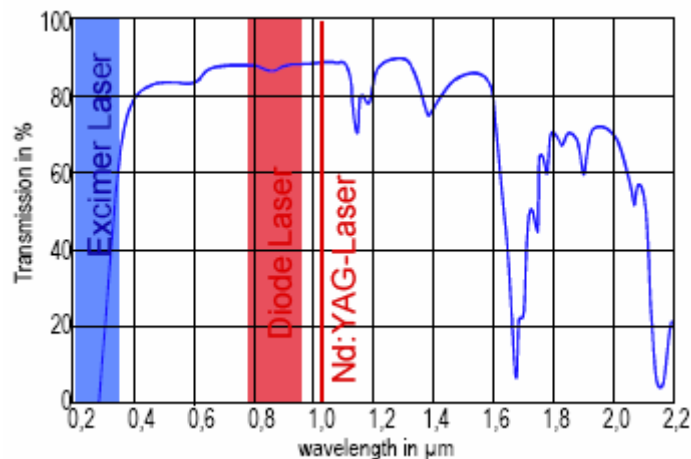


Figure 8. Characteristic absorption spectrum of polycarbonate (thickness 3,2 mm). [5]

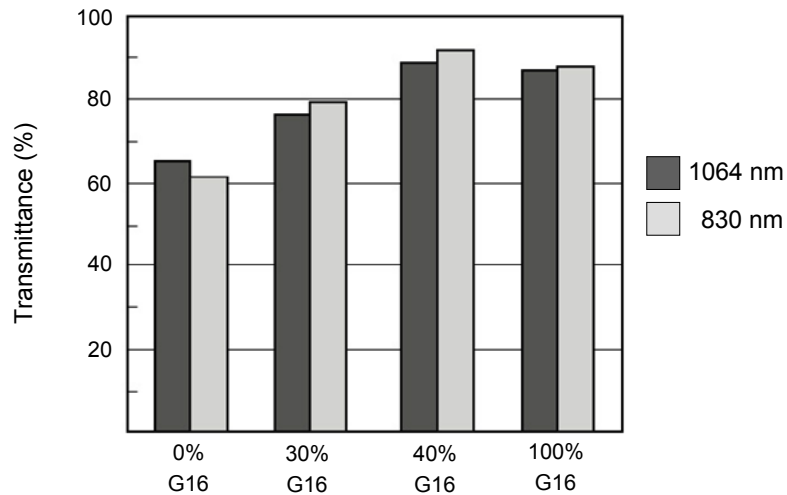


Figure 9. Influence of material crystallinity on transmittance properties for the blends of PA 6 with amorphous PA (G16). [11]

Because uncoloured polymers absorb the near infra red regions laser light a very little and in laser transmission welding transmissive and absorptive material is needed, the other plastic part must be blend with the laser light absorber additives. Also many products need certain colours and this may be a problem when one of the materials should be laser transparent and the other laser absorber. Nowadays lot of different colours are used in manufacturing of plastics and the colours (pigments and dyes) are developed to be more and more laser weldable. Every colour has it own transmission and absorption properties and the effect to the optical properties of plastic (Figure 10). Black colour used is commonly carbon black and it has very good absorption properties in the near infra red region. Some other black pigments have also been developed. There are visible black pigments, which are transmissive in near infra-red region and by using it as top plastic the welding of black parts is possible with trough transmission welding technique (Figure 11). Sometimes there is a need to weld uncoloured parts to each other. For these cases IR-absorptive additives which can be spread to the weld interaction or can be mixed into the bottom material is developed. [12]

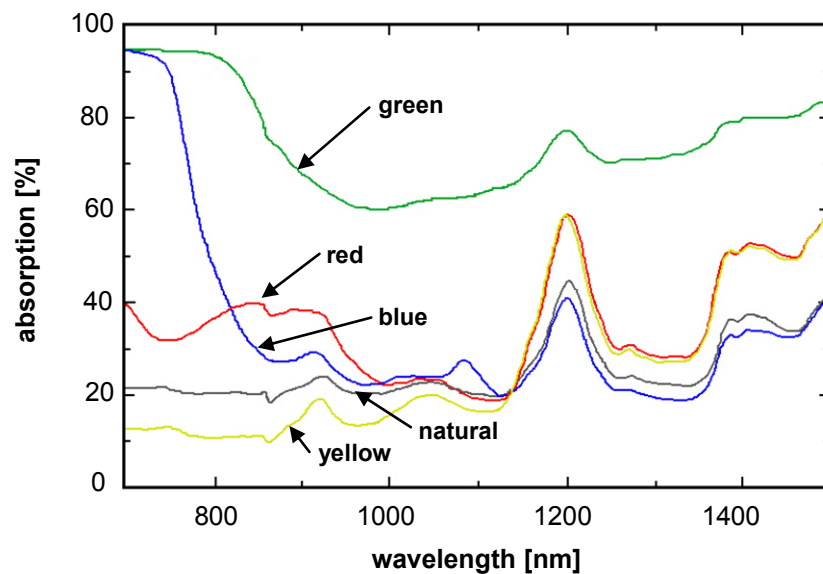


Figure 10. Absorption characteristics of different coloured polyamide. [13]

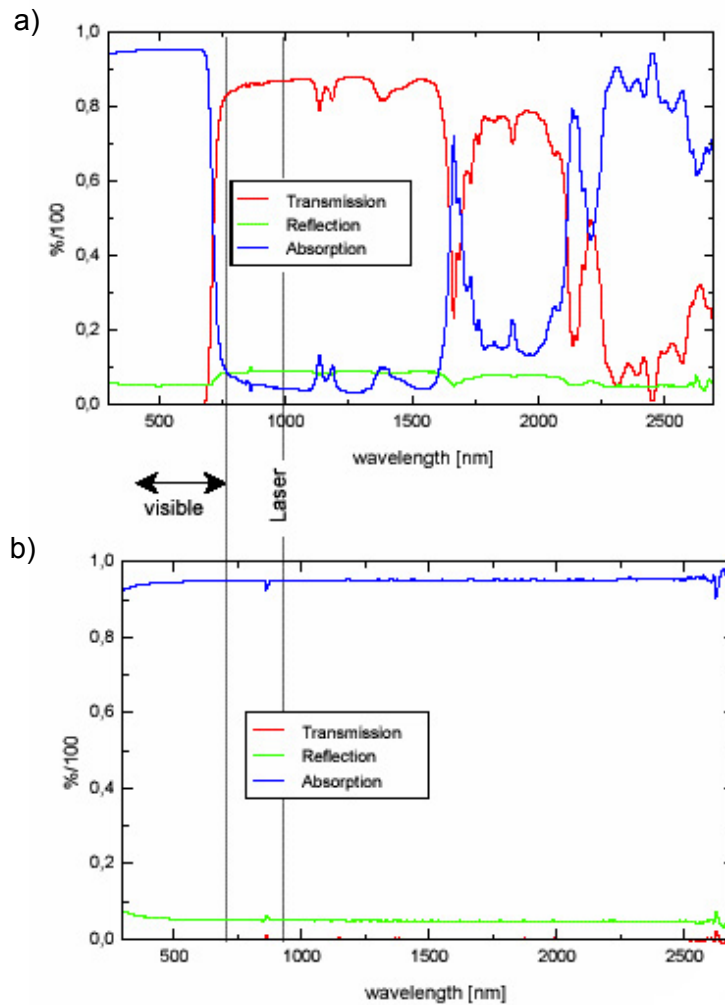


Figure 11. Transmission, reflection and absorption of a) IR transparent black and b) IR absorber black plastic. [14]

The amount of colorants affects to the transmission and absorption of laser light. Example the amount of carbon black effects to the optical depth and therefore to the depth of the melt (Figure 12). When the carbon black concentration is higher, the weld is more symmetrical. The size and shape of the pigment and dye particles effects also to optical properties, when the size of the particles is smaller the material is more homogenous and less scattering is appeared (Figure 13).

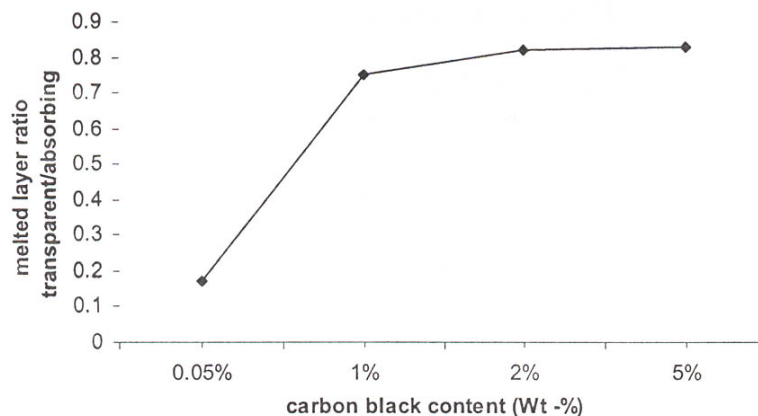


Figure 12. The effect of a carbon black concentration of PP to melt layer thickness ratio (transparent/absorbing). [4]

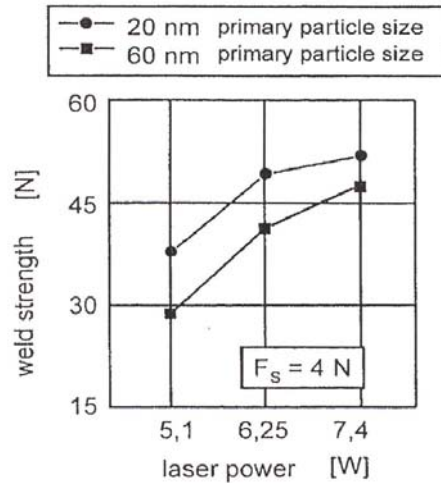


Figure 13. The effect of carbon black particle sizes on the weld strength. [15]

Most common additives used to better the strength of the material are reinforcements like fiber glass and minerals, different fillers and impact modifier. Generally these additives decrease the transmission of plastics (Figure 14). Reflection and scattering from the additives create the decreasing of transmission. The absorption of material increase slightly when the additives are blended into the material. The power needed increases when additive content is increased. The scattering of the laser light is dependent of the formula, concentration, size and the refractive index of the additives. Transmission properties are also depending on material thickness of blended materials. For example transmission of fiberglass blended plastic is decreased when the thickness of material is increased (Figure 15). [12], [16]

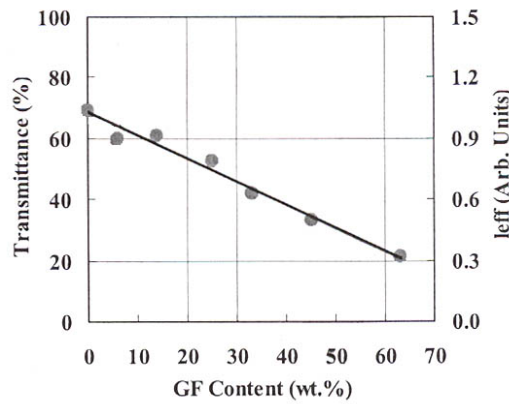


Figure 14. Transmittance of PA 6 with different fibreglass content. The wavelength is 1,064 nm, the fiber length is 180-320 μm and the fiber diameter is 10-13 μm . [17]

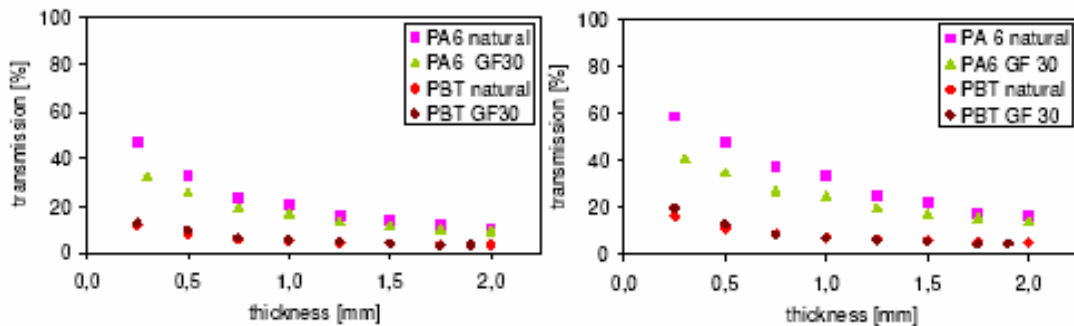


Figure 15. Transmittance of plastic for different wavelengths (left 810 nm, right 1064 nm) with the influence of fiber glass (GF) content and thickness. [18]

2.4.2. Thermal behaviour of plastics

Thermo-mechanical properties of plastics are factors what has to be taken into account when plastics are welded with the laser transmission technique. Most important properties are melting and decomposition temperatures, thermal expansion coefficient, volume increase of the melt and the viscosity of the melt.

The phase transitions with temperature are not clearly defined for polymer materials. On the contrary melting is taken place in a certain temperature range. Phase transition temperature is dependent on chain length, chain structure, crystallinity and other details of polymers. Because of that the temperature range is difficult exactly to specify. A temperature range with increasing volume and decreasing viscosity characterises the melt phase of polymers. Above a certain temperature the polymer decompose and is irreversibly destroyed. To weld two different polymers their melt temperatures and decomposition temperatures should be equal enough. Otherwise one polymer starts to destroy before the other is started to melt (Figure 16). The welding temperature effects also to the strength of the weld (Figure 17). When the temperature is low (low energy) the strength of the weld is low. When the temperature is too high (high energy) material starts to destroy and the strength of the weld decreases. Reinforcements like fibreglass and mineral fillers properties like thermal conductivity and heat capacity differs from the base polymers properties. Because of that the thermal properties (heating, welding and cooling time) of reinforced plastics are different than the properties of the base material.[5], [19], [20]

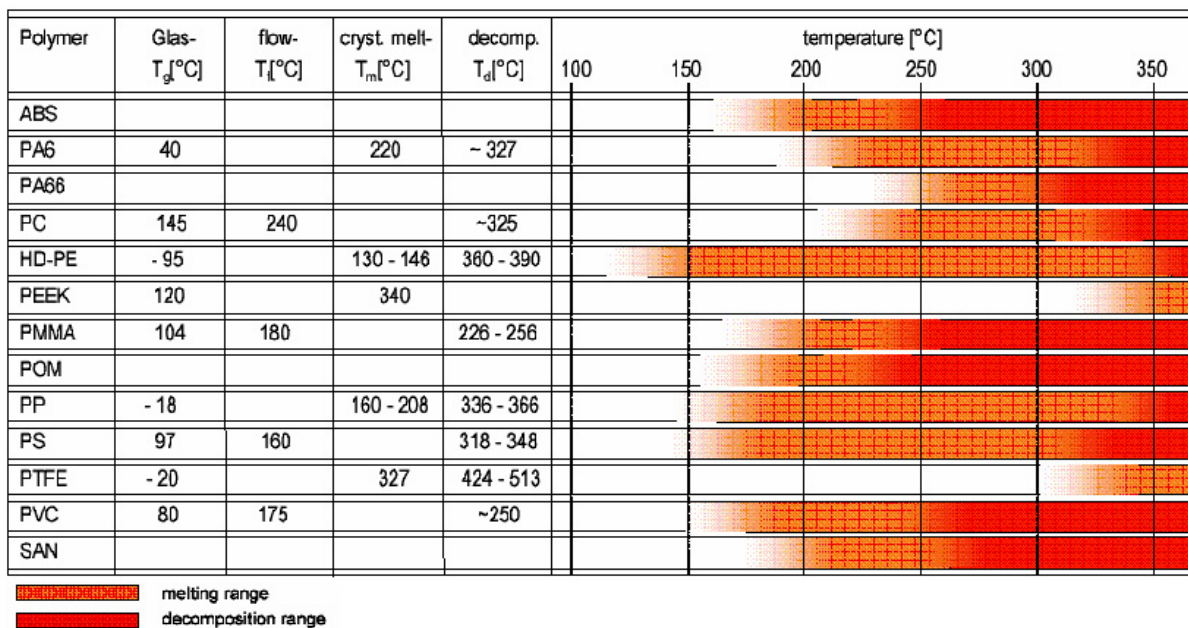


Figure 16. Melting and decomposition temperatures of plastics. [5]

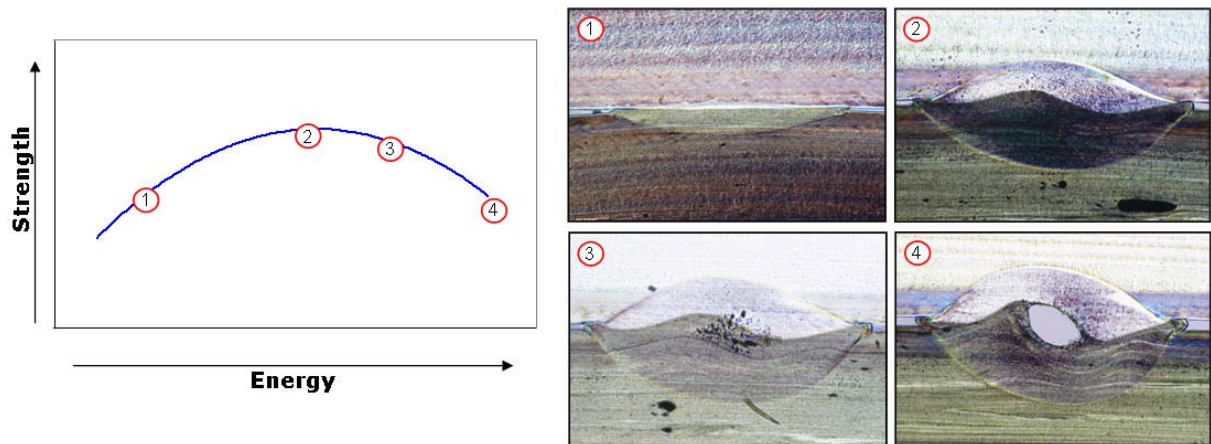


Figure 17. The effect of welding energy to the strength and the shape of the weld.

Plastics have a low capacity of heat transmission and high viscosity of melt. Because of that the mixing of the melts are slow. That's why the external pressing force is needed in welding. Pressure helps the transmission of the temperature and mixing of the melts. The thermal expansion coefficient and the volume increase of melt effects to the welding of polymers and especially to the external pressing force. When the volume of the melt increases the external pressure increases. The increasing of volume may be 15-20 %. In some case the increasing the pressure and volume may compensate the air gaps between the parts. [5]

3. Experimental setup

3.1. Equipment

In the welding tests three different types of lasers has been used. Mainly the tests have been done with diode laser, but some test has also been done with Nd:YAG laser and fiber laser.

3.1.1. Diode laser

Diode laser work cell (Figure 18) has been designed and built up in the beginning of the project (beginning of 2003) for quasi-simultaneous laser welding of plastics. It contain fiber coupled diode laser, scanner unit and different types of clamping devices. Also welding head equipped with pyrometer and CCD-camera belongs to the work cell.

Laser unit in the work cell is a Laserline LDF 400-200 fiber coupled diode laser. Laser powers up to 197 W can be used. The wavelength of the laser beam is 940 ± 10 nm and the beam quality is 40 mmxmrاد. Laser beam is guided via 400 μ m optical fiber to the welding head. In quasi-simultaneous laser welding the laser beam is moved with an Arges 2D scanner optic. Scanning head is fixed to the guide bar and the distance of the scanning head from work piece can be controlled manually. Clamping device, scanner head system and laser is fixed to the optical table.

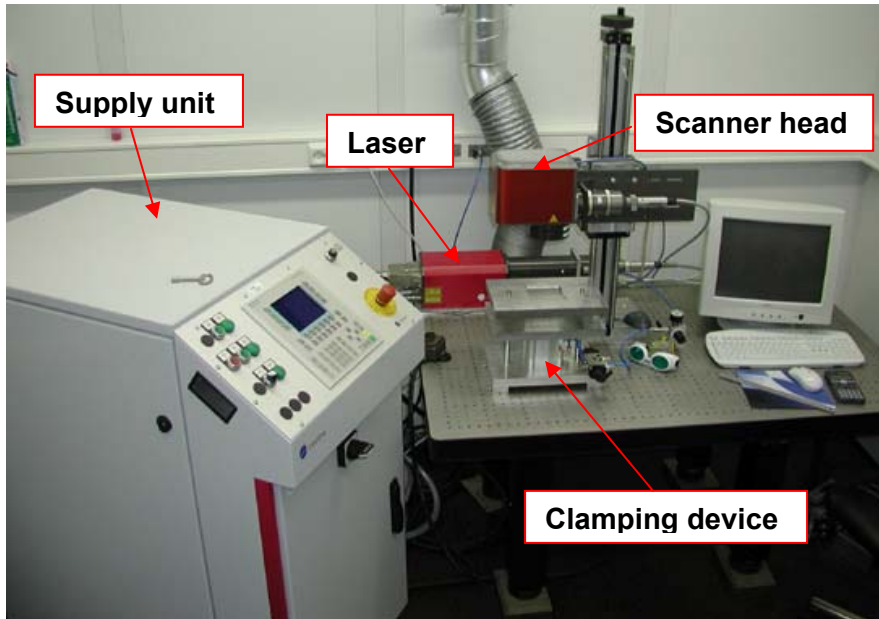


Figure 18. Diode laser work cell.

Five different types of optics can be used with this scanner, two F-theta optics (f 80 and f 163) and one F-theta combine optic with three different optic combinations (f 160, f 220 and f 434). Because the laser beam is moved with the scanning head the optics used determines the size of the working area and the size of the focal spot (Table 1). Properties of focal spot with different optics have been measured with Primes focus monitor laser beam analyzer (Figure 19 - Figure 23).

Table 1. Optics.

Focal length [mm]	Working distance [mm]	Focal spot diameter [mm]		Working area [mm ²]
		2. Mom	86%	
<i>f 80</i>	83	0,55	0,51	40 x 40
<i>f 163</i>	187	1,06	0,98	70 x 90
<i>f 160</i>	155	1,08	1,01	100 x 100
<i>f 220</i>	214	1,44	1,34	130 x 130
<i>f 434</i>	419	2,76	2,55	260 x 260

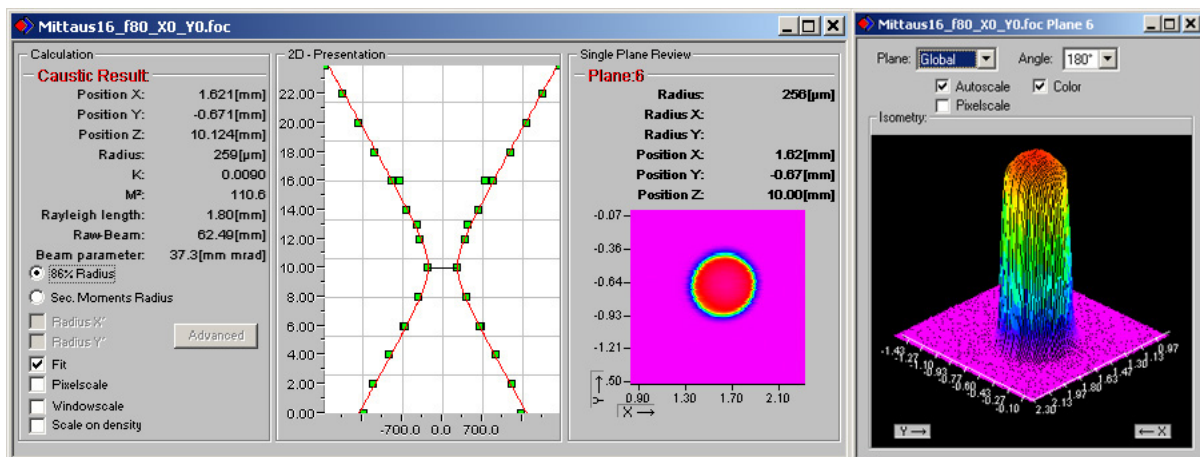


Figure 19. Laser beam analysis of f 80.

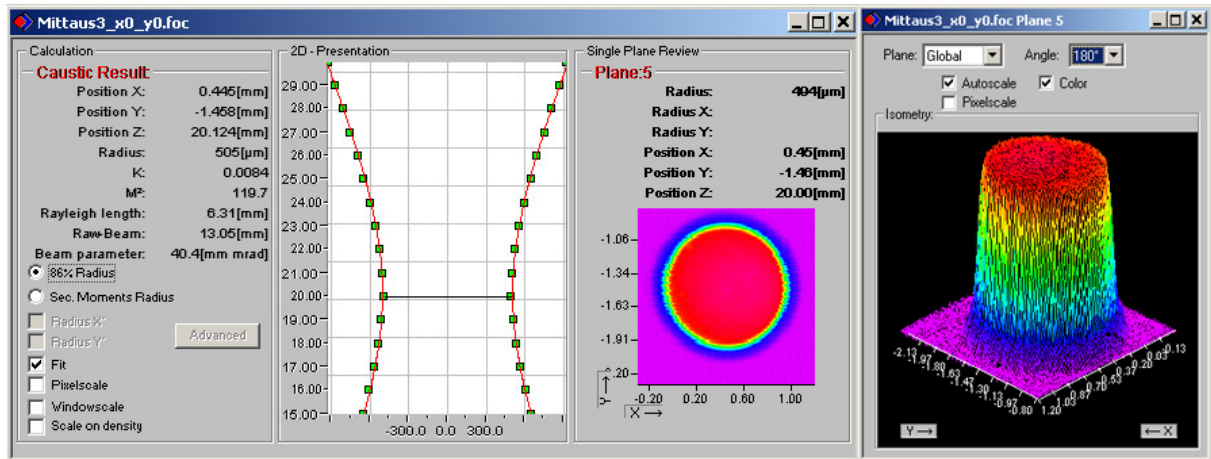


Figure 20. Laser beam analysis of f 163.

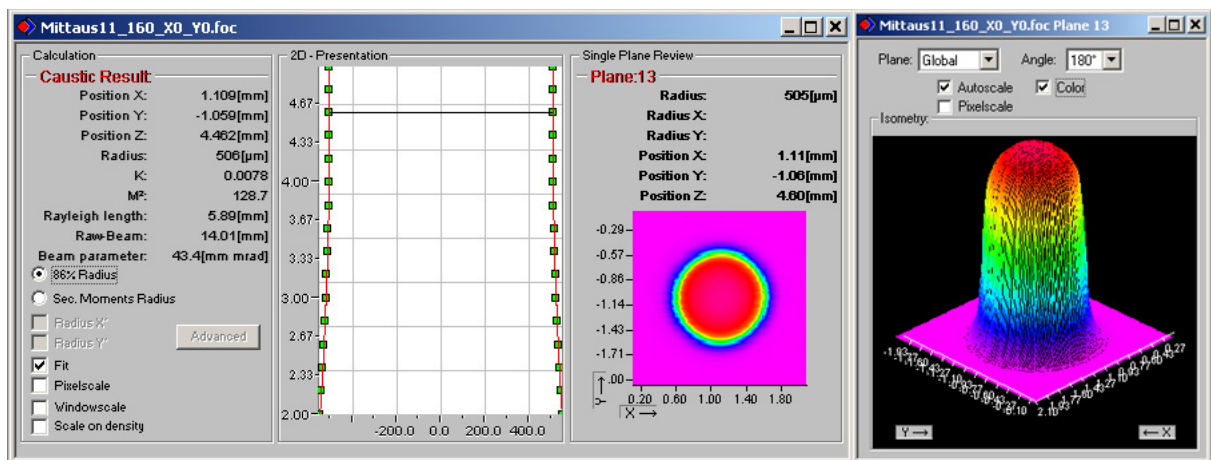


Figure 21. Laser beam analysis of f 160.

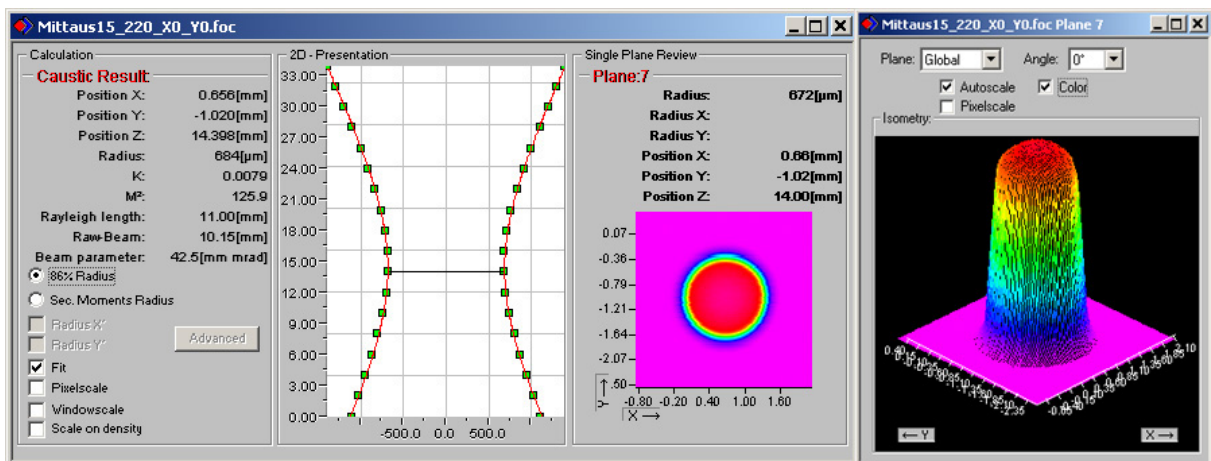


Figure 22. Laser beam analysis of f 220.

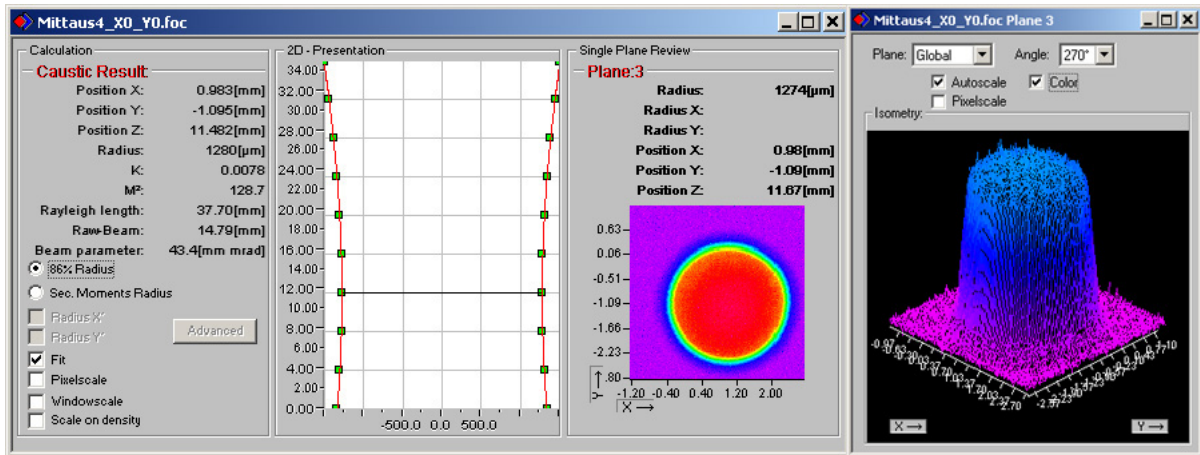


Figure 23. Laser beam analysis of f 434.

3.1.2. Nd:YAG laser

The Nd:YAG laser tests were performed with a Rofin RSM 100D diode pumped Q-switched Nd:YAG-laser, which has a 100W output power. The Nd:YAG laser operates at 1064 nm wavelength.

3.1.3. Fiber laser

The fiber laser used in the plastic welding tests was a high power SPI 100W fiber laser. The laser operated at 1090nm wavelength and the laser beam M^2 value is less than 1,1. The beam delivery optics (BDO) used produced a $\varnothing 6,0$ mm collimated beam, which was then guided to a Arges Fiber Rhino scanner. The tests were performed with a 300mm F-Theta scanner optics, which produced 0,15mm focal spot (Figure 24) in a 200mm x 200mm working area.

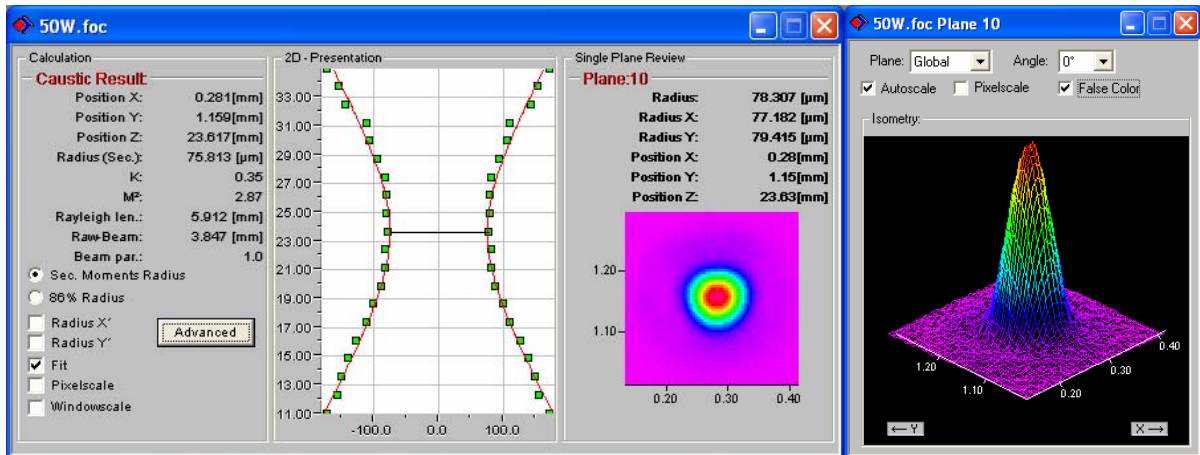


Figure 24. The fiber laser beam analysis of F-theta 300mm scanner optics.

3.1.4. Clamping devices

Two different kinds of clamping devices (Figure 25) have been used in welding tests. One clamping device is engineered for basic material tests and the other clamping device is more universal equipment to generate the clamping. The clamping device used in basic material tests was pneumatic equipment and the system was fit out with pressure control. The work pieces were pressed together by an aluminium plate, which had a groove machined in the middle and two hydraulic cylinders at both ends of the plate to supply the needed pressure on the work pieces during welding. A uniform pressure on the whole length of the joint was

generated by gasket tape attached on both sides of the groove on the aluminium plate. The other clamping device was also pneumatic and it was fit out with a pressure control. The work pieces were pressed against an optical class with an aluminium plate and hydraulic cylinder during the welding. The transmission of the optical glass in the wavelength of diode laser (940 nm) is about 91 %.

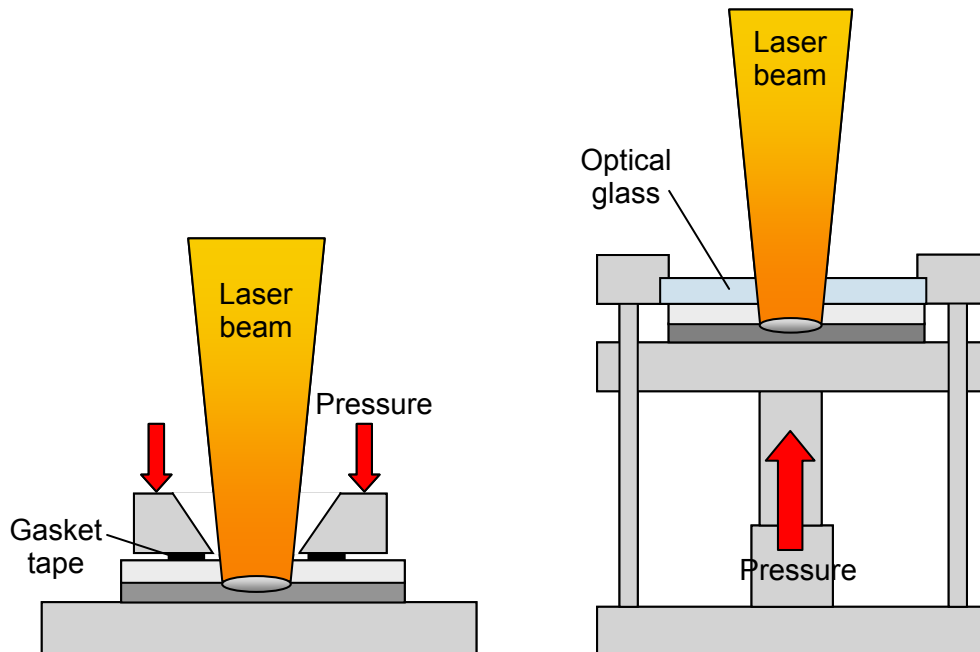


Figure 25. A schematic drawing of the clamping devices used in the welding experiments.

3.2. Welding tests

3.2.1. The effect of process parameters to welding of PP and PC

In these tests the effect of different process parameters has been studied. Materials used in these tests were polypropylene and polycarbonate. Some parameters have been tested with both materials but some of them have been tested only with one material. Parameters studied were welding speed, number of scans, pigment concentration, fiber glass concentration, air gap and welding time. In all experiments the effects of laser power and line energy have been analyzed.

The effects of welding speed and number of scans have been tested with PP and PC. More extensive tests were done with polypropylene. The effect of welding speed was tested first with five different welding speeds (number of scans was 50) (Table 2) and then with more extensive tests where eight different welding speeds have been used. The effect of number of scans has been tested with seven different number of scans values (Table 3). Also some tests were done with contour welding to compare it to the quasi-simultaneous welding (Table 4). In the first tests the transparent plastic was natural polypropylene and the absorbing plastic was polypropylene blended with 0,5 w% of carbon black. In the second tests the transparent plastic was natural polypropylene and the absorbing plastic was polypropylene blended with 1,0 w% of carbon black. With polycarbonate the effect of welding speed was investigated with five different welding speeds (number of scans was 50) (Table 5) and the effect of number of scans was studied with five different number of scans (welding speed was 2 m/s) (Table 6). In both cases the natural polycarbonate was used as transparent part and commercial black PC was used as absorber material.

Table 2. The parameters used in the first polypropylene welding tests (effect of welding speed).

Number of scans 50	Welding speed [m/s]				
	2	4	6	8	10
Laser power [W]	20 - 80	32 - 96	36 - 120	48 - 160	50 - 160

Table 3. The parameters used in the second polypropylene welding tests (effect of welding speed and number of scans).

Laser power [W]		Number of scans						
		2	5	10	20	30	50	100
Welding speed [m/s]	0,5	20 - 80	20 - 60	15 - 40	15 - 35	15 - 35	15 - 35	10 - 35
	1	30 - 110	25 - 85	25 - 70	25 - 60	25 - 50	20 - 40	15 - 40
	2	40 - 190	40 - 145	30 - 100	30 - 80	30 - 70	25 - 60	20 - 60
	3	50 - 197	50 - 197	45 - 135	40 - 115	35 - 100	30 - 80	20 - 70
	4	60 - 195	60 - 195	55 - 190	40 - 110	40 - 100	30 - 90	20 - 70
	6	120 - 197	120 - 197	80 - 197	50 - 160	50 - 140	40 - 110	40 - 80
	8	130 - 190	120 - 197	80 - 197	60 - 197	50 - 170	30 - 150	30 - 80
	10	197	140 - 197	120 - 197	80 - 197	60 - 180	40 - 140	30 - 110

Table 4. The parameters used in the polypropylene contour welding tests.

		Welding speed [m/min]						
		1	3	5	7	9	11	15
Laser power [W]		3 - 11	5 - 20	6 - 26	10 - 30	10 - 34	14 - 42	15 - 50
		Welding speed [m/min]						
		20	30	60	120	240	360	480
		20 - 70	30 - 80	45 - 135	70 - 190	100 - 197	150 - 197	197

Table 5. The parameters used in the polycarbonate welding tests (effect of welding speed).

Number of scans 50	Welding speed [m/s]				
	2	4	6	8	10
Laser power [W]	30 - 85	40 - 115	50 - 150	70 - 55	90 - 180

Table 6. The parameters used in the polycarbonate welding tests (effect of number of scans).

Welding speed 2 m/s	Number of scans				
	5	10	20	30	50
Laser power [W]	130 - 190	90 - 190	70 - 120	50 - 100	30 - 85

The effect of pigment concentration was studied with polypropylene (Table 7). The natural polypropylene was used as transparent material and absorber material used was

polypropylene blended with different carbon black concentrations. Welding speeds used were 2 m/s and 4 m/s, number of scans was 50.

Table 7. The parameters used in the pigment concentration tests (material PP).

Welding speed 2 m/s	Pigment concentration [w%]						
	0,05	0,1	0,2	0,3	0,5	1,0	1,5
Laser power [W]	36 - 80	36 - 72	28 - 56	32 - 60	20 - 80	20 - 60	20 - 56
Welding speed 4 m/s	Pigment concentration [w%]						
	0,05	0,1	0,2	0,3	0,5	1,0	1,5
Laser power [W]	64 - 144	48 - 104	32 - 96	40 - 96	32 - 96	24 - 88	24 - 88

Polypropylene was used when the effect of fiber glass was studied (Table 8). The natural polypropylene and polypropylene blended with different fiber glass concentrations was used as transparent material. Absorber material was polypropylene blended with different carbon black and different fiber glass concentrations. Three different types of material combinations were tested. In the first tests only the top plastic was blended with fiber glass, in the second tests bottom plastic was blended with fiber glass (and carbon black) and the top plastic was natural PP and in the last tests both parts were blended with fiber glass. Welding speed used was 2 m/s and number of scans was 50 in all experiments.

Table 8. The parameters used in the fiber glass concentration tests (material PP).

Laser power [W]	Fiber glass concentration of absorbing [w%] Carbon black concentration of absorbing [w%]										
	0	10			20			30			
	0,5	1,0	0,5	0,1	1,0	0,5	0,1	1,0	0,5	0,1	
FG of trans- parent [w%]	0	-	25-50	30-45	40-55	25-50	30-45	40-55	25-50	30-45	40-55
	10	32-56	30-50	-	-	-	-	-	-	-	-
	20	36-76	-	-	-	40-60	-	-	-	-	-
	30	40-88	-	-	-	-	-	-	50-80	-	-

The effect of air gap was tested with polypropylene (Table 9) and with polycarbonate (Table 10). In polypropylene tests two different welding speeds were used, number of scans was 50. Four different carbon black contents of absorbing material were used. Air gaps used were from 0,06 mm to 0,36 mm. In the air gap tests with polycarbonate the welding speed used was 2 m/s, the number of scans was 50 and air gaps used were from 0,06 mm to 0,36 mm.

Table 9. The parameters used in the air gap tests (material PP).

Laser power [W]		Carbon black concentration of absorbing [w%]				
		Welding speed [m/s]				
		0,05	0,1	0,5		1
		2	2	2	4	2
Air gap [mm]	0,06	40 - 72	32 - 60	28 - 60	32 - 80	24 - 52
	0,12	-	-	32 - 56	40 - 80	-
	0,18	-	-	40 - 70	-	-
	0,24	-	-	60 - 80	-	-
	0,30	-	-	80 - 100	-	-
	0,36	-	-	110 - 120	-	-

Table 10. The parameters used in the air gap tests (material PC).

	Air gap [mm]					
	0,06	0,12	0,18	0,24	0,30	0,36
Laser power [W]	50 - 100	70 - 120	90 - 120	100 - 110	100 - 110	100

The effect of the welding time was studied (Table 11 and Table 12). Welding times used were 0,5 to 4 s and material used were polypropylene and polycarbonate. In the tests the welding path was 150 mm and nine different number of scans was used. Welding speed was adjusted according to welding time and number of scans ((scans x length)/speed). Laser power used was “optimum laser power” as high as possible, so at the weld was visually acceptable, there were no pores in the weld.

Table 11. The parameters used in welding speed tests, material PP. Welding speed [m/s], number of scans and laser power [W]

Welding time 0,5 s											
[m/s]	0,3	0,9	1,5	3,0	4,5	6,0	9,0				
scans	1	3	5	10	15	20	30				
[W]	21-22	33	40	54	59-60	64	64-66				
Welding time 1 s											
[m/s]	0,15	0,45	0,75	1,5	2,25	3,0	4,5	6,0	7,5		
scans	1	3	5	10	15	20	30	40	50		
[W]	16	27	33	39	41	42	43	44	45		
Welding time 2 s											
[m/s]	0,075	0,225	0,375	0,75	1,125	1,5	2,25	3,0	3,75	5,625	7,5
scans	1	3	5	10	15	20	30	40	50	75	100
[W]	9	19	23	29	31	32	32	33	34	33-34	34

Welding time 3 s											
[m/s]	0,05	0,15	0,25	0,5	0,75	1,0	1,5	2,0	2,5	3,75	5,0
scans	1	3	5	10	15	20	30	40	50	75	100
[W]	8	15	18	25	27	27	28	29	29	29	29

Welding time 4 s											
[m/s]	0,038	0,113	0,188	0,375	0,563	0,75	1,125	1,5	1,875	2,813	3,75
scans	1	3	5	10	15	20	30	40	50	75	100
[W]	7	12	16	21	23	24	25	26	26	26	26

Table 12. The parameters used in welding speed tests, material PC. Welding speed [m/s], number of scans and laser power [W]

Welding time 0,5 s									
[m/s]	0,3	0,9	1,5	3,0	6,0	9,0			
scans	1	3	5	10	20	30			
[W]	35-45	60-80	70-90	110-140	110-150	110-150			

Welding time 1 s									
[m/s]	0,15	0,45	0,75	1,5	3,0	4,5	7,5		
scans	1	3	5	10	20	30	50		
[W]	10-45	30-90	40-120	45-145	50-160	45-185	50-190		

Welding time 2 s									
[m/s]	0,075	0,225	0,375	0,75	1,5	2,25	3,75	7,5	
scans	1	3	5	10	20	30	50	100	
[W]	13-20	20-30	30-40	40-70	50-80	60-80	50-80	60-80	

Welding time 3 s									
[m/s]	0,05	0,15	0,25	0,5	1,0	1,5	2,5	5,0	
scans	1	3	5	10	20	30	50	100	
[W]	10-14	18-22	20-29	45-60	55-65	55-65	55-70	55-70	

3.2.2. Elastomers

Some tests were done with elastomers. TPU (thermoplastics polyurethane elastomer) were welded to black PC+ABS plates (Table 13). Tests were done with five different welding speeds; number of scans was 50 in all tests.

Table 13. The parameters used in elastomers welding test.

Number of scans 50	Welding speed [m/s]				
	2	4	6	8	10
Laser power [W]	40 - 60	50 - 80	60 - 120	100 - 130	110 - 140

3.2.3. Transmission measurements

Transmission measurements were done at VTT Electronics in Oulu. The aim of the measurements was to determine the transmission, absorption and reflection of different plastics in different wavelengths. The measured wavelength range was 400...2000 nm. Transmission and reflection measurements were done with Varian Cary 5000 spectrometer and with integrating ball (Internal DRA 2500: 00 100811 00) (Figure 26). The resolution of measurements was 5 nm. Absorption was calculated from transmission and reflection values.

Measured plastics were natural polypropylene, PP blended with 10, 20 and 30 w% of glass fiber. Optical properties of natural PC, natural PMMA and PC+ABS (white, red, blue and black) were also measured. Some materials blended with absorbing additive Clearweld were tested. These materials were PP, PP+30% GF, PMMA, PC and PC+ABS samples blended with Clearweld LWA-267 and LWA-290 dyes.

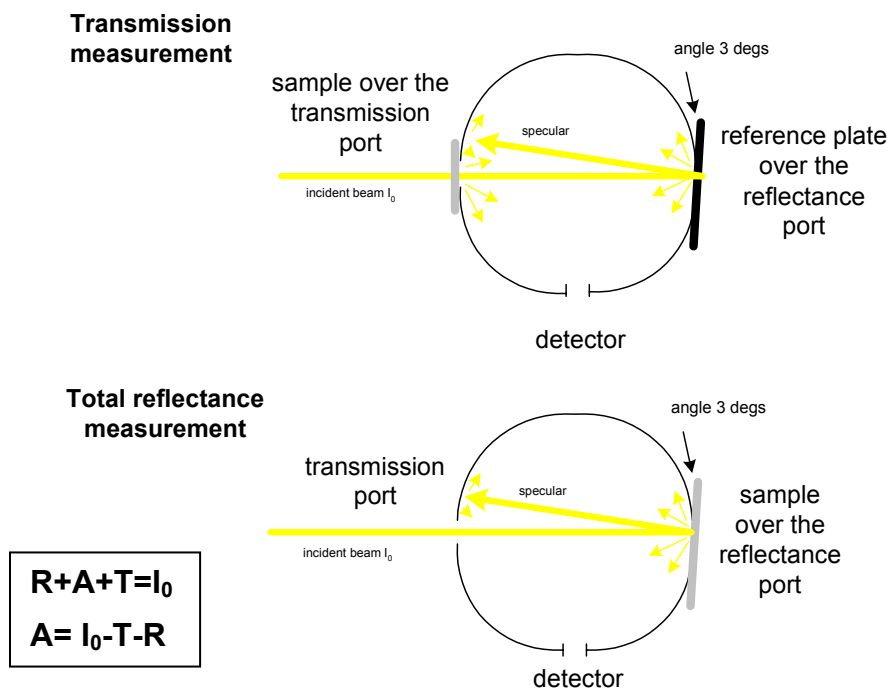


Figure 26. Measurements with integrating ball.

3.2.4. Clearweld welding tests

In these tests the effect of Clearweld dye blended to the bottom (absorbing) plastic has been studied. Tests have been done with different materials and different Clearweld dyes.

In the first tests (Table 14) the effect of different Clearweld concentration was tested with PMMA and PC+ABS. In all tests the transmissive top plastic was PMMA and it was welded to red and white PC+ABS materials which were blended with Clearweld additive. PMMA was also welded to PMMA which was blended with Clearweld. In these tests the number of scans was 50 and the welding speed was 2 m/s. Optic used was f-theta combine optic f 163 mm and the size of the focal spot was then ca. 1 mm.

Table 14. The parameters used in the Clearweld tests.

Laser power [W]		Material + colour		
		<i>PC+ABS red</i>	<i>PC+ABS white</i>	<i>PMMA</i>
Clearweld concentration [%]	0	50 – 130	-	-
	0,0025	-	-	197
	0,0030	-	120 – 150	-
	0,0035	50 – 110	-	-
	0,005	-	-	190
	0,006	-	90 – 130	-
	0,007	50 – 100	-	-
	0,010	-	-	90 – 150
	0,012	-	70 – 130	-
	0,014	50 – 90	-	-

In the second tests (Table 15) base materials were PP, glass filled PP, PMMA, PC+ABS and PC. These materials were blended with different concentrations of Clearweld dye and the tests were done with contour and quasi-simultaneous welding techniques. The strength of the welds was compared with tensile tests. The welding time was kept same in all tests with both welding techniques. The path was similar in all the tests and the welding speed was adjusted according to the number of scans used that the total welding time was 1 second. Each dye concentration was welded at least with 5 different laser powers with each welding speed and number of scans in order to find out the adequate laser power needed to weld the materials with different Clearweld concentrations. The welding tests with the LWA-267 was carried out with a fibre coupled ($\varnothing 400 \mu\text{m}$) diode laser (940 nm) and the welding tests with the LWA-290 was carried out with a fibre laser (1090nm) and with Nd:YAG laser (1064 nm). Optical properties of these materials were also measured.

Table 15. The materials used in the Clearweld tests.

CW [w%]		Diode	Nd:YAG	Fiber
PP	LWA-267	0,1 0,05 0,025 0,0125	-	-
	LWA-290	-	0,04 0,02 0,01	0,04 0,02 0,01
PC	LWA-267	0,1 0,05 0,025	-	-
	LWA-290	-	0,04	-
PP+ 30%GF	LWA-290	-	-	0,04 0,02 0,01
PC+ ABS	LWA-290	-	-	0,04 0,02 0,01

3.2.5. T-joint welding tests

In this project almost all the welding tests were done for the lap joint. Some tests were also done for the T-joint (Figure 27). Material used was 1 mm thick polycarbonate plates (black and natural). Welding path was 150 mm and welding time was kept constant 1 s. Number of scans used were 5, 10, 15, 20, 30 and 50. Welding speed was adjusted according to the number of scans so that the welding time was 1 s. Laser power was varied to find out the “optimum” laser power.

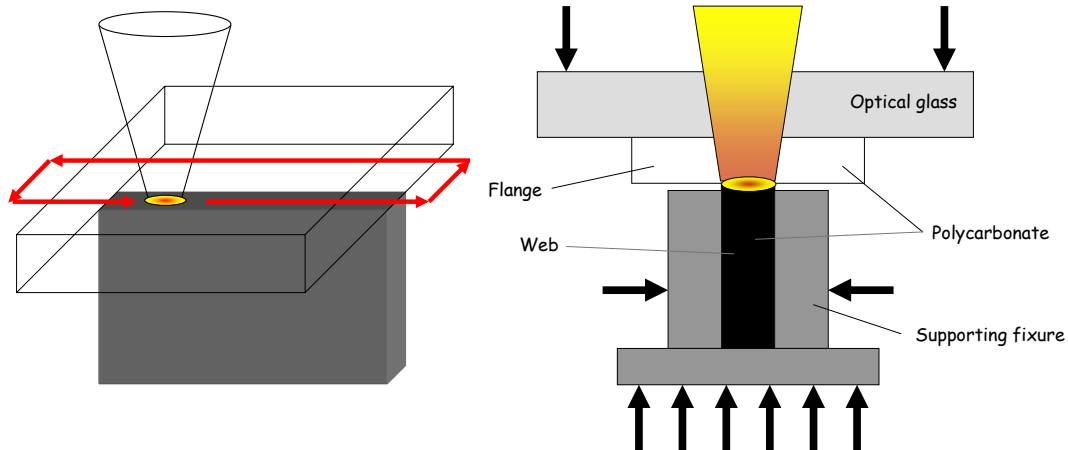


Figure 27. Experimental setup of the T-joint welding tests.

First test were done for the flat surfaces. In the second tests top plastic was 2 mm thick and there were one millimeter groove machined in it (Figure 28).

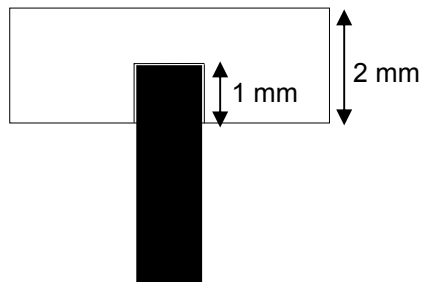


Figure 28. Test parts used in the second t-joint tests.

3.2.6. 3D welding tests

Three dimensional plastic components can be welded with several different techniques depending on the application. The choice of the technique will depend on many factors like required production time, size and shape of the part. Techniques suitable for 3D welding are contour welding, quasi-simultaneous welding and simultaneous welding. The traditional way to weld 3D joint geometries is to use the welding head or laser attached to an industrial robot. High requirements, like the reject fraction and through put time in case of mass-production enforced to develop new 3D welding techniques.

3D quasi-simultaneous laser welding is not possible with today's, robot guided laser welding technique. Only a scanner system with fast mirrors can reach the required welding speed. Using of scanners makes development of three dimensional welding techniques quite a challenging job. There are a few techniques to weld 3D joints with quasi-simultaneous welding 3D scanners, multiple scanners and scanners with mirrors can be used. Quasi-simultaneous welding of 3D joints has also own benefits and drawbacks. These properties differ a lot from the pros and cons of the contour welding. In the project two different types of 3D quasi-simultaneous welding techniques have tested and developed, multiple scanners and scanners with mirrors techniques.

In the multiple scanner system the weld seam is covered with multiple scanners, which are operated in turns such that the welding occurs continuously through the entire weld seam (Figure 29). The more the surface of the weld changes in the z-direction, the longer focal length is required. This technique is faster than other 3D quasi-simultaneous welding techniques and because of that it is well suitable for mass-production. In this technique either scanners can have their own laser source, or the beam on one laser can be divided to serve various scanners. If one laser is used, the laser power required for one laser is higher than in the case of multiple lasers.

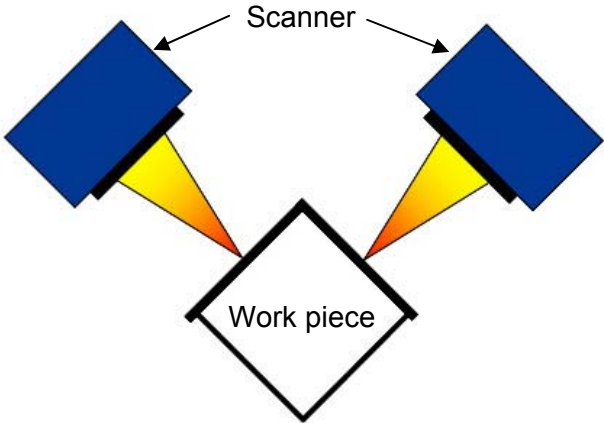


Figure 29. The principle of quasi-simultaneous 3D welding with a two-scanner system.

In a scanner and mirror system (Figure 30) the laser beam is guided via a mirror or mirrors to the weld seam that can't be reached with the 2D scanner. Laser beam is reflected via the mirrors such that the welding occurs continuously through the entire weld seam. A very long focal length and a long focal depth are required, because the position of the focal spot may vary in the z-direction depending on the size and shape of the product. The idea is to cover the changes of the surface of the work piece in the z-direction with a long focal depth. This technique is also fast and the investment costs are lower than in the multiple scanner system. By changing the number of mirrors almost any shape of the part can be welded.

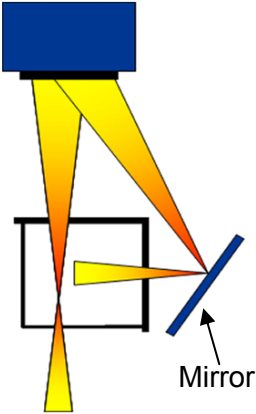


Figure 30. The principle of quasi-simultaneous 3D welding with a scanner and one mirror system.

3.3. Tensile tests

Two different types of joint were used in the welding tests, lap joint and T-joint. In the testing of these test parts two different type of tensile test method were used.

3.3.1. Lap joint

The 20 mm wide test specimens were cut from 1 mm thick and 60 mm wide plates which were welded together (Figure 31). Normally band saw with fine teeth blade was used, with some brittle materials also high pressure water jet cutting was used. Two 20 mm wide test bars from each welded specimen were used to test the strength of weld line. From the narrow parts of the specimen, which were not used in the tensile tests, were used to make a cross section microtome from where the weld width and depth were measured. The parts were numbered before cutting.

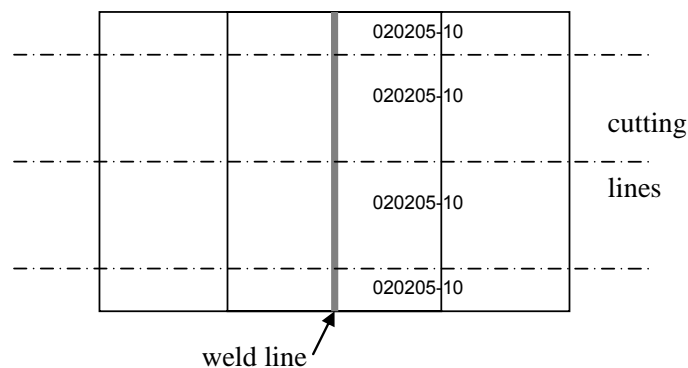


Figure 31. Cutting lines of the welded sample.

The 20 mm wide stripes were tested with the Instron tensile tester (Figure 32). The test speed was 5 mm/min. The width of every sample was measured. Maximum load divided by width [N/mm], maximum load [N], displacement at maximum load [mm] and the width of the sample were reported. Graphs with force – displacement curves were plotted from each test. Principally the test was shear test. With PP-material normally at the end of the test the test bar did bend so, that the stress was combination of shear, tension and peeling. The dashed lines show the bending. If the weld was weak, no bending did occur. With stiff materials as PC and PMMA, the bending was smaller.

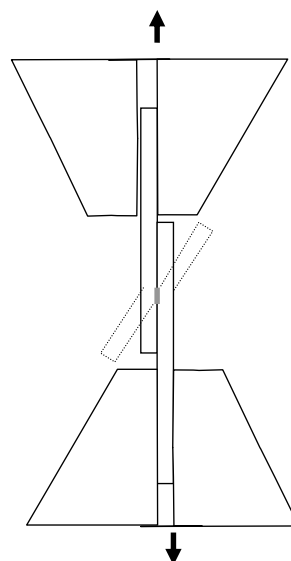


Figure 32. The principle of the tensile tests.

3.3.2. T-joint

T-joints were tested with bull out tests. The transmissive plate was fixed in the support jig and the absorbing part was drawn by wide clamping jaw apart from the clear plate (Figure 33). The test speed was 1 mm/min. Maximum load [N], displacement at maximum load [mm] and calculated tensile stress [MPa] at the absorbent plate was reported. The calculated tensile stress was used to compare these values to the data sheet value. Two types of joint were used. First test were done for the flat surfaces (1 mm). In the second tests top plastic was 2 mm thick and there were one millimetre groove machined in it.

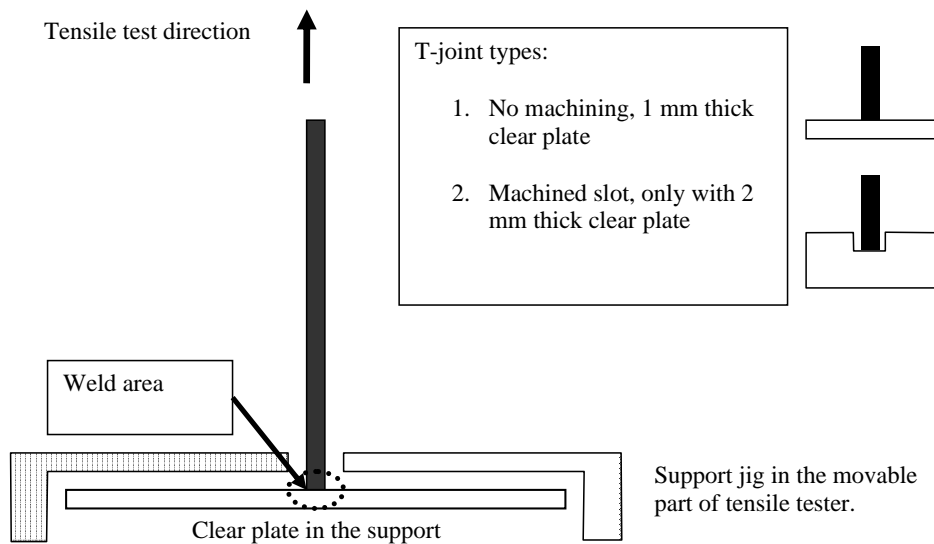


Figure 33. The principle of the bull out tests of the T-joint.

3.4. Thermodynamic modelling

3.4.1. Modelling approach

The quasi-simultaneous overlap welding where the upper plastic is transparent and the lower plastic is absorptive was analysed also by thermal modelling. Both plastics were 1 mm thick polypropylene plates.

The main target for the thermal modelling was to estimate the temperature distribution in the materials to be welded and especially to calculate the volume of molten material in order to estimate the welded area size for different input parameter values (laser power, welding speed, number of scans). The modelling of the size and the distribution of the melted area was considered important, because it is one of the main factors defining the strength of a weld.

Modelling was based on transient finite element thermal analysis and the laser beam was modelled as a moving heat source. Modelling was done using a commercial finite element code (Ansys, version 10.0). The Ansys solver has powerful scripting capabilities and the model was built so that all relevant variables (model dimensions, meshing parameters, laser parameters, material parameters etc.) are controlled by script input variables which can be changed easily. Many of the parameters can also be entered as arrays, so it is easy to run multiple cases automatically and the output results are also collected to separate files named automatically by relevant input parameters.

In the model, the laser energy was applied only at the lower, non-transparent material and the energy absorption was supposed to obey the Lambert-Beer exponential decay law with a constant absorption coefficient. Due to losses in the laser, reflection and absorption in the

upper plate and reflection between the plates, only some 70% of the nominal laser power was supposed to finally reach the lower plate. The energy flow in the model and the controlling parameters are shown in Figure 34.

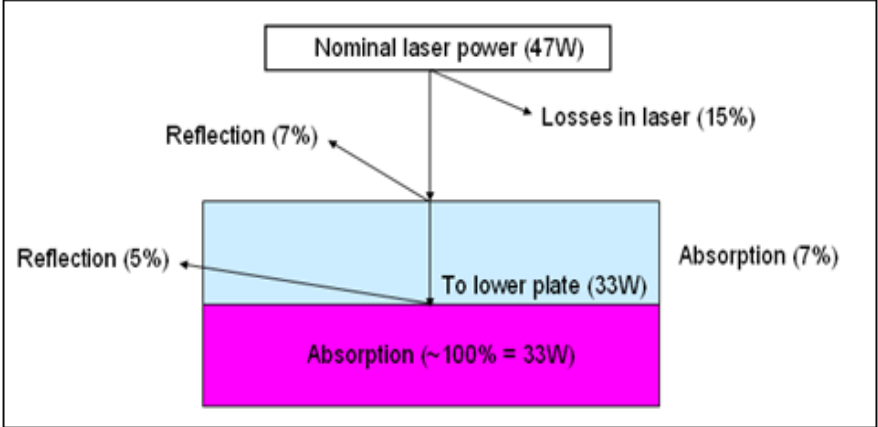


Figure 34. Laser energy flow in the model.

Modelling time step was set so that the heat source was moving forward always by one laser beam diameter during each time step. After each step the proper nodal heat generation values were set only at those nodes which were under the laser beam (heat source). Laser beam intensity was supposed to be constant across the beam area and consequently nodal heat generation values depended only on the distance from the beam centre line (outer segments are shorter and are covered by the laser beam for a shorter time) and on the depth measured from the plate surface (Lambert-Beer law). The moving heat source scheme is shown in Figure 35.

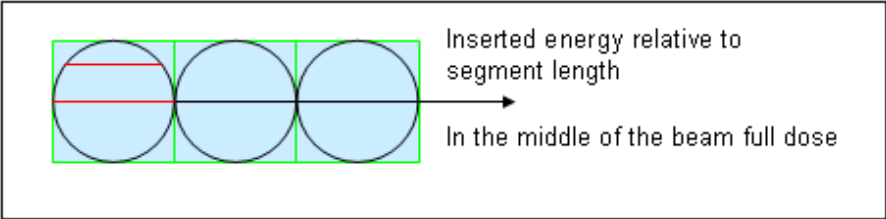


Figure 35. Moving heat source.

Only a small part of the actual 150 mm long weld path was modelled in the finite element model. The modelled section was 4 mm long and 4 mm wide. For the 1 mm laser beam this means that four heat generation steps must be applied at the model nodes during each scan. The rest of the weld path was modelled as a single cooling step, so each scan required five time steps. The model was considered to be symmetrical at the centre line of the beam, so the final model width was 2 mm and consequently the half of the laser beam covered 0.5 mm of the material in the width direction. The actual weld path and the modelled area are shown in Figure 36.

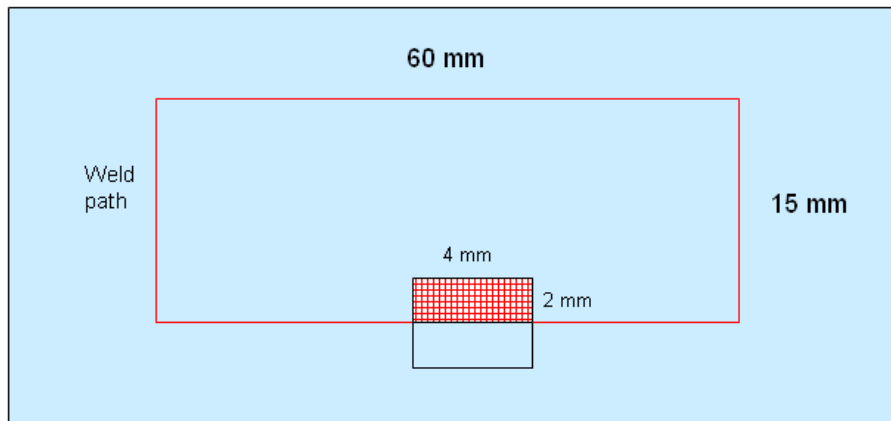


Figure 36. Modelled area.

The model was meshed using linear brick elements (about 80000 elements) and the mesh was densest at the symmetry line and between the plates where the element size was about 25-30 μm . A typical solution time for the thermal model was about 10 minutes per time step on a standard 3GHz pc-computer. The finite element model is shown in Figure 37. The left side is the symmetry plane and the lines drawn over the mesh describe the area between the welded plates and the laser beam outer radius.

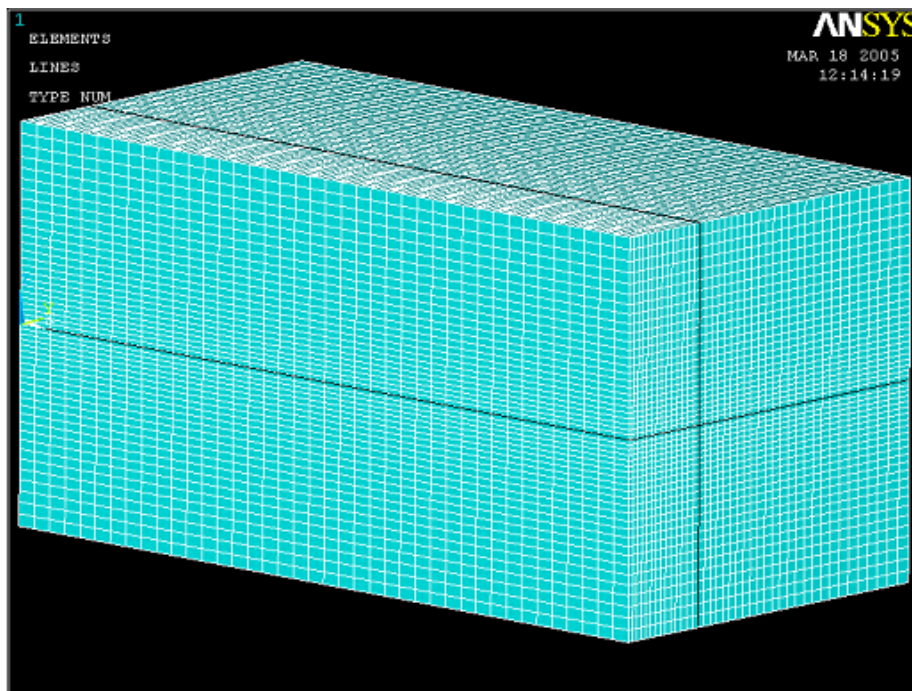


Figure 37. Finite element model.

No air gap was supposed between the welded plates, so there was a full thermal contact between the plates and the whole model was considered a single solid block. The upper surface of the upper plate and the lower surface of the lower plate were modelled as convective boundaries where heat transfer is by natural convection to ambient (room) temperature. At all other boundaries heat flux was set to be zero as if they were pure symmetry boundaries. This is actually not true at any of these surfaces, but due to very low heat conductivity of the material, this was considered as an acceptable approximation. To minimize the errors, all the modelling results were taken at the middle section of the model.

3.4.2. Material properties

When the laser light passes through the lower plastics is it gradually transformed into heat. Microscopically this is a complicated light-matter interaction process which is very difficult to model. However, it can be effectively described macroscopically by a simplified absorption process where only one material parameter, absorption coefficient, is needed.

If the laser beam power intensity at the surface of the lower plate is I_0 (W/m²) and α is the absorption coefficient (1/m), then according to the Lambert-Beer law the power intensity at the depth z (m) from the surface is (ref. Section 2.1):

$$I_z = I_0 e^{-\alpha z}$$

The absorption coefficient is a material specific property and it depends especially on the carbon black content of the polymer.

The inverse of absorption coefficient is called optical path length (or optical penetration depth, OPD) and it is related to how deep the laser beam can penetrate into the material before being absorbed. According to the Lambert-Beer law nearly two thirds of the energy is absorbed within one path length and after three path lengths already about 95% of the energy is absorbed.

For the thermal modelling a correct value of the absorption coefficient is quite essential. Some reference values for polypropylene were available from the literature, but in order to get characteristics for the polypropylene samples used in the current project, some absorption coefficient measurements were made by VTT Electronics in Oulu. The measured values (Oulu) and values taken from the literature [21], [22] are plotted in Figure 38. In the same figure is shown the fitted curve based on the inverse relationship between optical path length and carbon black content (weight-% of carbon black). Because the absorption coefficient is the inverse of optical path length, it can be concluded that absorption coefficient depends linearly on the carbon black content, at least when the content is less than few percents in weight.

In the modelling, the value of the optical path length was set to 25 μm and this corresponding to the carbon black content of about 1.0 wt-% for polypropylene.

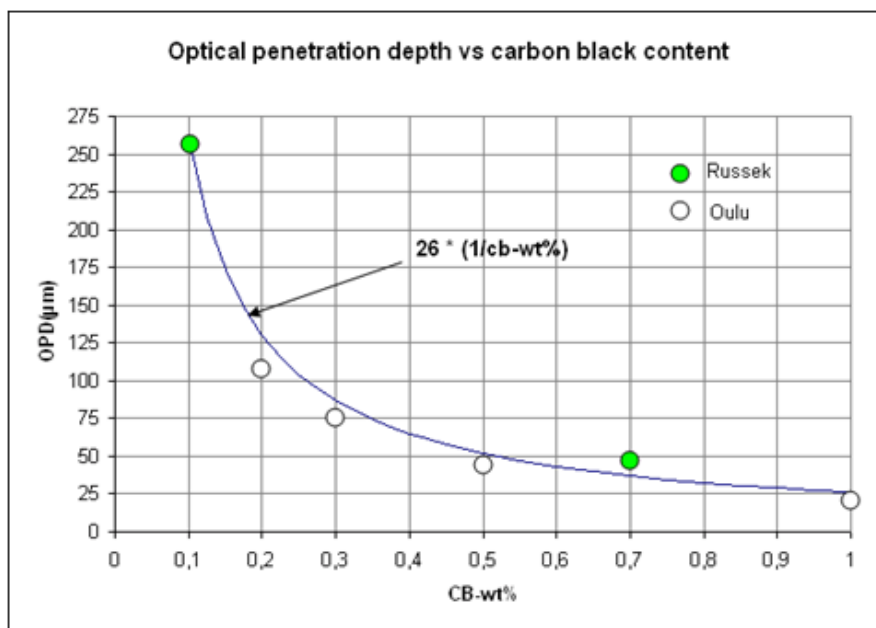


Figure 38. Optical penetration depth curve for polypropylene.

Other important material parameters for transient thermal modelling are heat conductivity, heat capacity and density.

The heat conductivity of plastics is generally quite low. In the literature the conductivity values for polypropylene are typically in the range of 0.2-0.3 W/Km with some temperature dependency. However, in the current modelling a constant value of 0.25 W/Km was used in all simulations.

The heat capacity and the density of polypropylene are temperature dependent and this was taken into account in the modelling. The heat capacity curve is shown in Figure 39, where especially the strong phase change effect around melting temperature (about 160 °C) is clearly visible. To model the phase change effects the enthalpy method was used and the enthalpy curve was calculated using temperature dependent heat capacity and density curves.

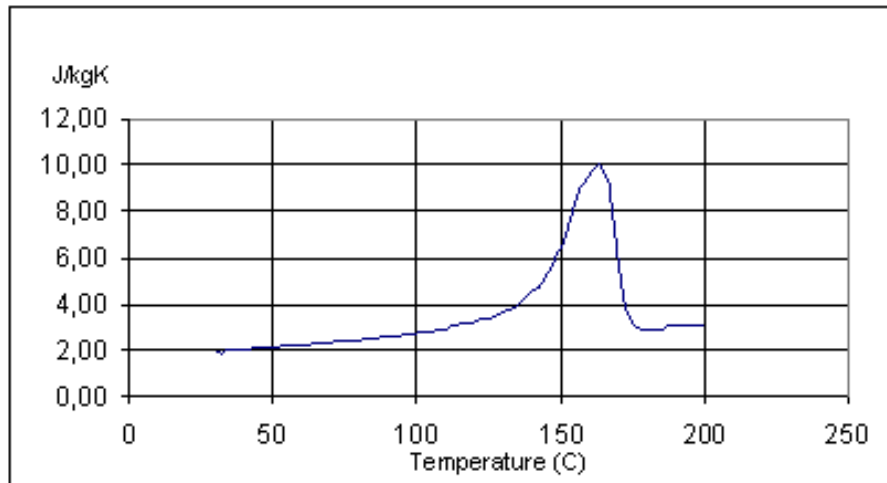


Figure 39. Heat capacity curve of polypropylene.

4. Results and discussion

4.1. The effect of process parameters on welding of PP and PC

4.1.1. The effect of welding speed

Welding speed is a very important parameter when mass-production components are welded. It has together with the number of scans the largest effect in the welding time. The strength of the weld per length was found to decrease as the welding speed increased (Figure 40 - Figure 43). With polypropylene the drop of the weld strength per length was larger with welding speeds from 0,5 m/s to 3 m/s, but with speeds from 3 m/s to 10 m/s only a slight decrease of the weld strength per length was found. Also with polycarbonate the drop of the maximum weld strength per length became smaller when the welding speed increased. The reason for this could be that the energy input (Figure 40 and Figure 41) was higher when the strength per length was higher and the welding speed was lower. It was also found that to form a weld the laser power has to be increased when the welding speed is increased. But with higher welding speeds the laser power window is wider (Figure 42 and Figure 43). The same phenomenon was found regardless what the number of scans was. The maximum weld strength per length was higher with polycarbonate than with polypropylene because of the higher material strength of polycarbonate. The strength of the polycarbonate base material was 72 MPa and the strength of the polypropylene base material was 33 MPa. Also the differences in maximum strengths per length between different welding speeds were larger with polycarbonate than polypropylene.

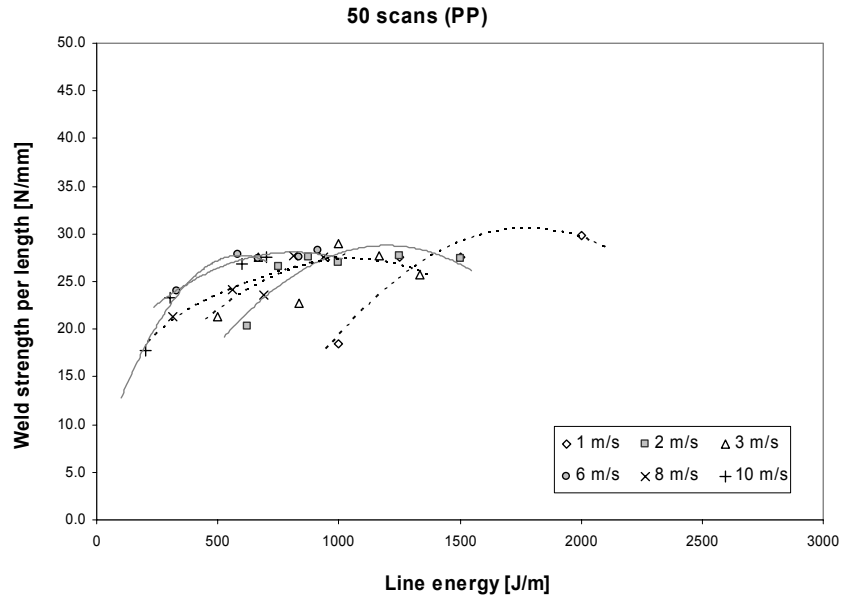


Figure 40. The maximum force per weld unit length as the function of line energy obtained with different welding speeds (polypropylene).

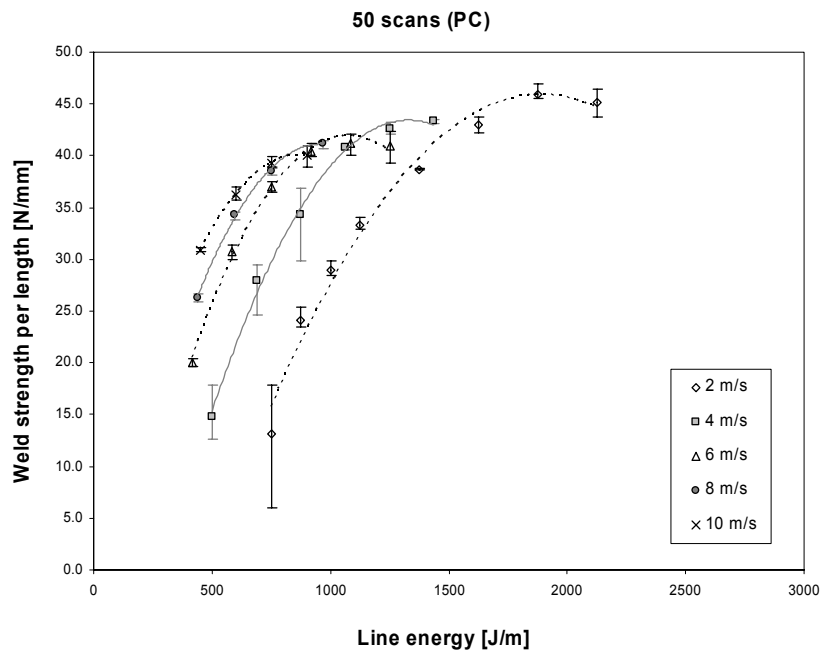


Figure 41. The maximum force per weld unit length as the function of line energy obtained with different welding speeds (polycarbonate).

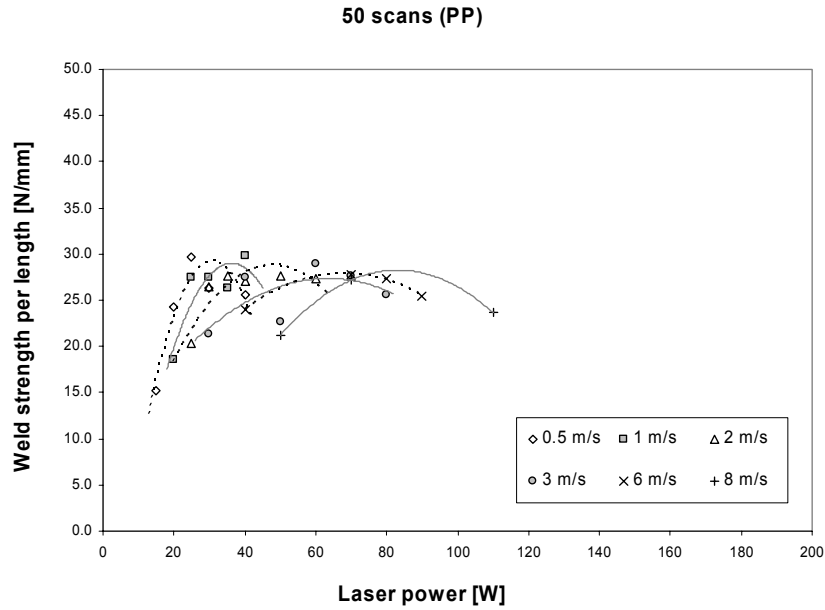


Figure 42. The maximum force per weld unit length as the function of laser power obtained with different welding speeds (polypropylene).

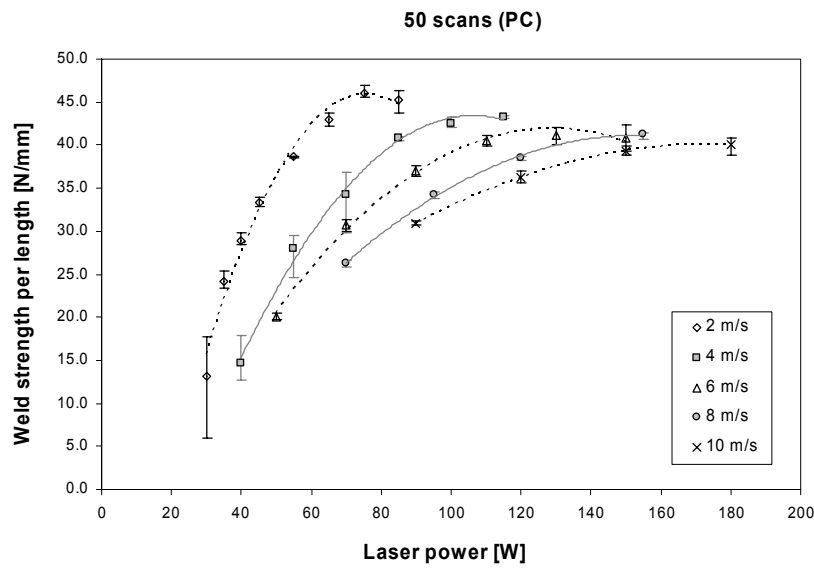


Figure 43. The maximum force per weld unit length as the function of laser power obtained with different welding speeds (polycarbonate).

Welding speed effects also to the size and shape of the weld. When polypropylene was welded it was found that the size of the weld decreased when the welding speed was increased. Both the width of the weld and the height of the weld are smaller with higher welding speeds (Figure 44 and Figure 45). Also the shape of the weld is flatter with higher welding speeds (Figure 46). The reason for this could be the lower energy input with the higher welding speeds.

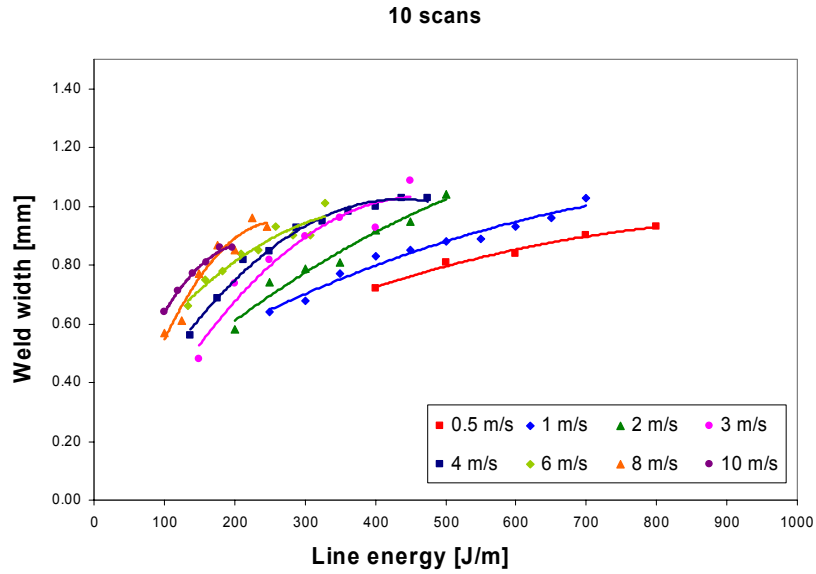


Figure 44. The width of the weld obtained with different welding speeds (polypropylene).

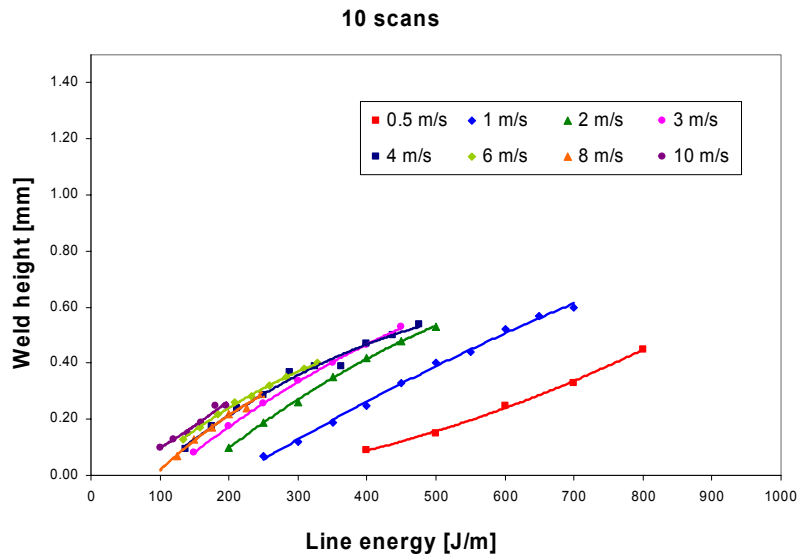


Figure 45. The height of the weld obtained with different welding speeds (polypropylene).

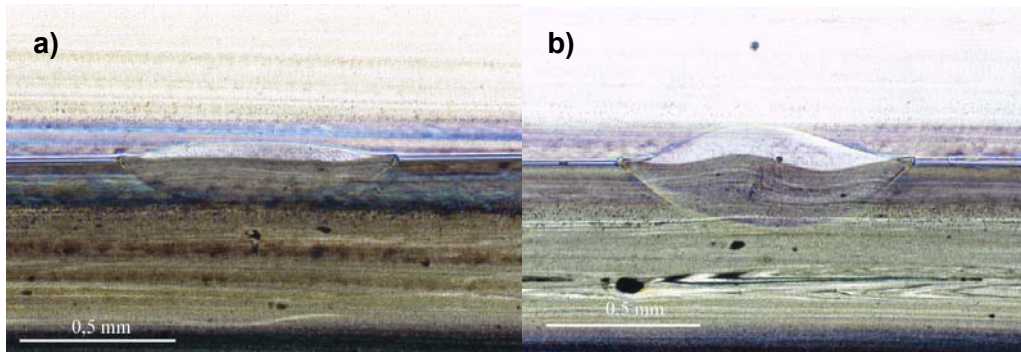


Figure 46. Cross-section micrographs of quasi-simultaneous welded polypropylene samples. The welding parameters used was a) 45 W, 1 m/s, 10 scans and strength per length was 28,9 N/mm and b) 160 W, 10 m/s, 10 scans and strength per length was 26,3N/mm.

4.1.2. The effect of number of scans

The number of scans mostly determines the time used to weld each component. The welding time per component can be also reduced by increasing the welding speed, but only to a certain extent. With higher speeds the accuracy of the scanner isn't as good as with low speeds, especially in sharp corners. Therefore the number of scans must be taken into consideration.

In Figure 47 and Figure 48 the effect of the number of scans to the weld strengths per length can be found. It can be also noticed that a higher weld strength per length was achieved by increasing the number of scans. Although a higher laser power is needed when the weld is scanned only a few times, it didn't lead to a high weld strength per length (Figure 49 and Figure 50). The laser power range, where the maximum strength is obtained, is wider with lower number of scans. By increasing the number of scans and keeping the welding speed constant, the energy input increases, which creates more molten material and a larger weld. This can explain the fact that the weld strength per length increased when the number of scans was increased. The maximum weld strength per length is higher with polycarbonate than polypropylene because of the higher material strength of polycarbonate. The differences between the maximum strength per length with different number of scans were also larger with polycarbonate than with polypropylene.

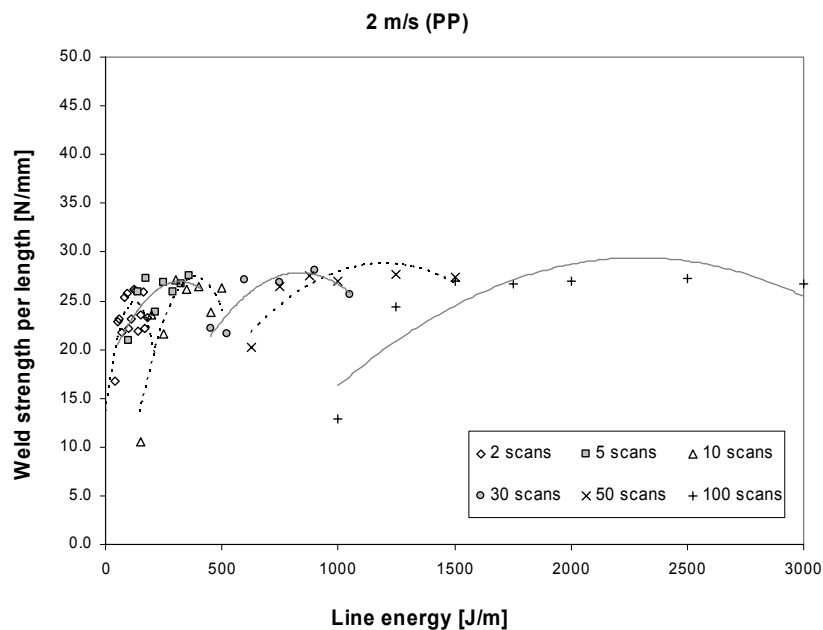


Figure 47. The maximum force per weld unit length as the function of line energy obtained with different number of scans (polypropylene).

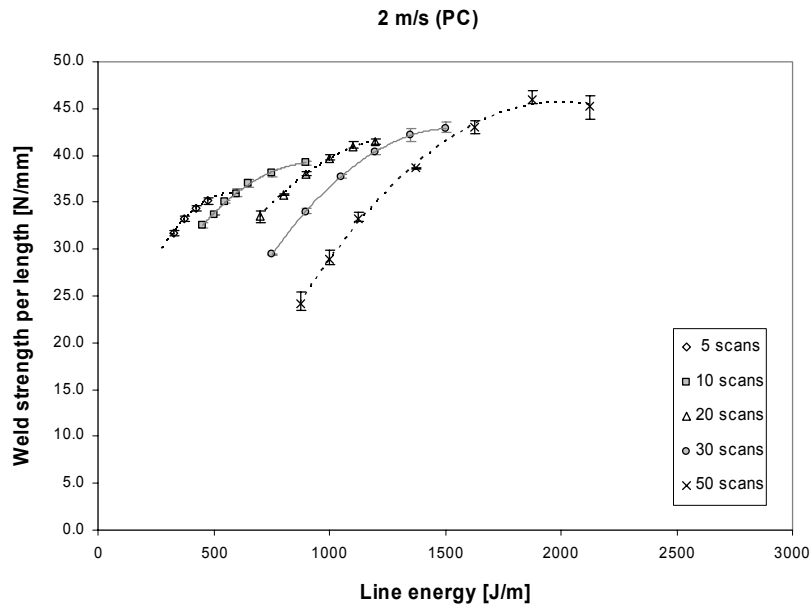


Figure 48. The maximum force per weld unit length as the function of line energy obtained with different number of scans (polycarbonate).

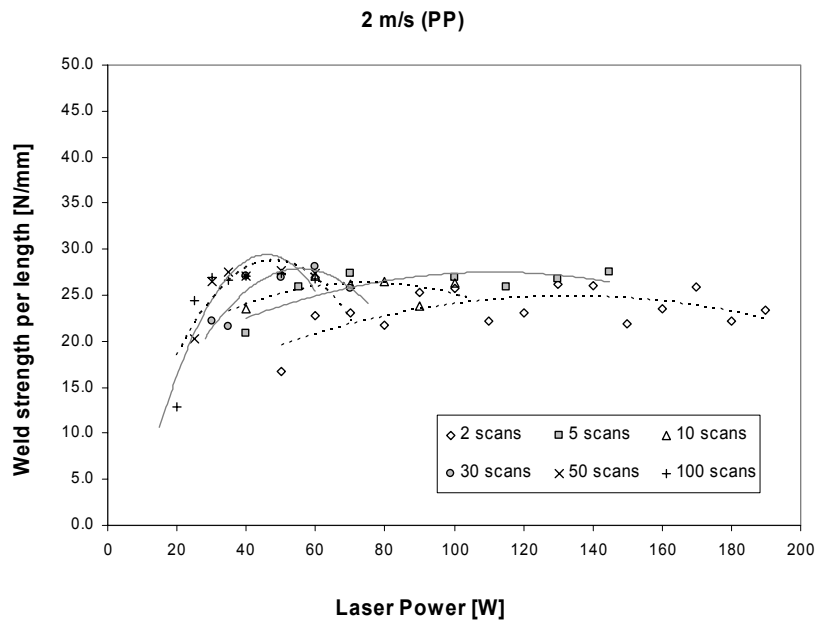


Figure 49. The maximum force per weld unit length as the function of laser power obtained with different number of scans (polypropylene).

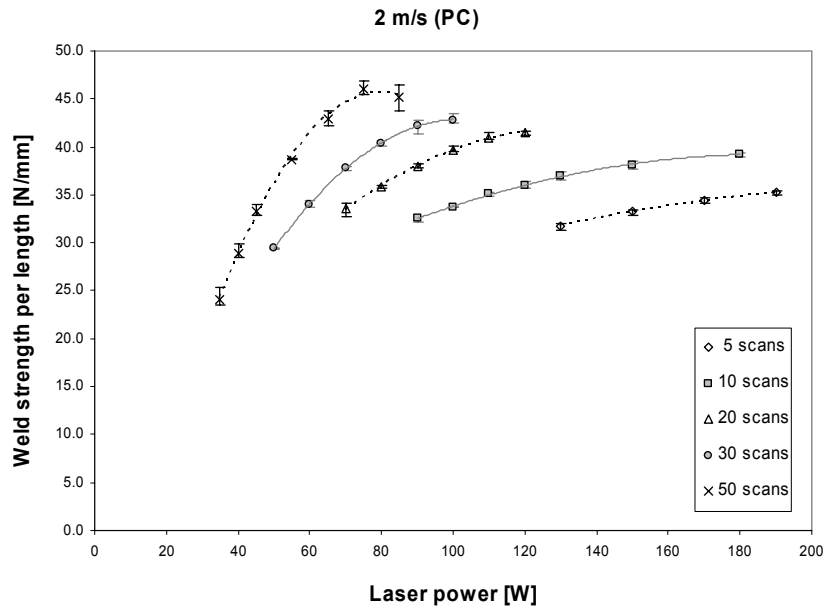


Figure 50. The maximum force per weld unit length as the function of laser power obtained with different number of scans (polycarbonate).

The number of scans effects also to the size and shape of the weld. In Figure 51 it can be found the effect of the number of scans to the width and the height of the polypropylene weld. It can be noticed that as the number of scans is increased also the width and the height of the weld are increased. This can be explained with higher energy input as the number of scans increase and create more molten material. The same phenomenon can be seen with all welding speeds from 0,5 m/s to 10 m/s. With a higher number of scans the weld height increases more than the weld with and is almost the same as the width, the shape of the weld is more circular. This is due to the higher energy input which leads into larger molten volume. Therefore it can be predicted that by increasing number of scans will lead into larger gap bridging capability.

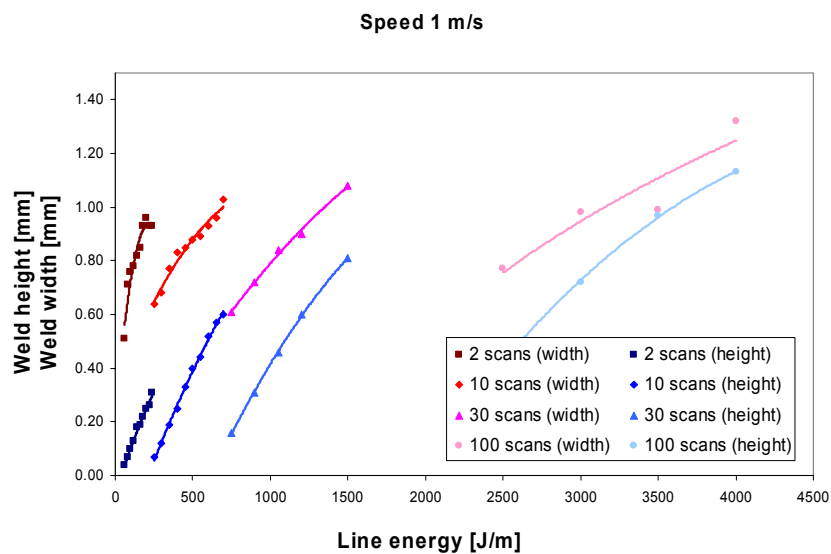


Figure 51. The width and the height of the weld obtained with different number of scans (polypropylene).

4.1.3. The effect of pigment concentration

The effect of pigment concentration was studied with different carbon black concentrations in absorbing polypropylene samples. In these experiments the welding results indicated that higher weld strengths could be achieved with higher carbon black content (Figure 52). With lower carbon black content power needed is higher than with higher carbon black content. Laser beam is absorbed to the carbon black additives that are blended to the plastic. When carbon black content is low plastic is more transparent for the laser light and the absorption is lower than with higher carbon black contents used. When carbon black content is higher laser beam is absorbed near to the surface of the plastic and weld formed is more symmetrical (Figure 53). With carbon black content 0,5 w% symmetrical weld could be achieved and increasing of carbon black content didn't effect to the shape of the weld. Maximum tensile strengths per length with different carbon black content were ca 21-24 N/mm and the powers needed were 45-65 W when the scanning speed was 2 m/s.

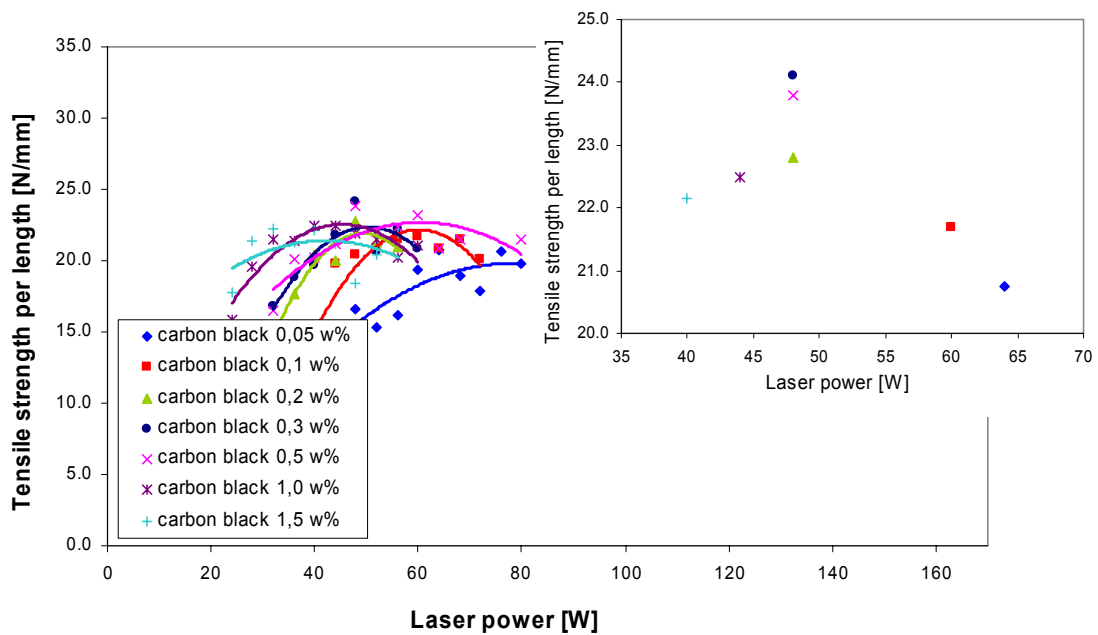


Figure 52. The effect of carbon black content to the tensile strength per length. Welding speed was 2 m/s.

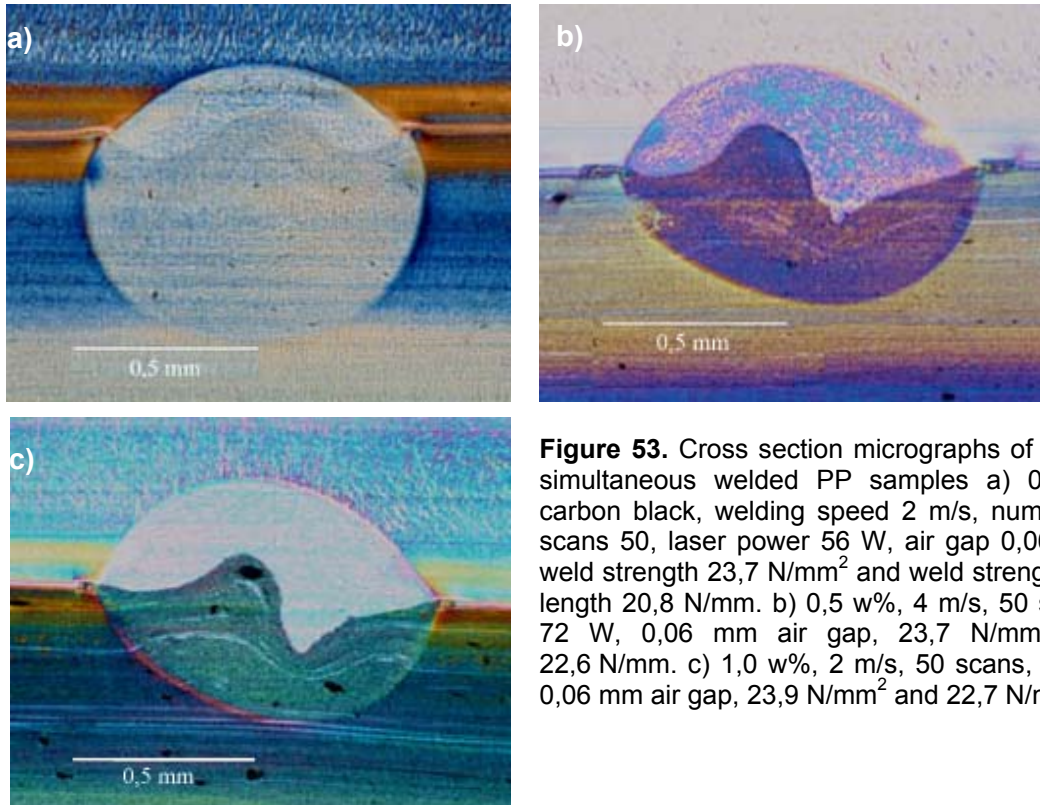


Figure 53. Cross section micrographs of quasi-simultaneous welded PP samples a) 0,1 w% carbon black, welding speed 2 m/s, number of scans 50, laser power 56 W, air gap 0,06 mm, weld strength 23,7 N/mm² and weld strength per length 20,8 N/mm. b) 0,5 w%, 4 m/s, 50 scans, 72 W, 0,06 mm air gap, 23,7 N/mm² and 22,6 N/mm. c) 1,0 w%, 2 m/s, 50 scans, 48 W, 0,06 mm air gap, 23,9 N/mm² and 22,7 N/mm.

4.1.4. The effect of fiber glass

The effect of fiber glass blended into the plastic was studied. Tests were done with different fiber glass content in transparent and in absorbent polypropylene part (10 w%, 20 w% and 30 w% of fiber glass). Highest tensile strength was achieved when both parts were blended with fiber glass. When the fiberglass content was increased the strength of the weld was increased.

When fiber glass was blended only to transparent material, it was noted that increasing of fiberglass increases the tensile strength (23,8-27,8 N/mm). However the needed laser power was also increased (Figure 54). The reason for that was a decreasing of transmission of transparent material when fiber glass content was increased. Highest tensile strength per length was achieved with fiber glass content of 30 w%. Tensile strength was then 27,8 N/mm, welding speed was 2 m/s and laser power needed was 88 W.

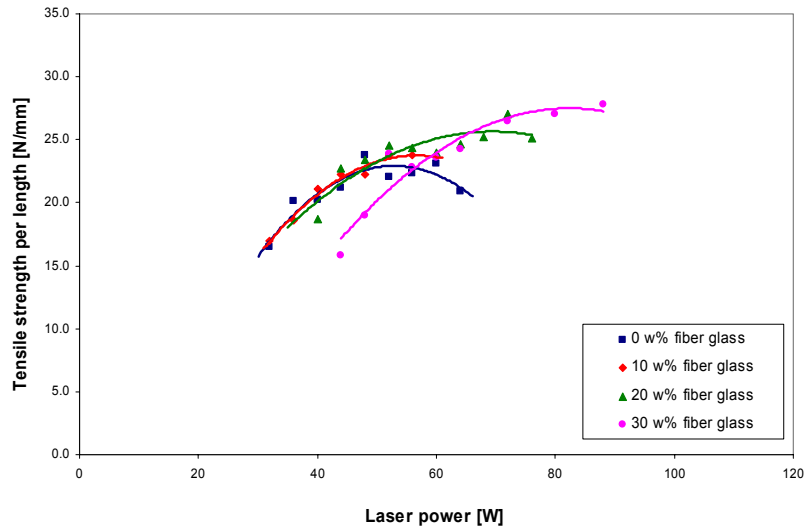


Figure 54. The maximum force per weld unit length as the function of laser power obtained with different fiber glass content of transparent material. The welding speed was 2 m/s, number of scans 50 and the carbon black content of absorbent material was 0,5 w%.

Welding tests were done also for absorbing polypropylene blended with fiber glass. Three different fiber glass contents were used (10 w%, 20 w% and 30 w%) and three different carbon black contents were used (0,1 w%, 0,5 w% and 1,0 w%). Transparent material was natural polypropylene. Highest tensile strength was achieved with highest fiber glass and carbon black contents.

Tests for transparent and absorbing material blended with fiber glass were also done. Highest tensile strength was achieved when both parts were blended with fiber glass. Increasing of the fiberglass content of both materials increases the tensile strength (24,8-30,2 N/mm) and the needed laser power was also increased (Figure 55).

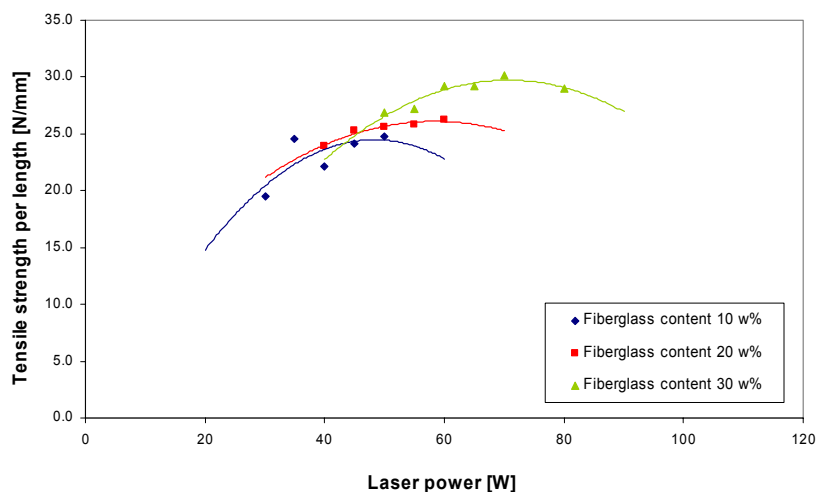


Figure 55. The maximum force per weld unit length as the function of laser power obtained with different fiber glass content of transparent and absorbing material. The welding speed was 2 m/s, number of scans 50 and the carbon black content of absorbent PP was 1,0 w%.

When decomposition of the weld was investigated visually and from cross-sectioned specimens, it was noticed that the best quality of the weld was achieved just before the maximum tensile strength per length was achieved. Same effect can be seen with all

different fiber glass concentrations. In Figure 56 there are some cross-section picture examples from welds with different fiber glass contents.

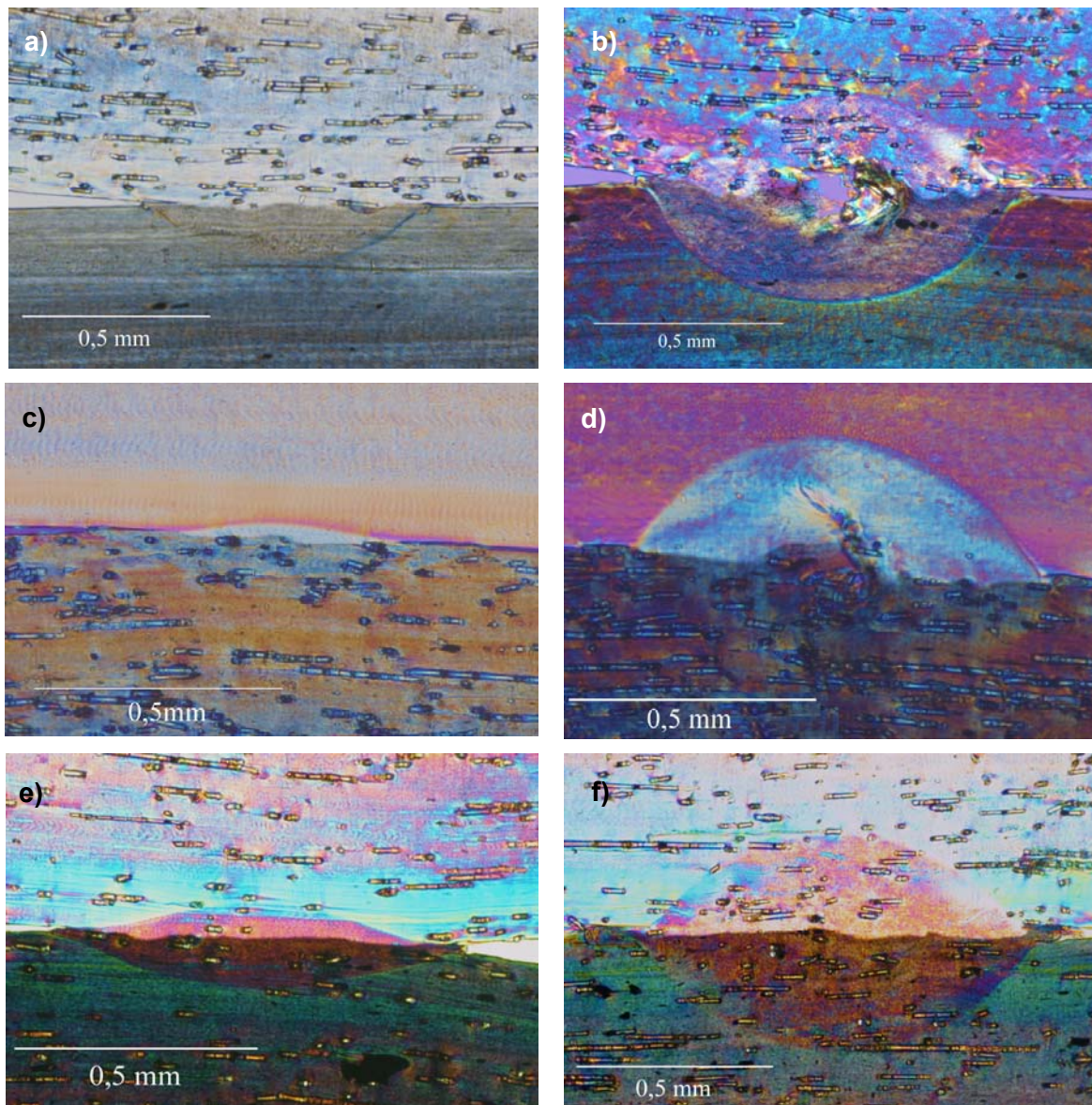


Figure 56. Cross-section pictures from fiber glass blended PP welds. Welding speed was 2 m/s, number of scans 50 a) fiber glass content of transparent 10 %, fiber glass content of absorbent 0 %, carbon black content of absorbent 0,5 %, laser power 36 W and tensile strength per length 18,6 N/mm b) FG of transparent 10 %, FG of absorbent 0 %, CB 0,5 %, 52 W and 23,8 N/mm c) FG of transparent 0 %, FG of absorbent 20 %, CB 0,5 %, 30 W and 16,7 N/mm d) FG of transparent 0 %, FG of absorbent 20 %, CB 0,5 %, 45 W and 21,9 N/mm e) FG of transparent 10 %, FG of absorbent 10 %, CB 1,0 %, 35 W and 24,6 N/mm f) FG of transparent 10 %, FG of absorbent 10 %, CB 1,0 %, 50 W and 24,8 N/mm.

4.1.5. The effect of air gap

The quasi-simultaneous welding technique showed great potential in bridging air gaps. Larger air gaps could be bridged with the quasi-simultaneous welding technique compared to the contour welding technique both with polypropylene and polycarbonate samples.

With PP a 0.30 mm air gap could be bridged with quasi-simultaneous welding without any critical decrease in the maximum tensile strengths per length (Figure 57). An air gap over 0.30 mm wasn't bridgeable anymore. In contour welding only a 0.06 mm air gap in PP could

be bridged without critical decrease in the maximum tensile strength per length of the weld. The weld strength per length of PP wasn't in the acceptable range anymore, when air gaps were over 0.06 mm. Maximum tensile strengths per length in quasi-simultaneous welding were almost same with different air gaps (0,06-0,30 mm) ca 21-23 N/mm when welding speed was 2 m/s.

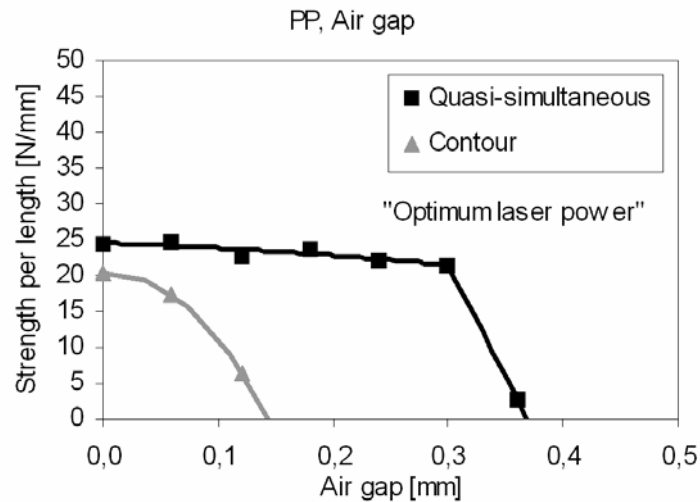


Figure 57. The maximum force per weld unit length of PP obtained with different air gaps in contour welding and quasi-simultaneous welding with optimum laser power. Welding speed for contour welding was 3 m/min and for quasi-simultaneous welding the welding speed was 2 m/s and the number of scans was 50.

With PC an air gap of 0.18 mm could be bridged without critical decrease in the maximum tensile strength per length of the weld (Figure 58). At an air gap of 0.24 mm the tensile strength per length with PC was ca. 50% of the strength for no air gap, which wasn't acceptable anymore. In contour welding only a 0.06 mm air gap in PC could be bridged. In quasi-simultaneous welding the maximum tensile strengths per length up to 0,18 mm air gap were about 38...47 N/mm. The higher volume increase of the melt of PP might favour the gab bridging ability PP compared to PC (Figure 59).

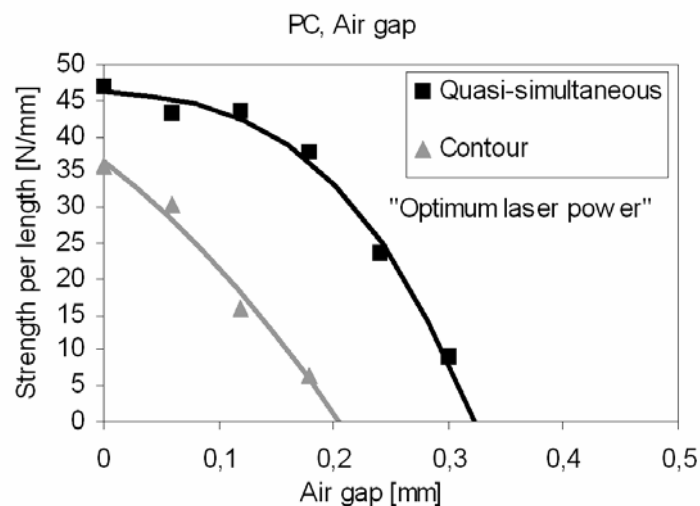


Figure 58. The maximum force per weld unit length of PC obtained with different air gaps in contour welding and quasi-simultaneous welding with optimum laser power. Welding speed for contour welding was 3 m/min and for quasi-simultaneous welding the welding speed was 2 m/s and the number of scans was 50.

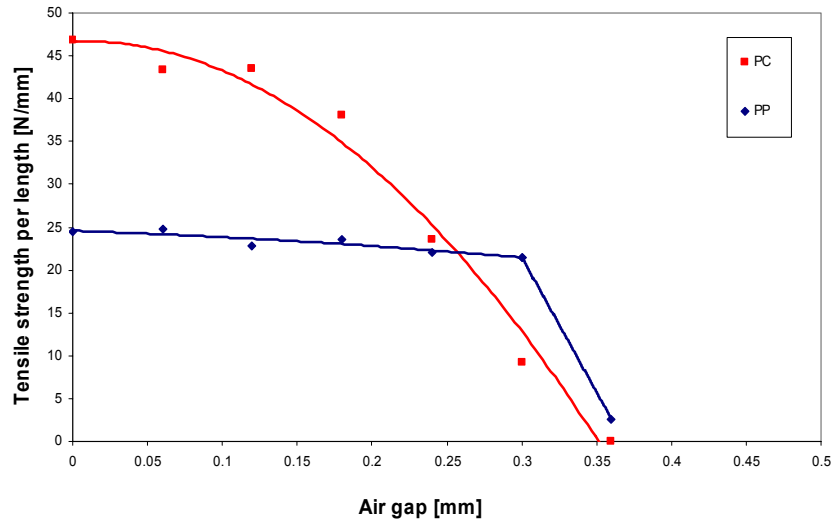


Figure 59. The tensile strength per length of polycarbonate and polypropylene obtained with different air gaps, welding speed was 2 m/s.

When there was an air gap between the parts there may be some bubbles in the weld, if the volume of the melt wasn't big enough to fill the air gap. When air gap was 0,06 mm there was enough molten material to bridge the air gap, but with higher air gaps there comes some bubbles to the weld. However there wasn't any critical decrease in the maximum tensile strengths per length until with the air gap of 0,36 mm. In Figure 60 and Figure 61 are some cross sections of the welds with different air gaps. We can also notice that with higher air gaps the width of the weld increases and some molten material was extruded to the air gap.

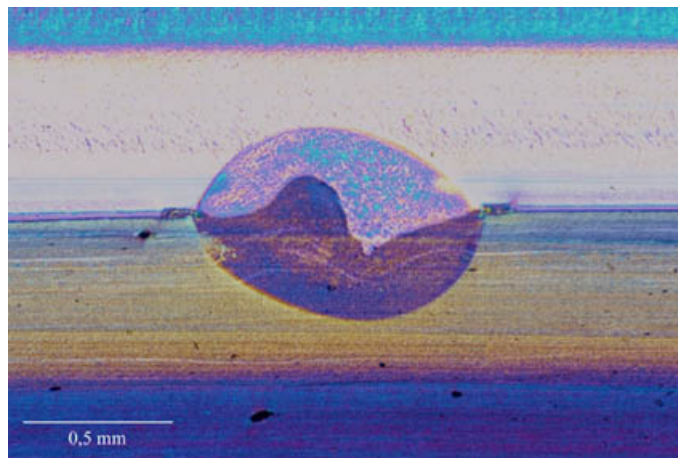


Figure 60. Cross section micrographs of quasi-simultaneous welded PP samples. Air gap was 0,06 mm, welding speed 4 m/s, number of scans 50 and laser power 72 W. The strength of the weld was 23,7 N/mm² and the strength per length 22,6 N/mm.

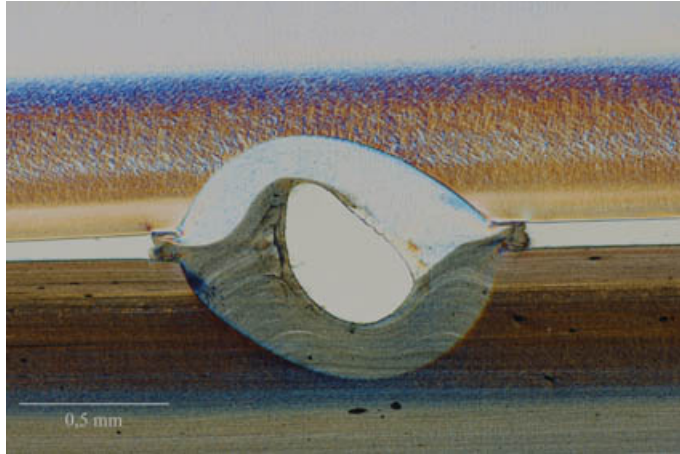


Figure 61. Cross section micrographs of quasi-simultaneous welded PP samples. Air gap was 0,12 mm, welding speed 4 m/s, number of scans 50 and laser power 80 W. The strength of the weld was 20,7 N/mm² and the strength per length 22,4 N/mm.

4.1.6. The effect of welding time

In mass-production welding times needed are often only a few seconds. Usually the cycle time of the production line is determined beforehand and therefore welding time isn't a parameter that can be varied. Consequently welding time can be considered as the most important parameter in mass-production. With quasi-simultaneous welding a short welding time can be achieved with different parameter combinations.

In Figure 62 and Figure 63 can be seen the strength per length values welded with different parameter combinations when the welding time was ca. 2 s with polypropylene and ca. 1 s with polycarbonate. The length of the welding path was 210 mm. It was found when welding polypropylene and polycarbonate that nearly the same maximum weld strengths per length are obtained with all the tested parameter combinations, if the welding time is the same.

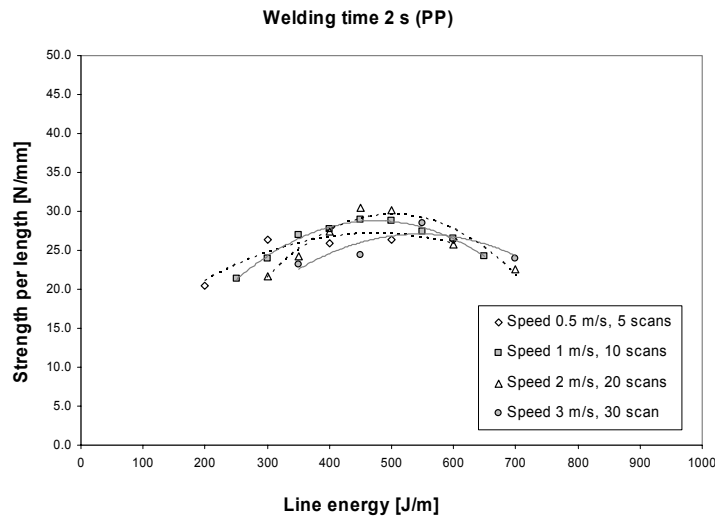


Figure 62. The maximum force per weld unit length of polypropylene obtained with different welding parameters. Welding time is ca. 2 s.

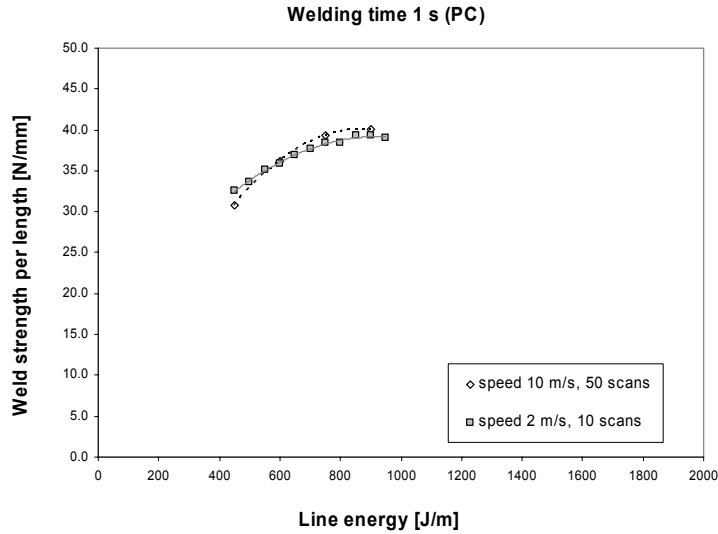


Figure 63. The maximum force per weld unit length of polycarbonate obtained with different welding parameters. Welding time is ca. 1 s.

With different parameter combinations the size of the weld was same if the welding time is same (Figure 64). Also at the maximum weld strength per length the shape of the weld was the same with different parameter combinations if the welding time was same. The reason could be that an equal amount of energy was distributed into the material and therefore the strength per length of the weld was also the same.

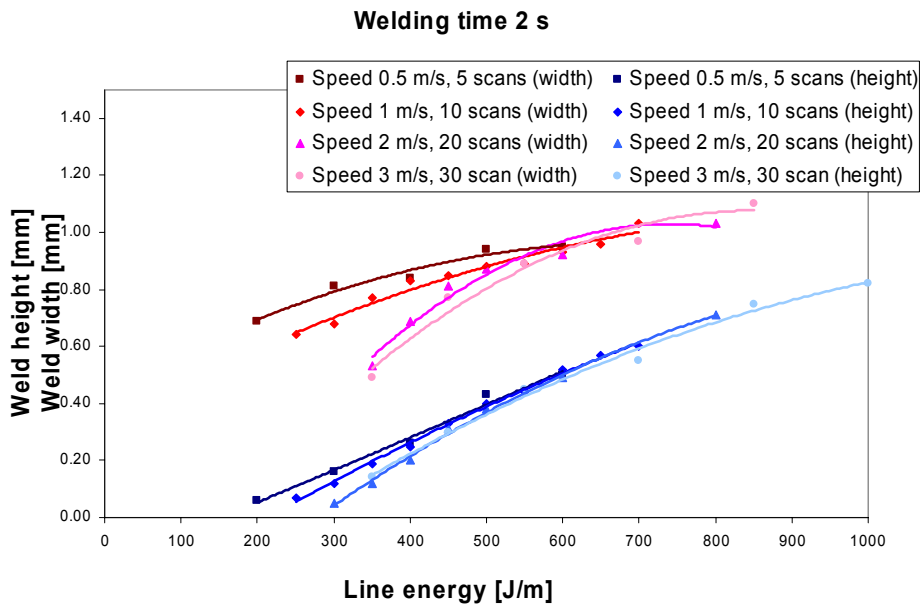


Figure 64. The width and height of the weld obtained with different welding parameters. Welding time is about 2 s.

The weld strength with similar welding times of quasi-simultaneous welding and contour welding of polypropylene was compared. With the same welding time higher weld strength per length can be achieved with quasi-simultaneous welding than with contour welding (Figure 65). But in quasi-simultaneous welding a higher energy is needed to achieve short welding times and higher strengths. Probably because of the higher energy needed in quasi-simultaneous welding the achieved weld strength per length is higher.

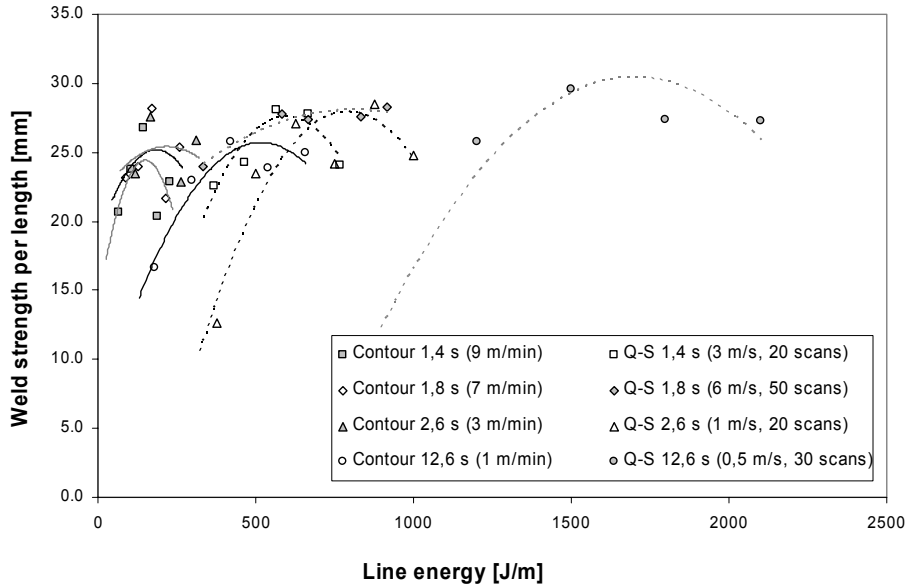


Figure 65. The maximum force per weld unit length obtained with different welding parameters and welding times with contour and quasi-simultaneous techniques. The length of the welding path was 210 mm.

4.1.7. Welding time of 0.5 s – 4 s

A constant welding time of 1 second and a weld seam length of 150 mm were used in order to determine the effect of different parameters to the tensile strength of the weld. The laser power was adjusted such that the weld was visually acceptable and the welding speed was adjusted according to the number of scans used such that the total welding time was always 1 second. The tensile strength of the welds was found to increase slightly with PP as the number of scans was increased (Figure 66). The lowest tensile strength values for PP were around 21 N/mm² with 1 scan and the highest tensile strength values were above 23 N/mm² with 50 scans. Also with PC the tensile strength increased as the number of scans was increased (Figure 67), but the increase was larger with PC than with PP. The lowest tensile strength values for PC were around 28.5 N/mm² with 1 scan and the highest tensile strength values were around 33 N/mm² with 50 scans. With PC the tensile strength didn't increase anymore when the number of scans used was 10.

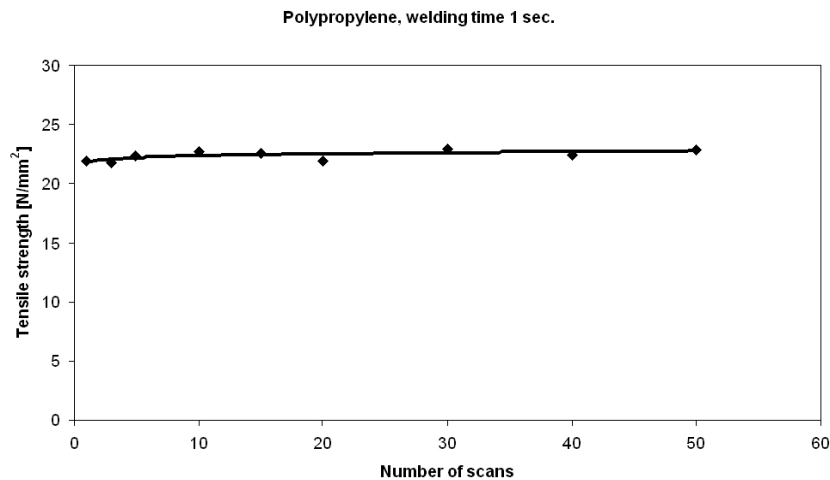


Figure 66. Tensile strength of polypropylene welded with different number of scans, total welding time 1 second and optimum laser power to achieve visually acceptable welds.

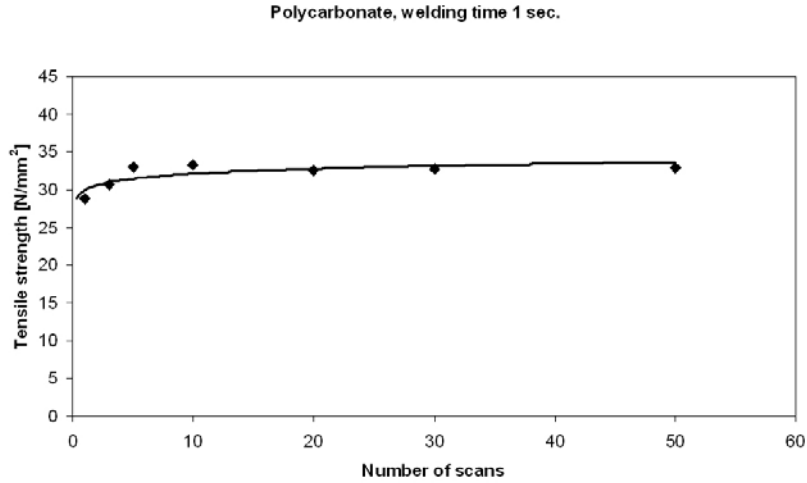


Figure 67. Tensile strength of polycarbonate welded with different number of scans, total welding time 1 second and optimum laser power to achieve visually acceptable welds.

The weld dimensions of PP were found to be strongly dependent on how many times the weld seam was scanned during the 1 second total welding time. The highest number of scans resulted in narrow, but high welds, whereas a low number of scans resulted in welds wide as the focal spot diameter used, but in this case the welds weren't very high. The measured PP weld widths and heights as a function of the number of scans used are presented in Figure 68. The widest weld (width 0.97 mm and height 0.11 mm, Figure 69a) was achieved with 1 scan, 16 W laser power and 150 mm/s welding speed. The highest weld (width 0.81 mm and height 0.28 mm, Figure 69b) was achieved with 50 scans, 45 W laser power and 7500 mm/s welding speed.

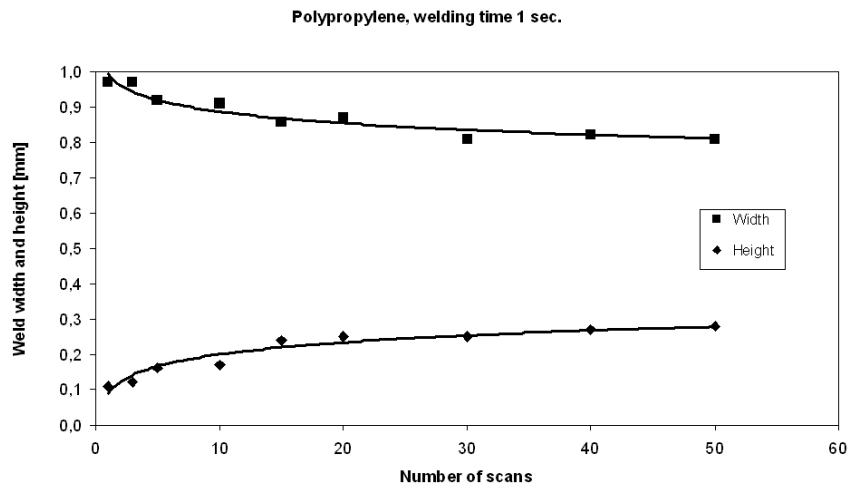


Figure 68. Weld width and height of polypropylene welded with different number of scans, total welding time 1 second and optimum laser power.

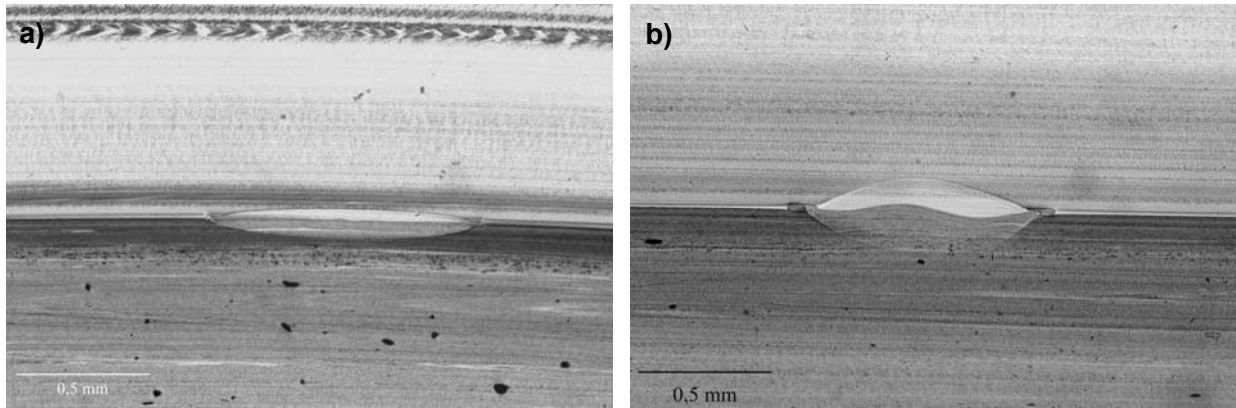


Figure 69. Cross-sections of quasi-simultaneously welded polypropylene samples a) welding speed 150 mm/s, laser power 16 W, 1 scan, welding time 1 s., b) welding speed 7500 mm/s, laser power 45 W, 50 scans, welding time 1 s.

The temperature measurements with an IR-camera showed very clearly how the temperature was distributed along the seam. Just with a single scan the weld already starts to cool down from the beginning of the seam (Figure 70a). Also with 3 scans the weld is already cooling down from the beginning when the total welding time is 1 second (Figure 70b). An even heat distribution along a 150 mm long weld seam can be achieved by scanning the welding 10 times or more during 1 second (Figure 70c).

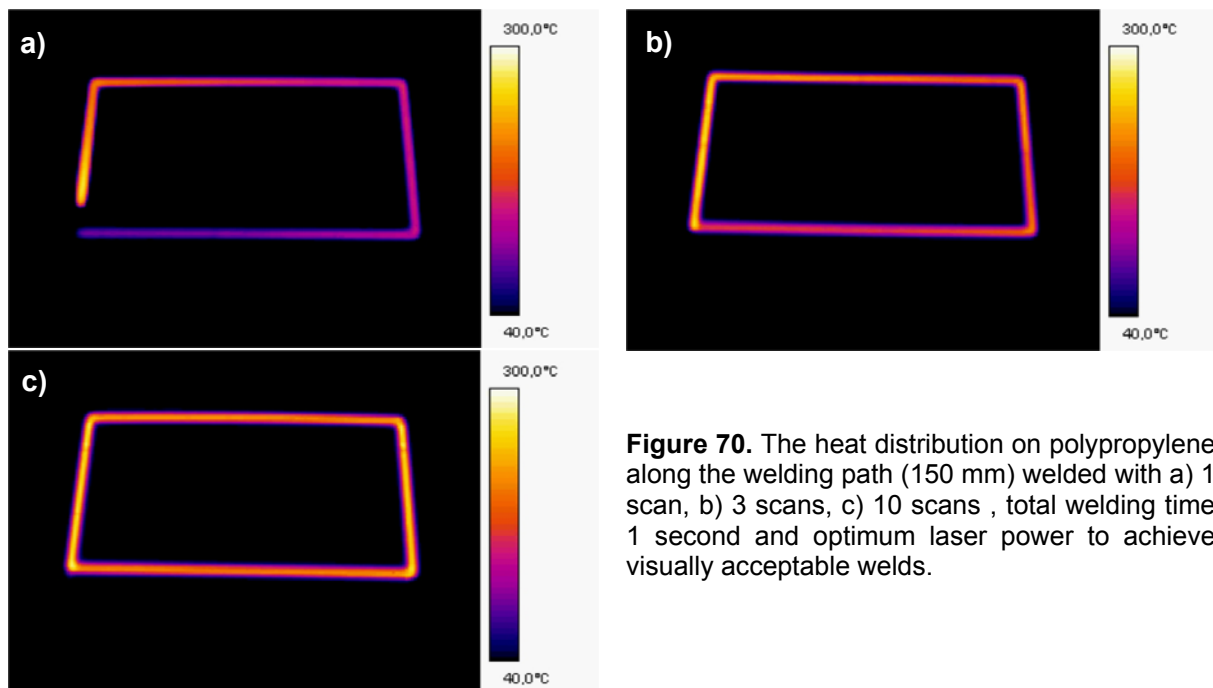


Figure 70. The heat distribution on polypropylene along the welding path (150 mm) welded with a) 1 scan, b) 3 scans, c) 10 scans , total welding time 1 second and optimum laser power to achieve visually acceptable welds.

The temperature measurements with the IR-camera were done without the top plastic. In each case the total welding time was always 1 second, welding path 150 mm and the welding speed was adjusted according to the number of scans used. The measured temperature values differ slightly from the real values, because the measurements were done without the top plastic. It can be also assumed that the measured peak temperatures would be lower with the top plastic and it would also affect the cooling of the weld between the scans. Still the temperature measurements clearly showed differences in the thermal behaviour of the quasi-simultaneous welding technique when number of scans was varied and they can be also used to get a better understanding of the quasi-simultaneous welding process.

With a single scan the temperature rises to the melting temperature of the plastic very quickly and then it starts to cool down (Figure 71a). Up to 10 scans the plastic is heated up very rapidly with the first scan and also the cooling down step can be seen very clearly (Figure 71a-d). The temperature rise was found to be very moderate when the number of scans was above 20 (Figure 71e-h). Also the cooling down step was found to decrease as the number of scans was increased.

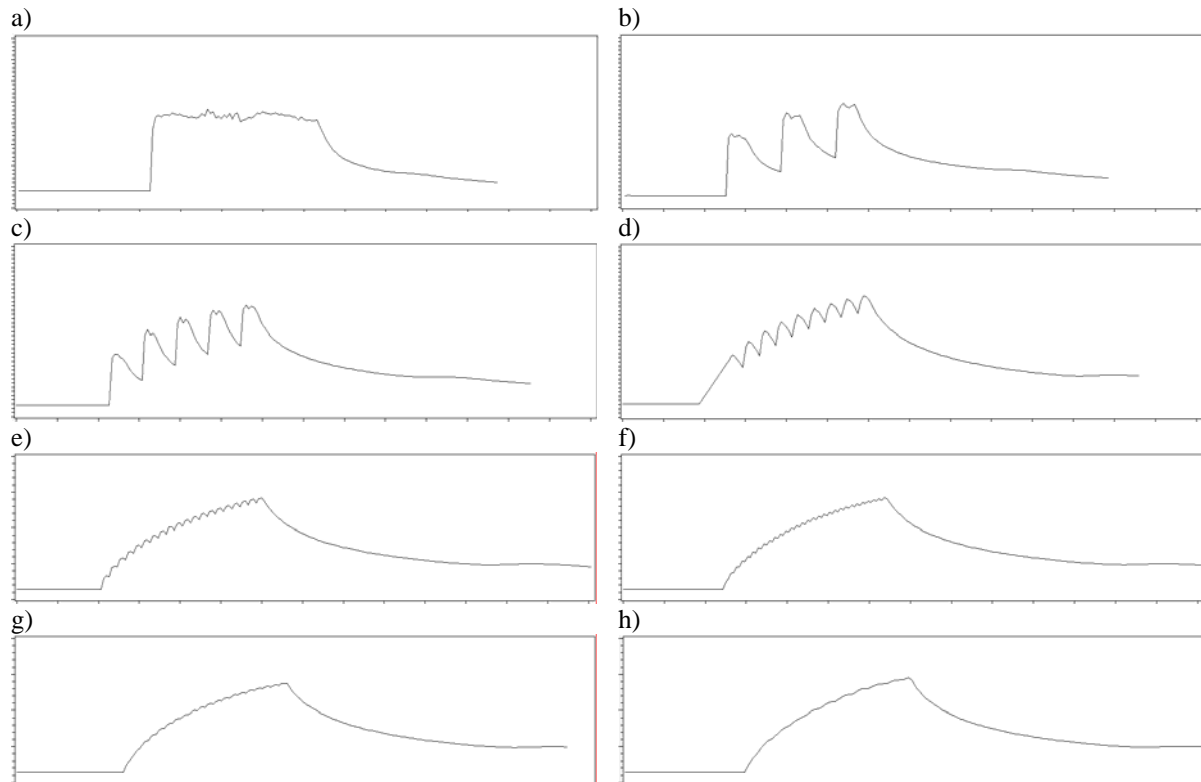


Figure 71. Temperature measurements at a certain point of the weld seam as a function of welding time. Measurements were done with an IR-camera and without the top plastic. The measured temperatures can be assumed to be higher than with the top plastic. Material PP, weld seam length 150 mm, total welding time 1 second a) number of scans 1 and welding speed 150 mm/s, b) number of scans 3 and welding speed 450 mm/s, c) number of scans 5 and welding speed 750 mm/s, d) number of scans 10 and welding speed 1500 mm/s, e) number of scans 20 and welding speed 3000 mm/s, f) number of scans 30 and welding speed 4500 mm/s, g) number of scans 40 and welding speed 6000 mm/s, h) number of scans 50 and welding speed 7500 mm/s

4.2. Elastomers

Some tests were done also for elastomer materials. TPU were welded to black PC+ABS plates. Tensile strength tests were done (Figure 72). Achieved weld strengths were not so high. Tests were done with different welding speeds and with 50 scans.

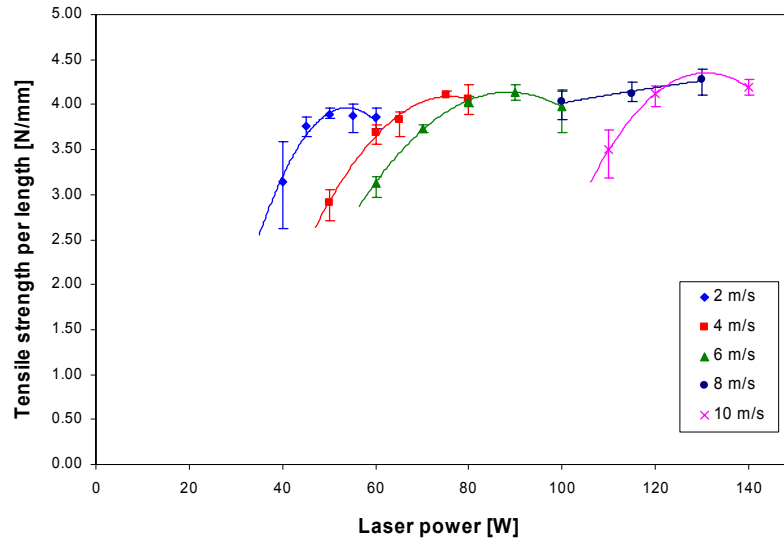


Figure 72. The maximum force per weld unit length as the function of laser power obtained with different welding speeds.

4.3. Transmission measurements

Results from transmission measurements are summarized in Figure 73 - Figure 80. In Table 16 it is summarized the optical properties of different materials in the wavelength of 940 nm (diode laser).

Table 16. Measured and calculated values of T, R and A in 940 nm.

Material	Transmission (%)	Reflection (%)	Absorption (%)
PP	85,96	7,73	6,31
PP10	78,23	12,51	9,26
PP20	68,01	19,86	12,13
PP30	58,14	27,27	14,59
PMMA	92,29	7,37	0,34
PC	90,40	9,51	0,09
PC+ABS white	6,74	92,51	0,75
PC+ABS blue	0,03	10,30	89,67
PC+ABS black	0	5,51	94,49
PC+ABS red	4,44	22,73	72,83

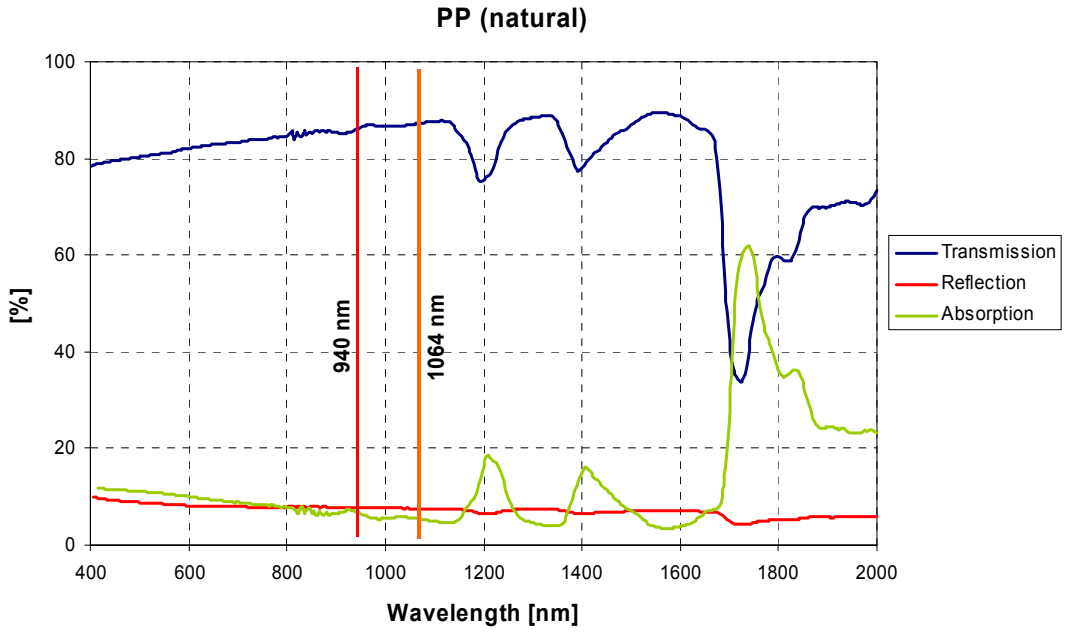


Figure 73. Optical properties of natural polypropylene.

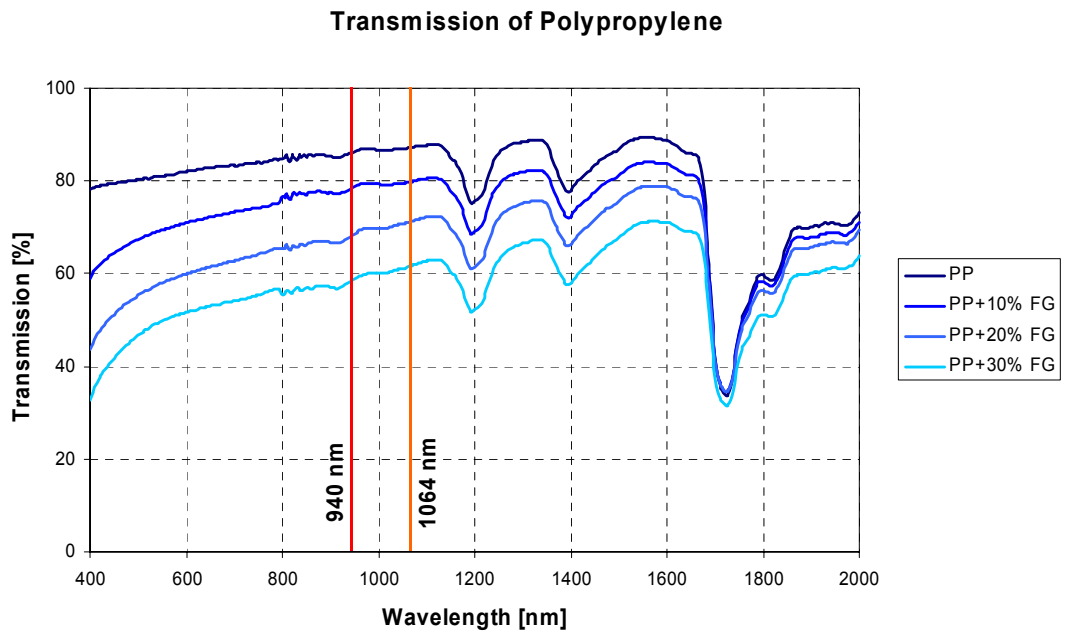


Figure 74. Transmission of polypropylene blended with different fiber glass content.

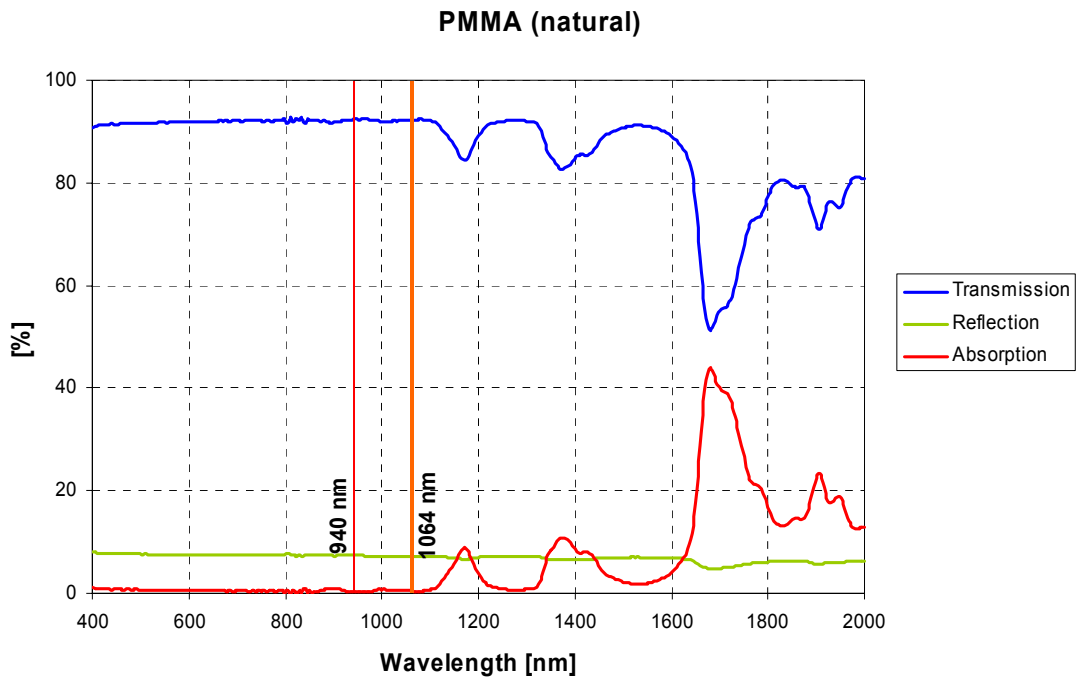


Figure 75. Optical properties of natural PMMA.

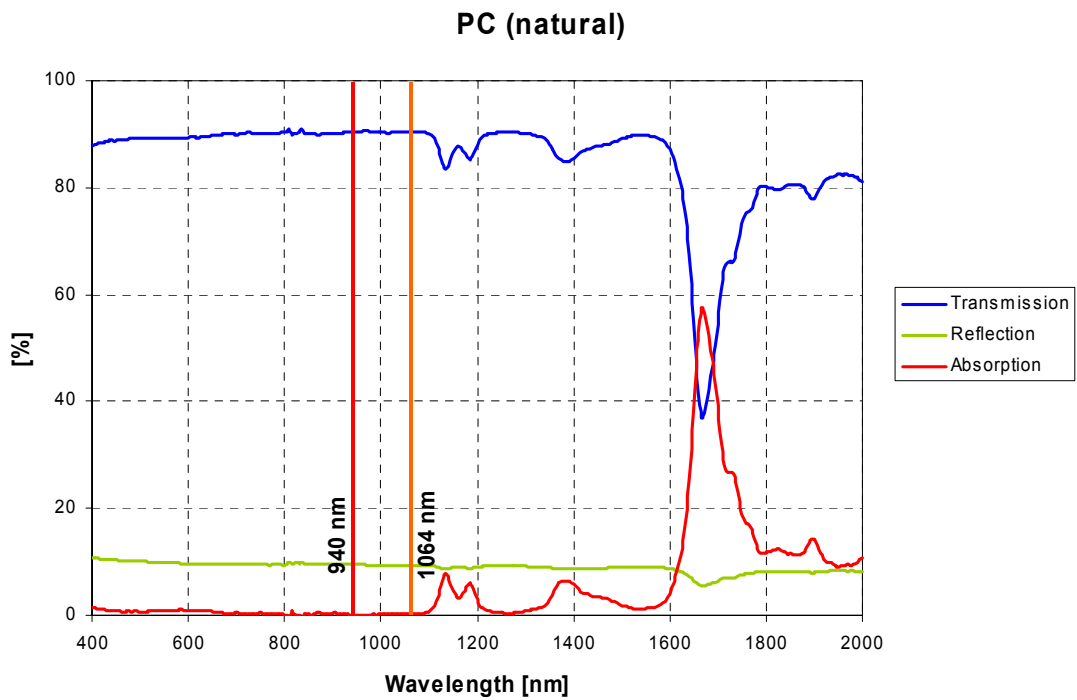


Figure 76. Optical properties of natural PC.

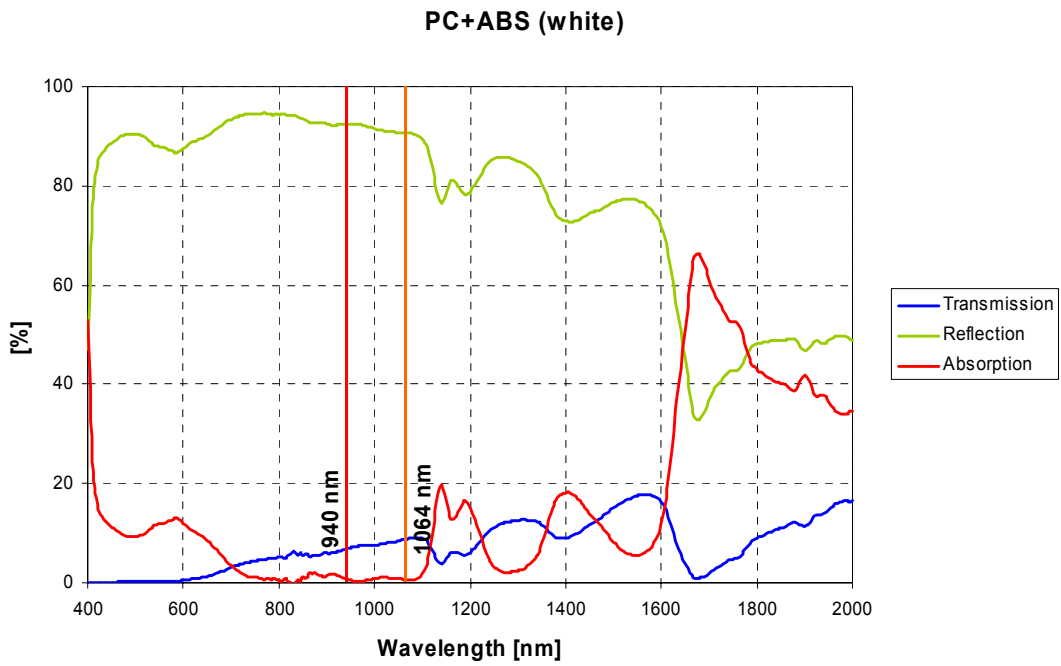


Figure 77. Optical properties of white PC+ABS.

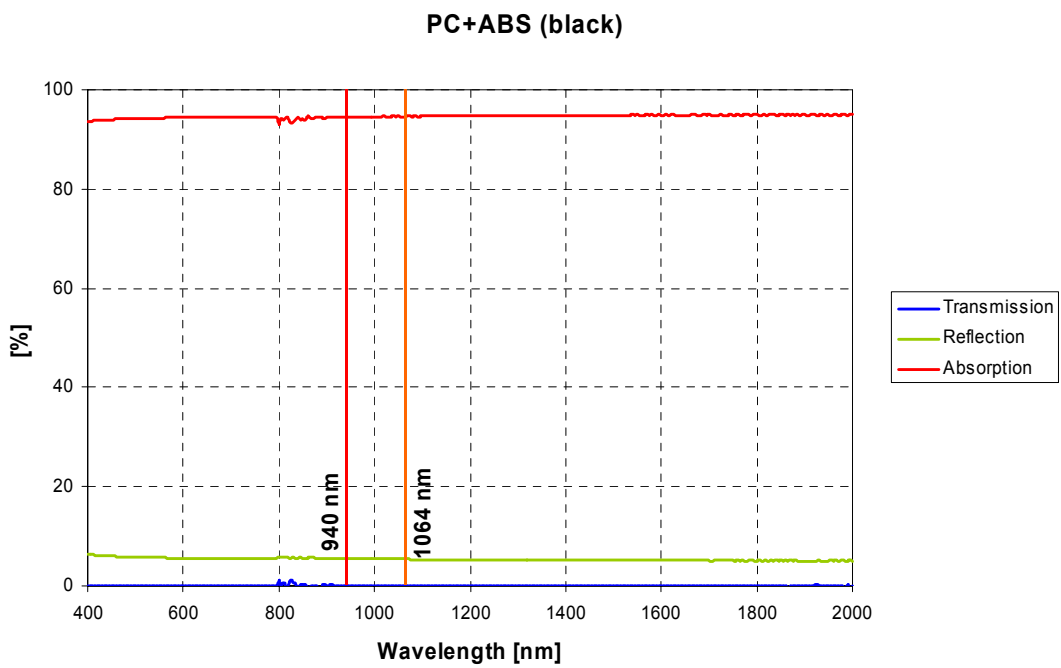


Figure 78. Optical properties of black PC+ABS.

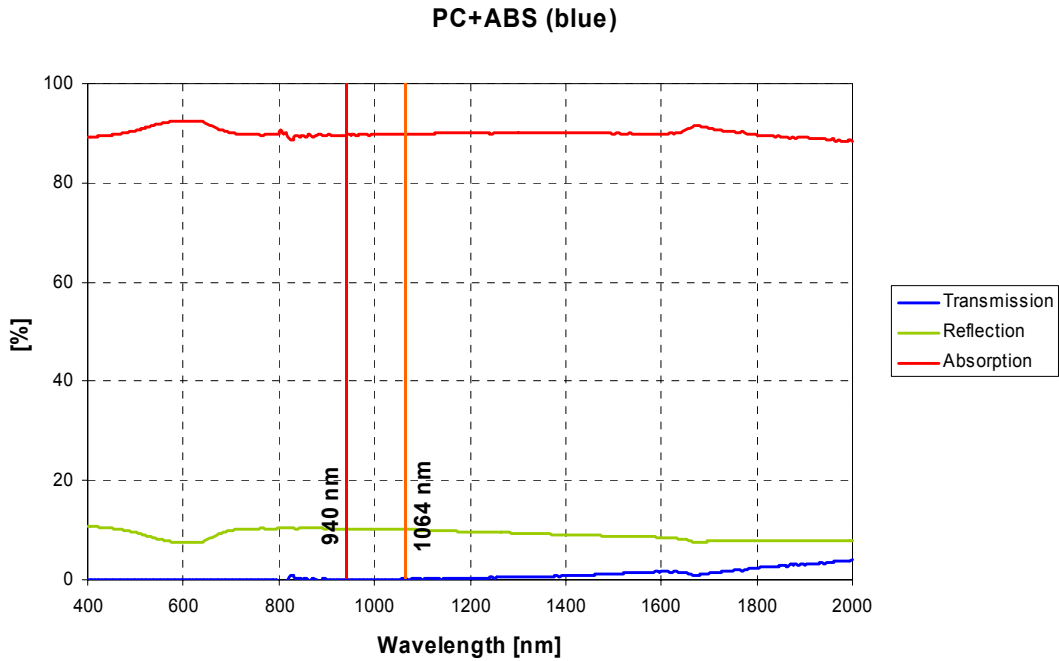


Figure 79. Optical properties of blue PC+ABS.

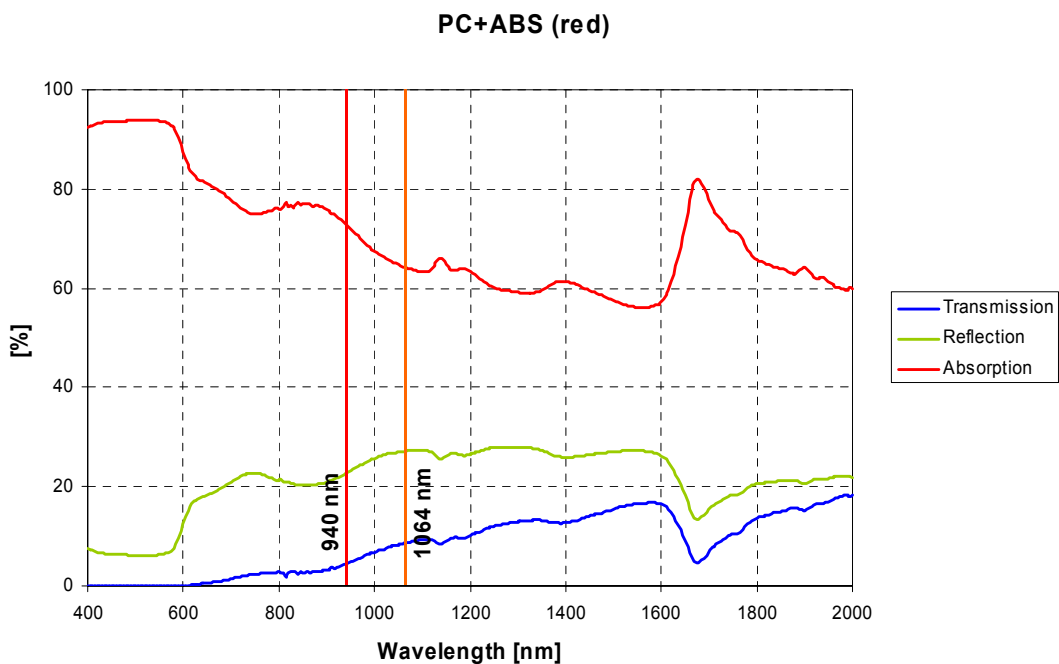


Figure 80. Optical properties of red PC+ABS.

PP, PMMA and PC+ABS materials were mixed with different Clearweld absorbing dyes and with different dye concentrations. Clearweld dyes LWA-267 (for diode lasers) and LWA-290 (for Nd:YAG lasers) were used. Optical properties of these materials (Table 17) were tested. Results from the measurements are summarized in Figure 81 - Figure 88. Clearweld dye LWA-290 did not survive in injection moulding of PMMA and PC materials, which can be seen lower absorption of plastics when lower Clearweld concentrations were used (Figure 85 and Figure 87).

Table 17. Measured Clearweld materials and concentrations.

Material	PP		PP+ 30% GF	PMMA		PC		PC+ABS
CW dye	LWA- 267	LWA- 290	LWA- 290	LWA- 267	LWA- 290	LWA- 267	LWA- 290	LWA- 290
CW [w%]	0,1 0,05 0,025 0,0125 0,00625	0,1 0,05 0,025 0,0125 0,00625	0,1 0,05 0,025 0,0125 0,00625	0,1 0,05 0,025 0,0125 0,00625	0,1 0,05 0,025 0,0125 0,00625	0,1 0,05 0,025 0,0125 0,00625	0,1 0,05 0,025 0,0125 0,00625	0,1 0,05 0,025 0,0125 0,00625

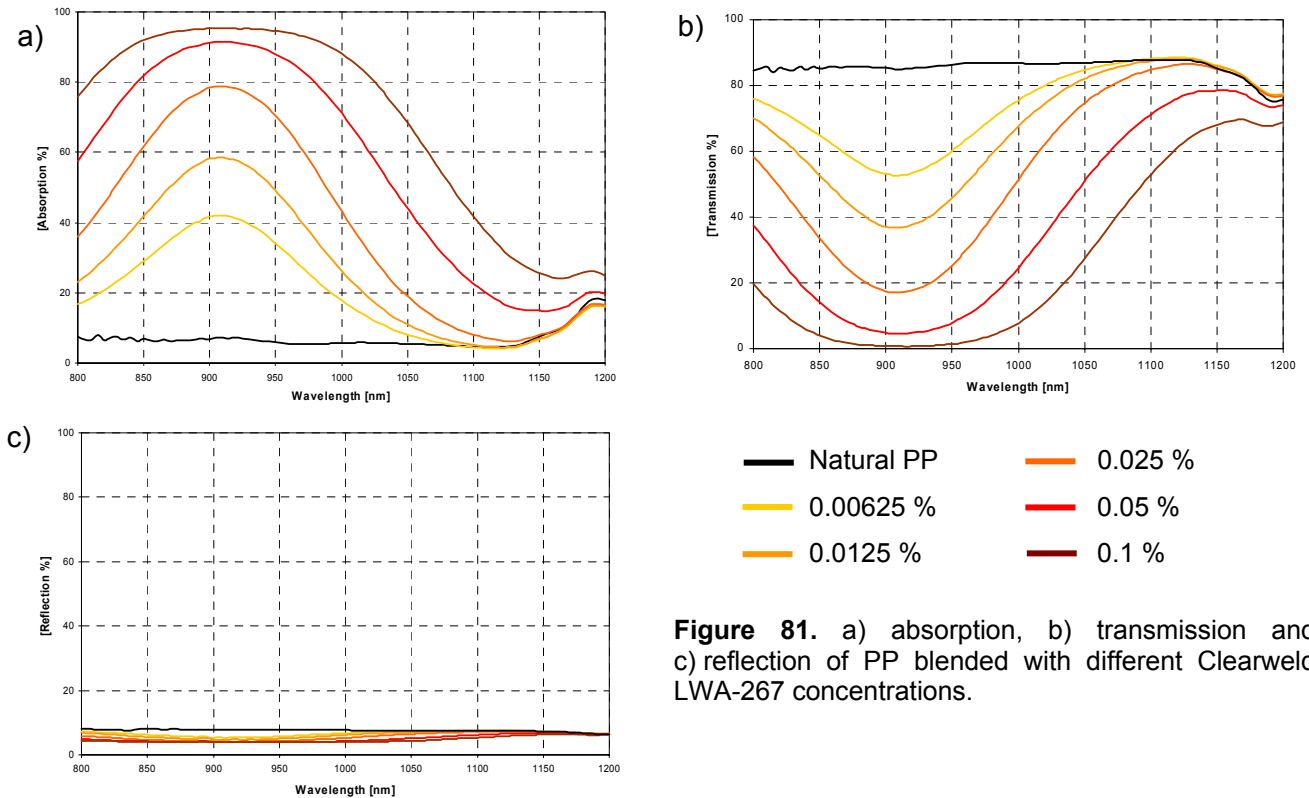
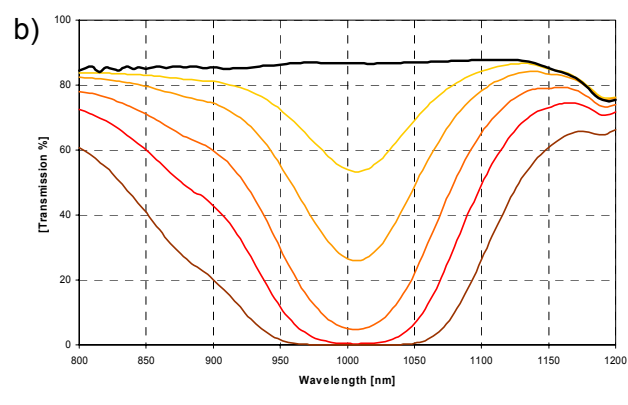
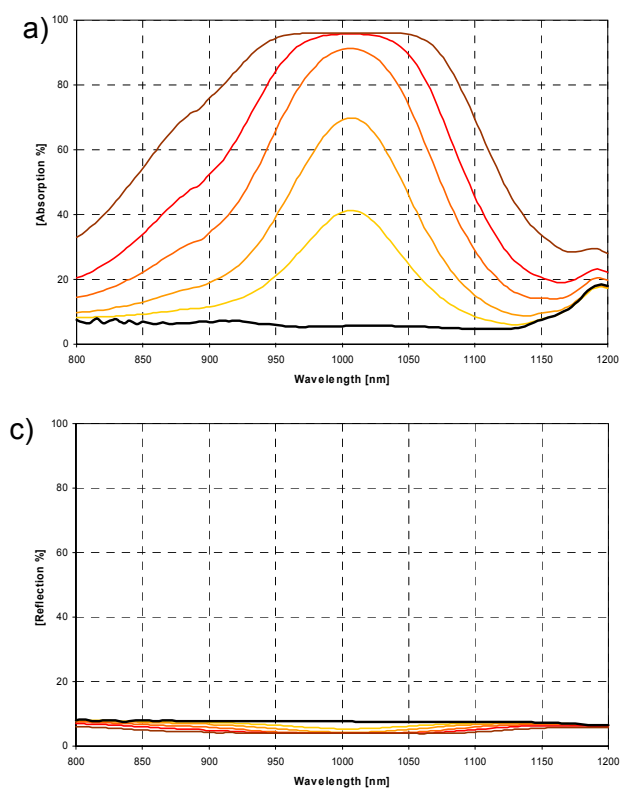
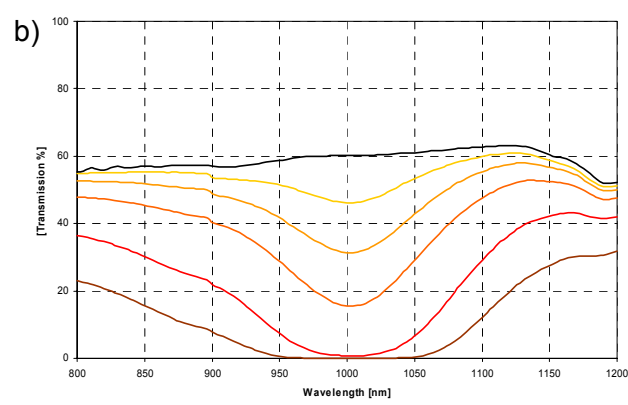
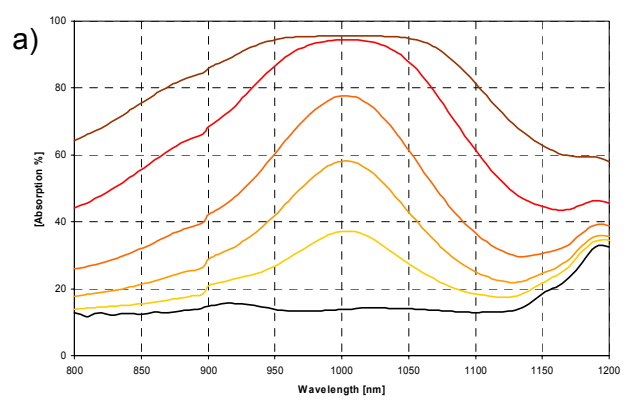
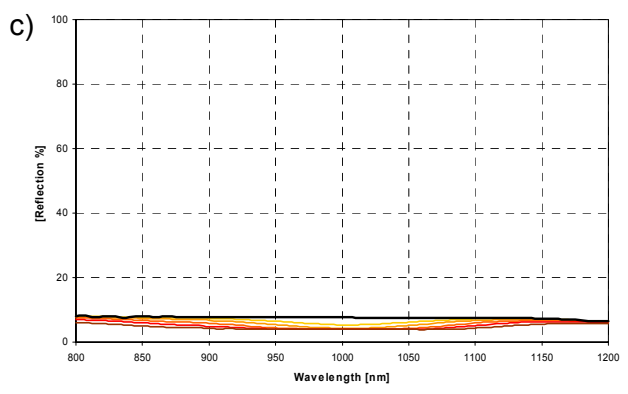


Figure 81. a) absorption, b) transmission and c) reflection of PP blended with different Clearweld LWA-267 concentrations.



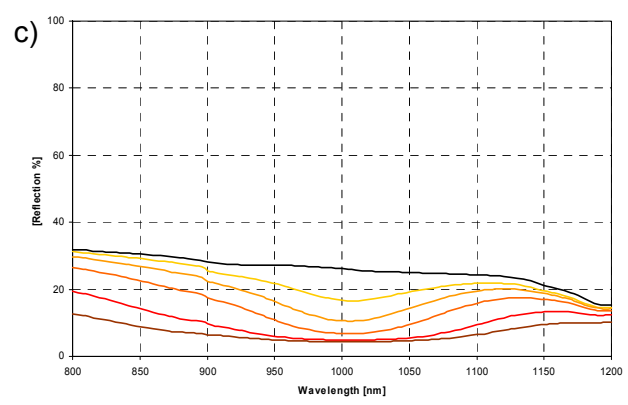
— Natural PP — 0.025 %
 — 0.00625 % — 0.05 %
 — 0.0125 % — 0.1 %

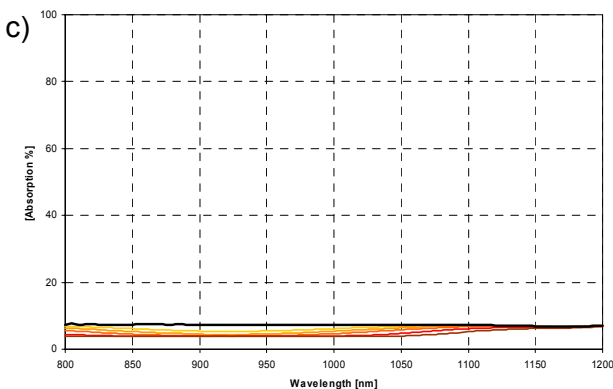
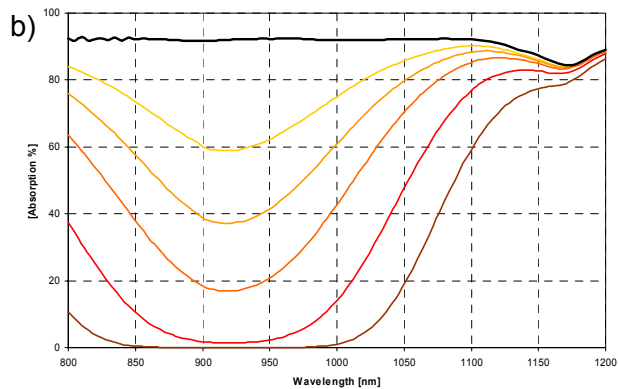
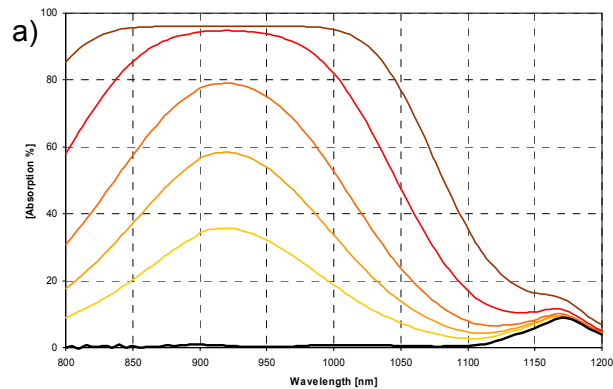
Figure 82. a) absorption, b) transmission and c) reflection of PP blended with different Clearweld LWA-290 concentrations.



— PP + 30 % GF — 0.025 %
 — 0.00625 % — 0.05 %
 — 0.0125 % — 0.1 %

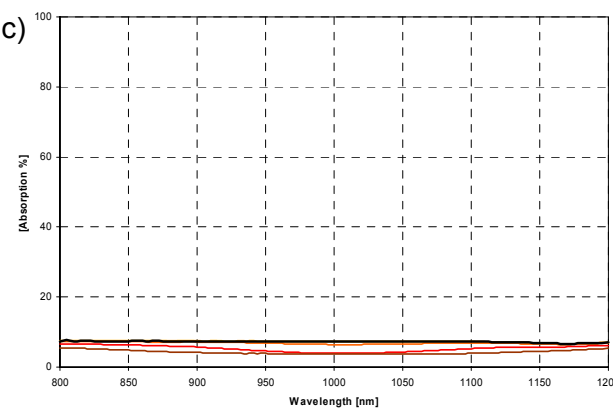
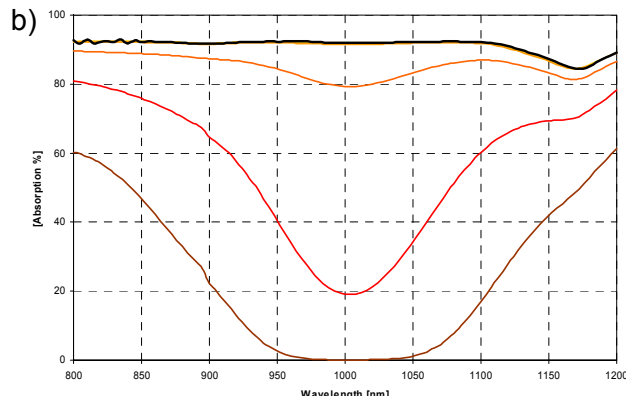
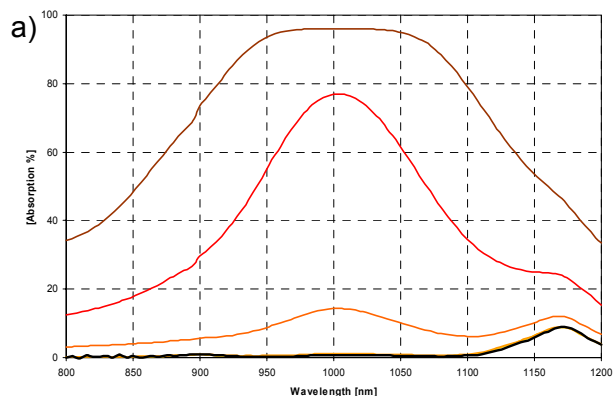
Figure 83. a) absorption, b) transmission and c) reflection of PP + 30% GF blended with different Clearweld LWA-290 concentrations.





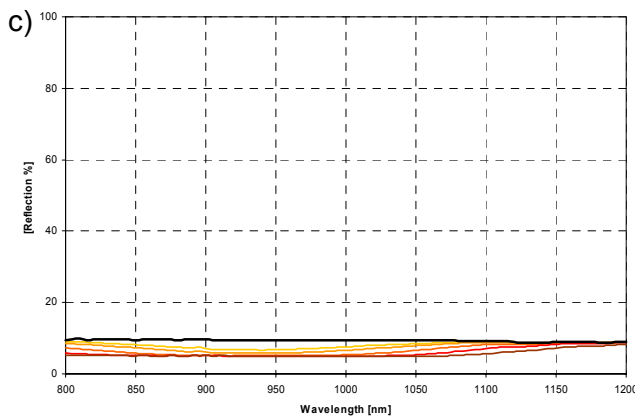
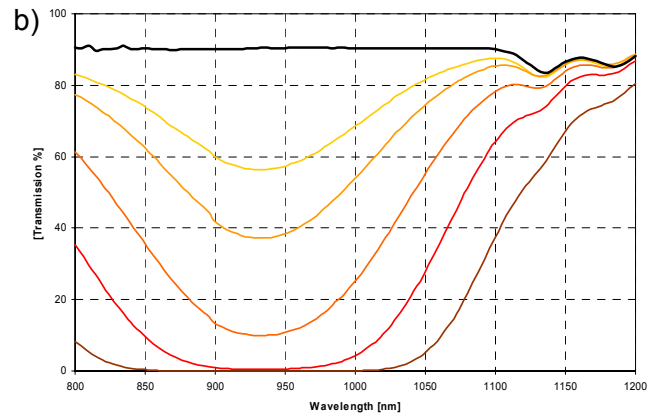
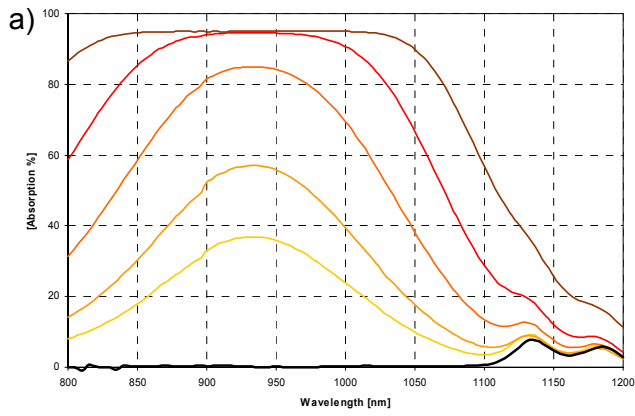
— Natural PMMA — 0.025 %
 — 0.00625 % — 0.05 %
 — 0.0125 % — 0.1 %

Figure 84. a) absorption, b) transmission and c) reflection of natural PMMA blended with different Clearweld LWA-267 concentrations.



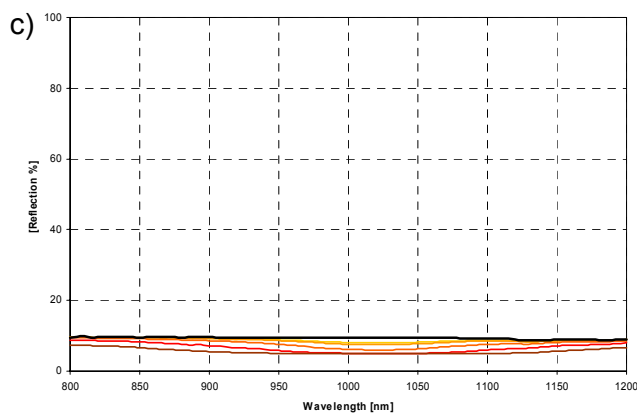
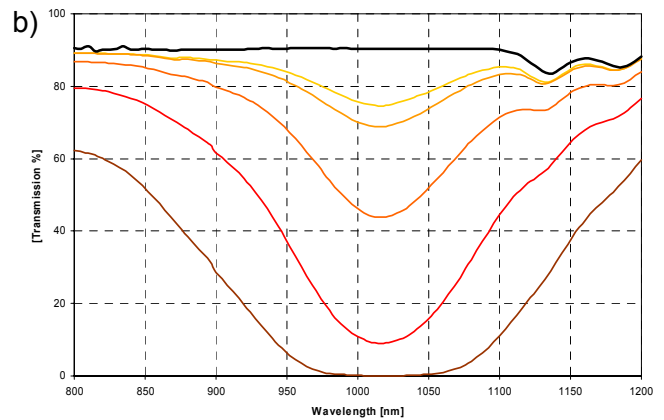
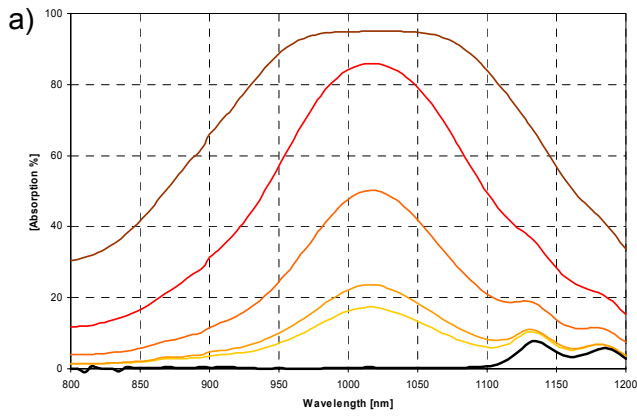
— Natural PMMA — 0.025 %
 — 0.00625 % — 0.05 %
 — 0.0125 % — 0.1 %

Figure 85. a) absorption, b) transmission and c) reflection of natural PMMA blended with different Clearweld LWA-290 concentrations.



— Natural PC — 0.025 %
 — 0.00625 % — 0.05 %
 — 0.0125 % — 0.1 %

Figure 86. a) absorption, b) transmission and c) reflection of natural PC blended with different Clearweld LWA-267 concentrations.



— Natural PC — 0.025 %
 — 0.00625 % — 0.05 %
 — 0.0125 % — 0.1 %

Figure 87. a) absorption, b) transmission and c) reflection of natural PC blended with different Clearweld LWA-290 concentrations.

b)

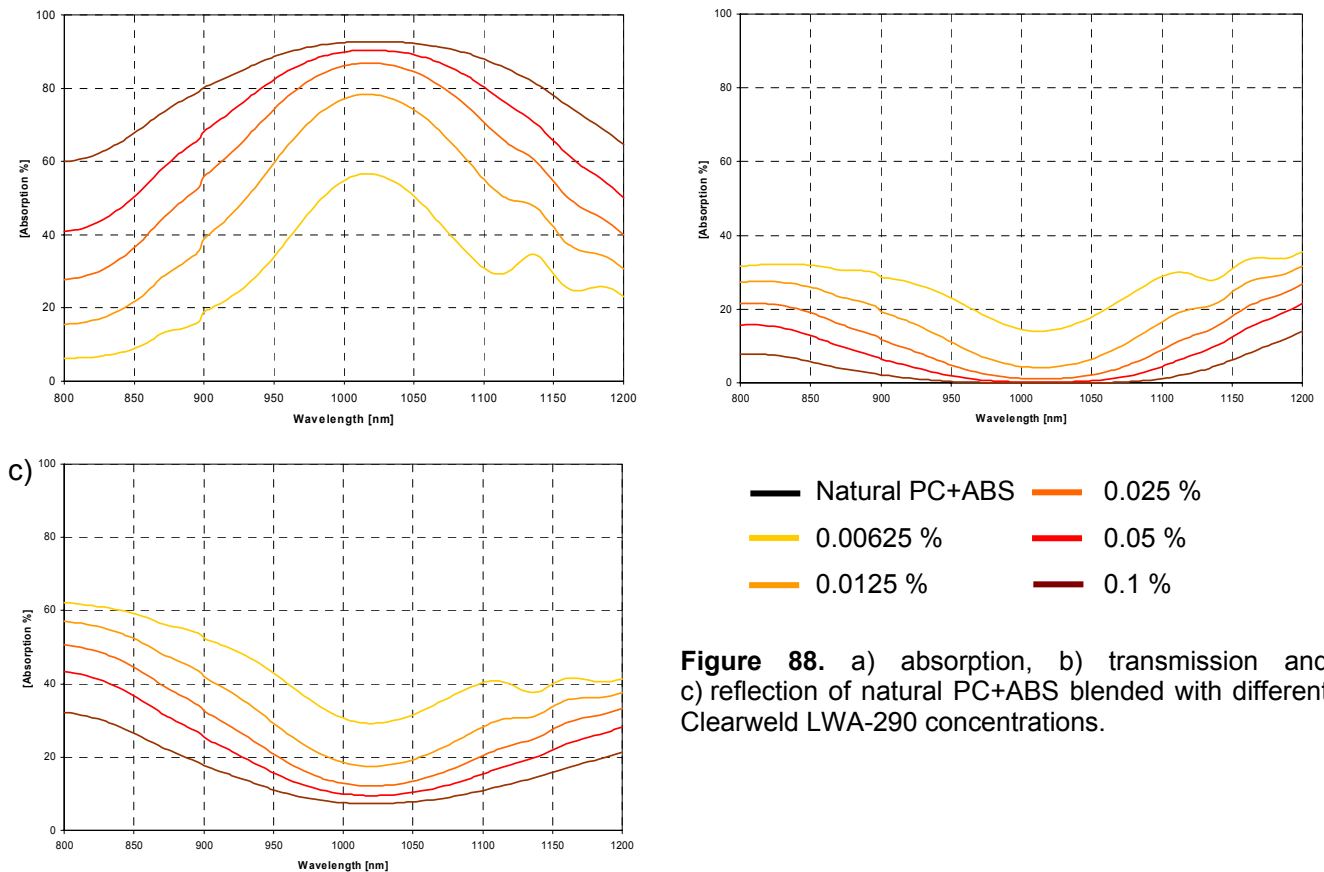


Figure 88. a) absorption, b) transmission and c) reflection of natural PC+ABS blended with different Clearweld LWA-290 concentrations.

4.4. Clearweld welding tests

4.4.1. Clearweld tests 1

Red and white PC+ABS materials were blended with different concentration of Clearweld dyes. In the welding tests PC+ABS was used as absorbing material and natural PMMA was used as transmissive material. Welding tests were done with quasi-simultaneous welding technique. The number of scans used was 50 and the welding time was 2 m/s in all tests. The quality of the weld was measured with tensile tests. From each weld two measurements were taken and the mean value of these tests was used in the results. Visual inspection of welds was also done and some cross section picture from weld was taken. There were some difficulties to make cross section specimens because of the breakable nature of PMMA.

Red PC+ABS was blended with 0 % (0 g), 0,0035 % (3,5 g), 0,007 % (7 g) and 0,014 % (14 g) of Clearweld. In the welding tests it was noted that red PC+ABS was weldable without Clearweld. Although tensile test results shows that mixing of Clearweld to the material makes the absorption of the material better. With higher Clearweld concentrations needed laser powers are not so high than with lower concentrations (Figure 89). Highest tensile strength per length values (32...33 N/mm) are still near the same with all Clearweld concentrations. Best tensile strength (25 N/mm²) was achieved with the highest Clearweld concentration. Clearweld concentration affected also to the width of the weld (Figure 90). With higher Clearweld concentration the weld width was higher when the laser power used was same. Cross section pictures of the welds with Clearweld concentration of 0,0035 % can be seen in Figure 91.

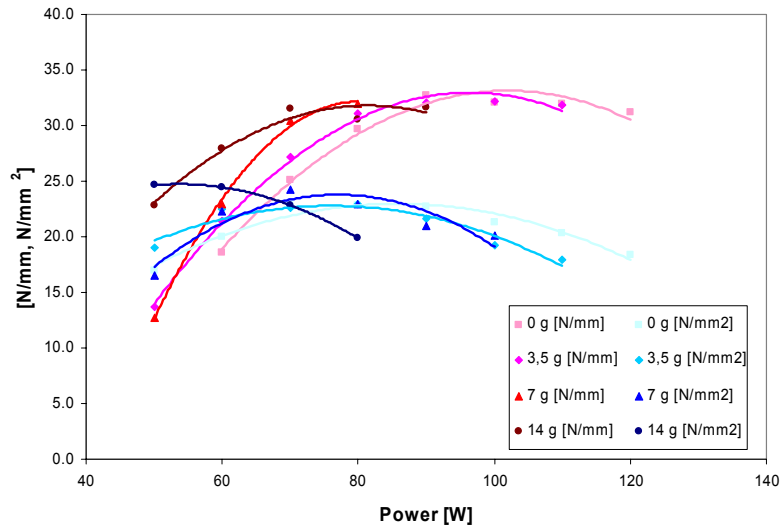


Figure 89. The effect of laser power to the weld strength per length and weld strength in quasi-simultaneous welding of red PC+ABS and PMMA with different Clearweld concentrations.

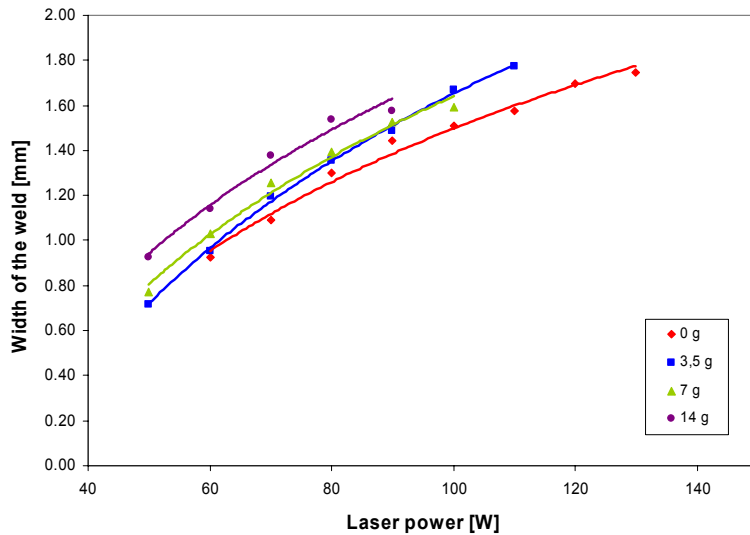


Figure 90. The effect of laser power to the width of the weld in quasi-simultaneous welding of red PC+ABS and PMMA with different Clearweld concentrations.

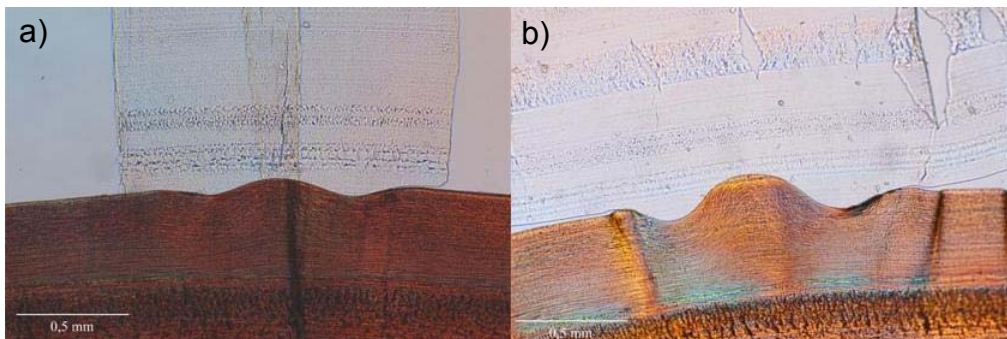


Figure 91. Cross section pictures of red PC+ABS (clearweld 0,0035 %) and PMMA, a) laser power was 80 W, tensile strength per length 31 N/mm and tensile strength 23 N/mm² b) laser power was 100 W, tensile strength per length 32 N/mm and tensile strength 19 N/mm².

White PC+ABS was blended with 0,003 % (3 g), 0,006 % (6 g) and 0,012 % (12 g) of Clearweld. White PC+ABS was not weldable without Clearweld additive because white pigment reflects almost all near infra red laser light. With all Clearweld concentrations weld was formed, but the best result was achieved with highest Clearweld concentration. Highest tensile strength per length (30 N/mm) and tensile strength (27 N/mm^2) was achieved with the highest Clearweld concentration (Figure 92). The Clearweld concentration affected also to the width of the weld (Figure 93), with higher Clearweld concentration the weld width was higher when the laser power used was same. Cross section pictures of the welds with Clearweld concentration of 0,006 % and 0,012 % can be seen in Figure 94.

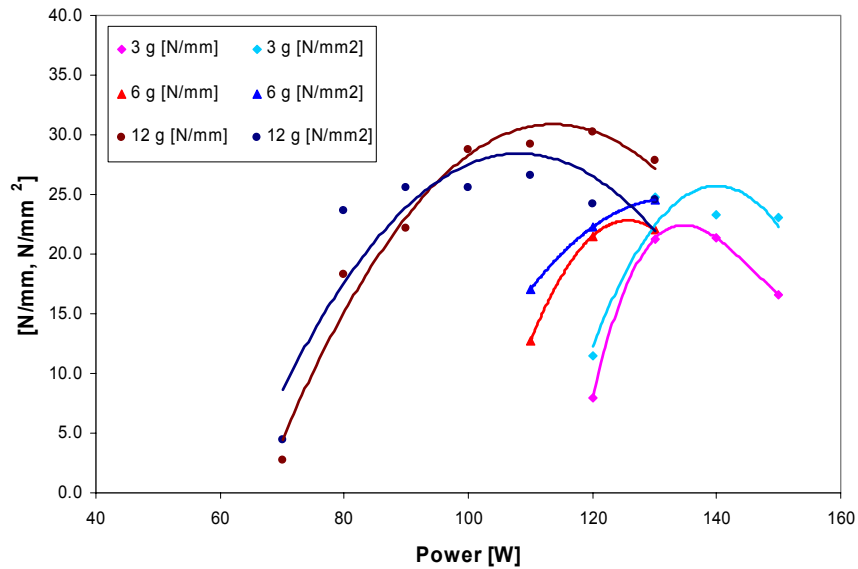


Figure 92. The effect of laser power to the weld strength per length and weld strength in quasi-simultaneous welding of white PC+ABS and PMMA with different Clearweld concentrations.

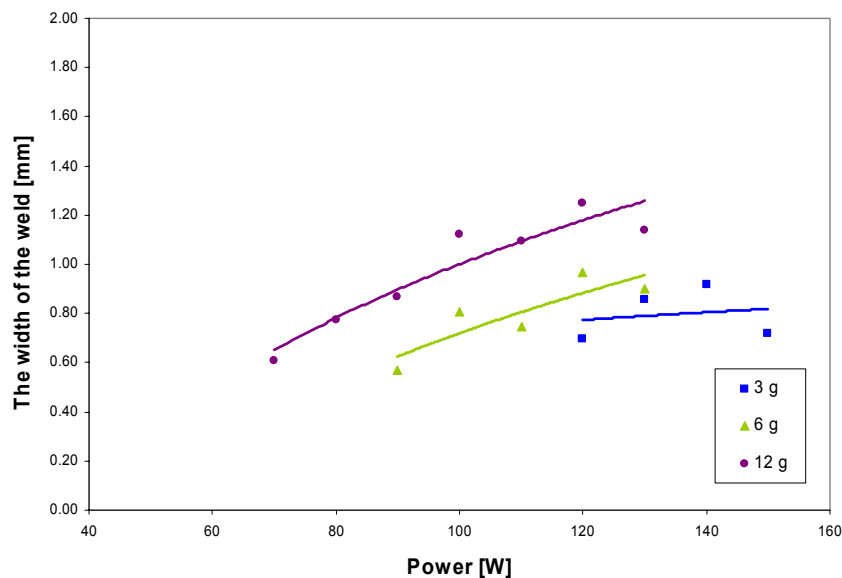


Figure 93. The effect of laser power to the width of the weld in quasi-simultaneous welding of white PC+ABS and PMMA with different Clearweld concentrations.

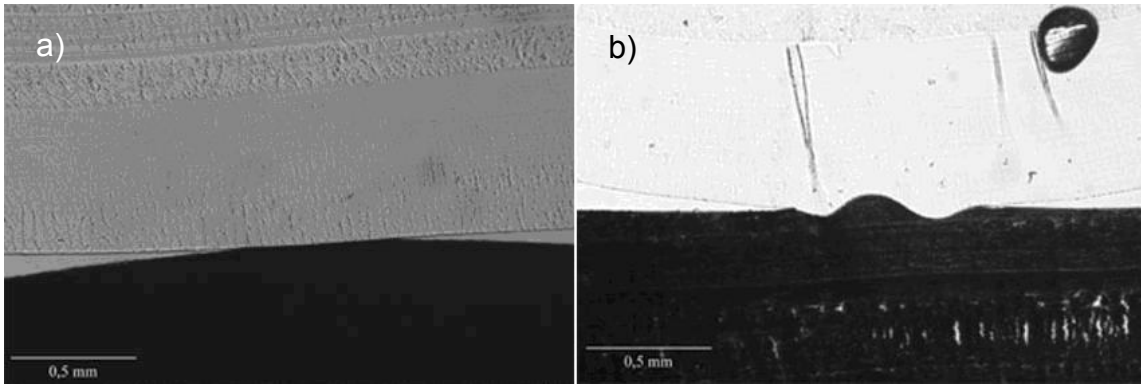


Figure 94. Cross section pictures of white PC+ABS and PMMA, a) Clearweld 0,006 %, laser power 130 W, tensile strength per length 22 N/mm and tensile strength 25 N/mm² b) Clearweld 0,012 %, laser power 110 W, tensile strength per length 29 N/mm and tensile strength 27 N/mm².

PMMA was blended with different concentration of Clearweld dye (0,0025 %, 0,005 % and 0,01 %). In the welding tests PMMA+Clearweld was used as absorbing material and natural PMMA was used as transmissive material. Welding tests were done with quasi-simultaneous welding, the number of scans used was 50 and the welding time was 2 m/s in all the tests. The quality of the weld was measured with tensile tests. Visual inspection of welds was also done. Cross section specimens can not be done because of the breakable nature of PMMA. The weld was acceptable with Clearweld concentration of 0,01 %, but with other two concentrations the forming of the weld was difficult. With the concentration of 0,005 % the tensile strength per length was 32 N/mm and with the concentration of 0,0025 % the tensile strength per length was only 4 N/mm. With highest concentration (0,01 %) the tensile strength per length of the weld was 40 N/mm. The irregular distribution of the Clearweld dye in the material can be seen as difference in the tensile strength per lengths of the weld (Figure 95).

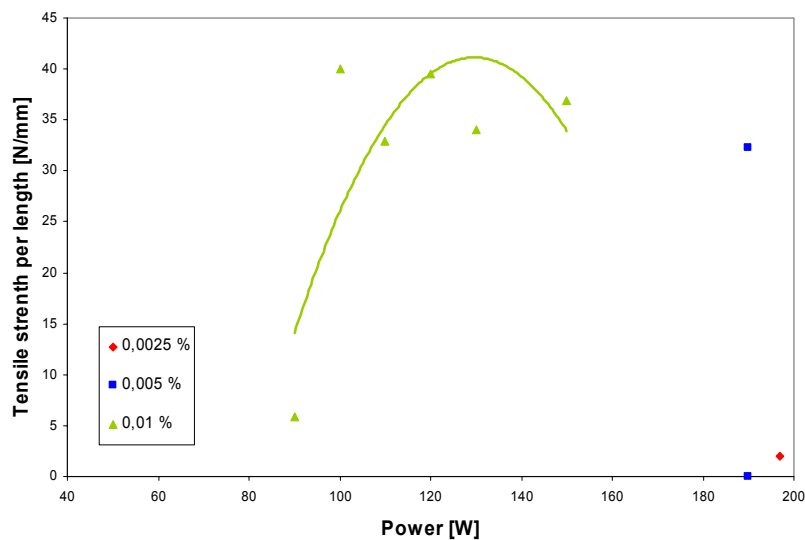


Figure 95. The effect of laser power to the weld strength per length in quasi-simultaneous welding of PMMA with different Clearweld concentrations.

4.4.2. Clearweld tests 2

PP, PC+ABS and PC materials blended with different concentrations of Clearweld dye were welded with contour and quasi-simultaneous welding techniques. The strength of the welds was compared with tensile tests. The welding tests for the materials blended with Clearweld LWA-267 was carried out with a fibre coupled diode laser (940 nm) and the welding tests for

the LWA-290 was carried out with a fibre laser (1090nm) and with Nd:YAG laser (1064 nm). The welding time was kept the same 1 s and the welding speed was adjusted according to the number of scans used.

First the PP material was tested with the diode laser. The absorbing plastic used was PP blended with LWA-267 dye and the top plastic used was natural PP. The effect of number of scans can be seen in Figure 96. In the case of PP the highest tensile strength per length was achieved with lowest number of scans. As we can see from Figure 97 - Figure 98 the weld is more symmetrical with higher number of scans and in the case of 1 scan at the highest tensile strength value the weld was destroyed badly. The effect of the LWA-267 concentration in PP can be seen in Figure 99. Highest tensile strength was achieved with the highest Clearweld concentration (0,1 w%).

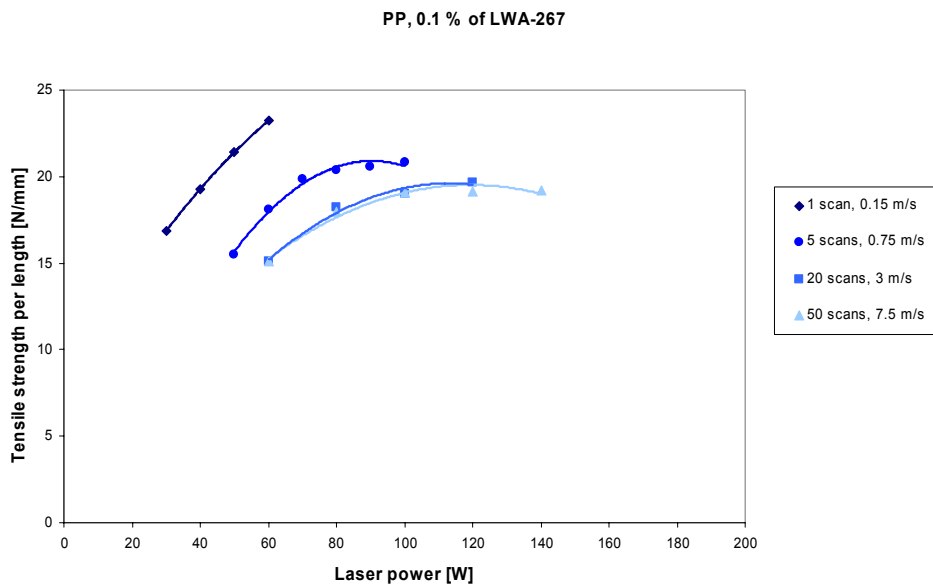


Figure 96. The effect of the number of scans to the weld strength per length for PP + 0,1 % of LWA-267 (diode laser).

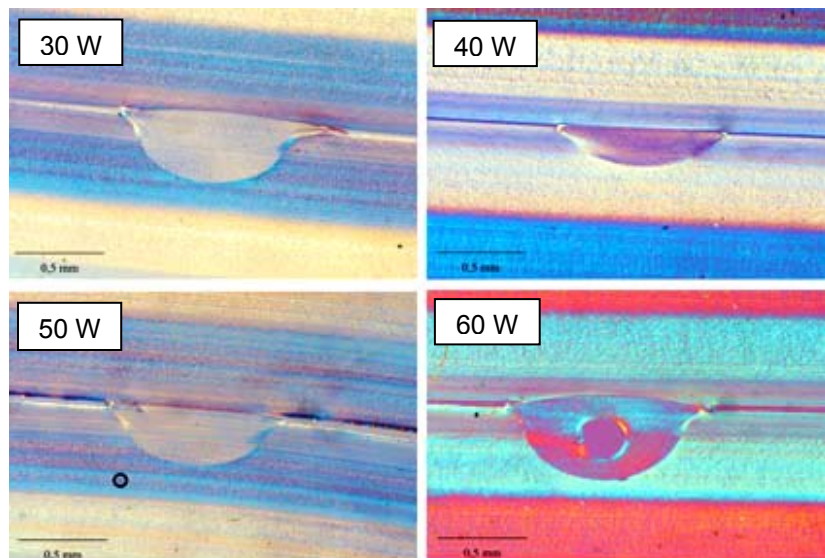


Figure 97. Cross section of PP + 0,1 % of LWA-267 welds, number of scans 1 and welding speed 0,15 m/s (diode laser).

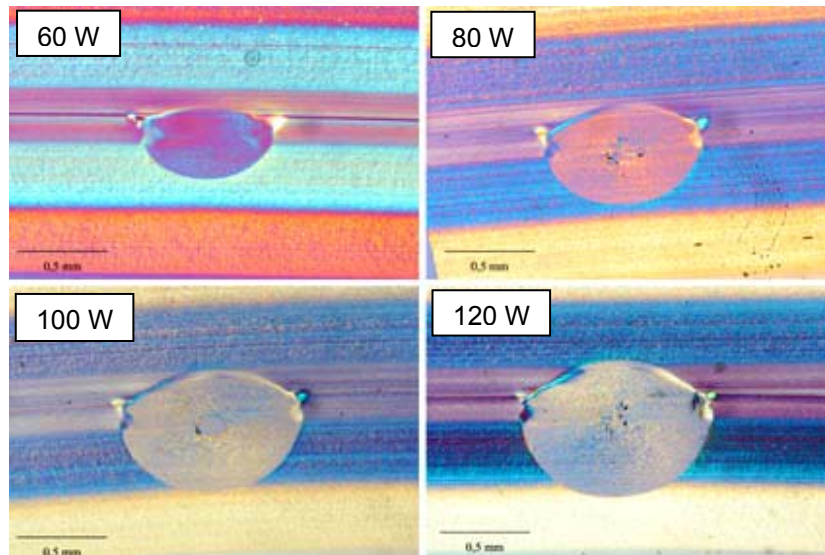


Figure 98. Cross section of PP + 0,1 % of LWA-267 welds, number of scans 50 and welding speed 7,5 m/s (diode laser).

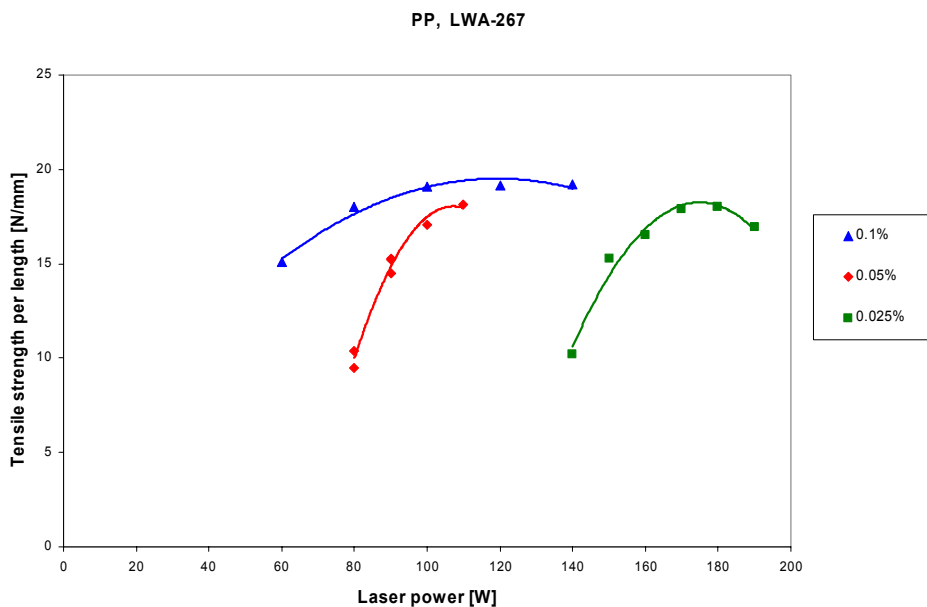


Figure 99. The effect of the Clearweld concentration the weld strength per length for PP + LWA-267. Welding speed was 7,5 m/s and the number of scans was 50 (diode laser).

Second material tested with diode laser was PC. Clearweld dye in the bottom PC plastic was LWA-267 and top plastic used was natural PC. The effect of number of scans can be seen in Figure 100. In the case of PC highest tensile strength per length was achieved with number of scans 20 and 50. Tensile strength is near the same with 20 and 50 scans and bubbles started to form at same laser power in both used number of scans values. The effect of the LWA-267 concentration in PC can be seen in Figure 101. Highest tensile strength was achieved with the highest Clearweld concentration (0,1 w%). PC with 0,025 % of LWA-267 was not weldable with 1 scan. Weld was achieved with 20 and 50 scans but it was not visually acceptable because there were some bubbles in the welds with all used laser powers.

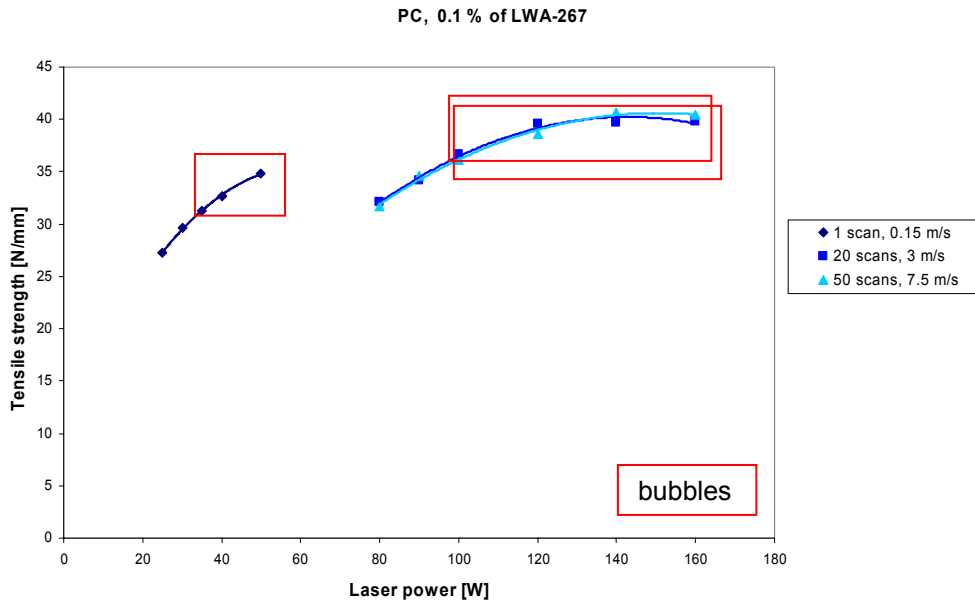


Figure 100. The effect of the number of scans to the weld strength per length for PC + 0,1 % of LWA-267 (diode laser).

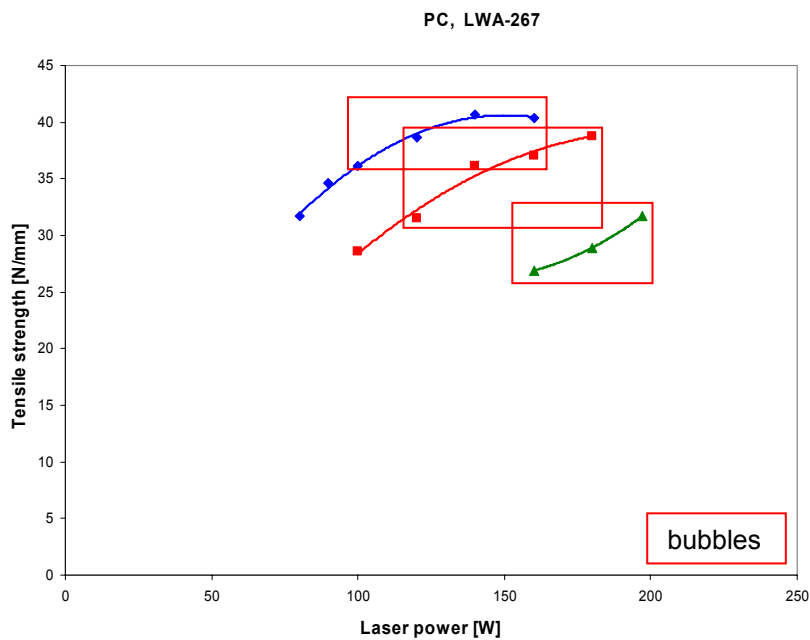


Figure 101. The effect of the Clearweld concentration to the weld strength per length for PC + 0,1 % of LWA-267. Welding speed was 7,5 m/s and the number of scans was 50 (diode laser).

Some tests were done also with fiber laser and with Nd:YAG laser. The PP material was tested with both lasers and the dye in resin in these tests was LWA-290. During the Nd:YAG tests the laser was misaligned, which was found out after the tests. That can have effect to the results. The effect of number of scans and the effect of the Clearweld concentration in the Nd:YAG tests can be seen in Figure 102. The misalignment of the laser can be seen in the results ca. 10...30 % lower weld strengths. Like in the diode laser tests the highest weld strengths was achieved with one scan. When we compare the results to the black+natural joint of PP welded with Nd:YAG laser (Figure 103) we can see that achieved weld strengths with Clearweld were a little bit higher with one scan and a little bit lower with 20 scans.

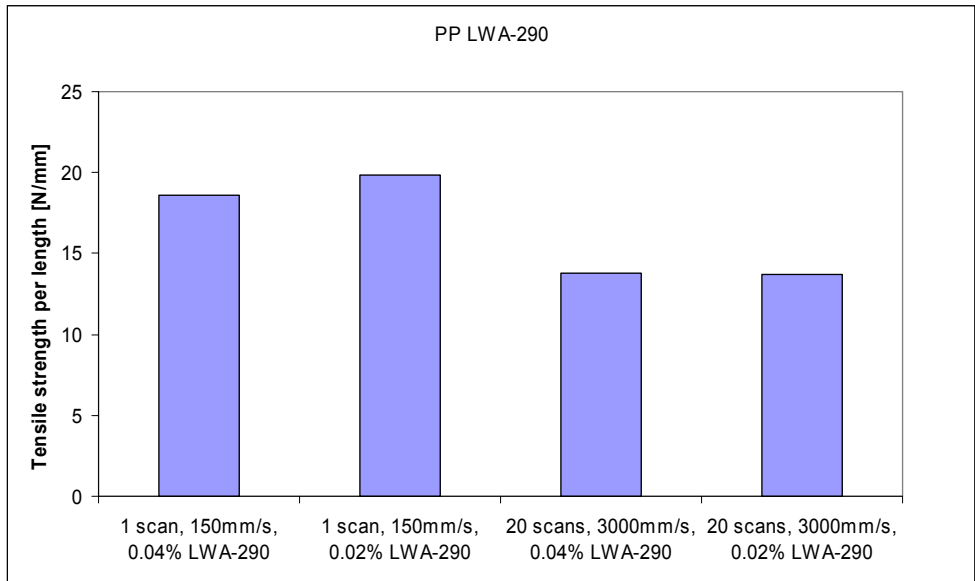


Figure 102. The effect of the number of scans and the effect of the Clearweld concentration to the weld strength per length for PP + LWA-290 in the Nd:YAG laser welding.

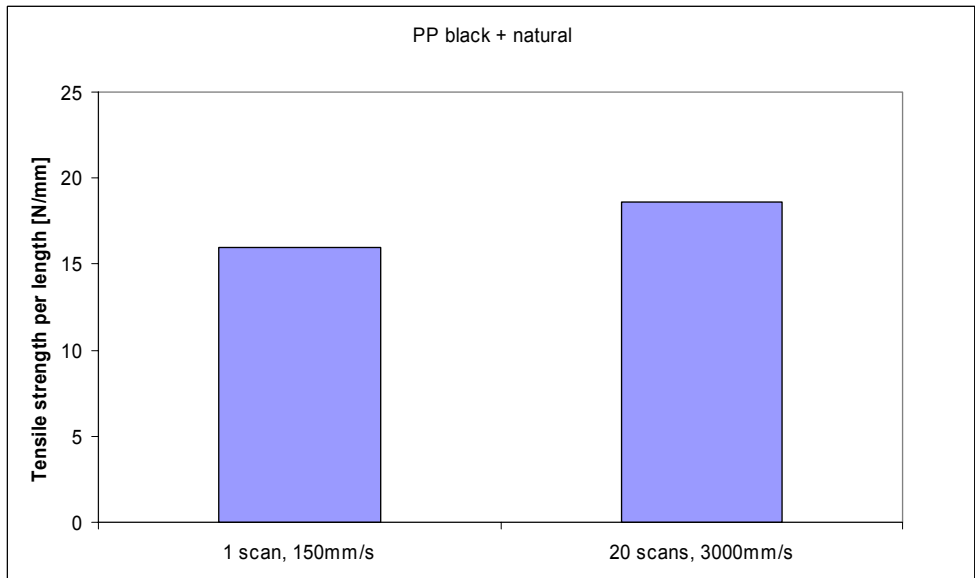


Figure 103. The effect of the number of scans to the weld strength per length for PP black + natural welds in the Nd:YAG laser welding.

PP + LWA-290 was tested also with a fiber laser. The effect of number of scans can be seen in Figure 104. Unlike in diode laser and Nd:YAG laser tests the highest tensile strength per length was achieved with the highest number of scans. The effect of the LWA-290 concentration to the weld strength can be seen in Figure 104. With the 0,02 % concentration the weld was not formed with the number of scans 50 and with the 0,01 % concentration the weld wasn't form at any used parameters.

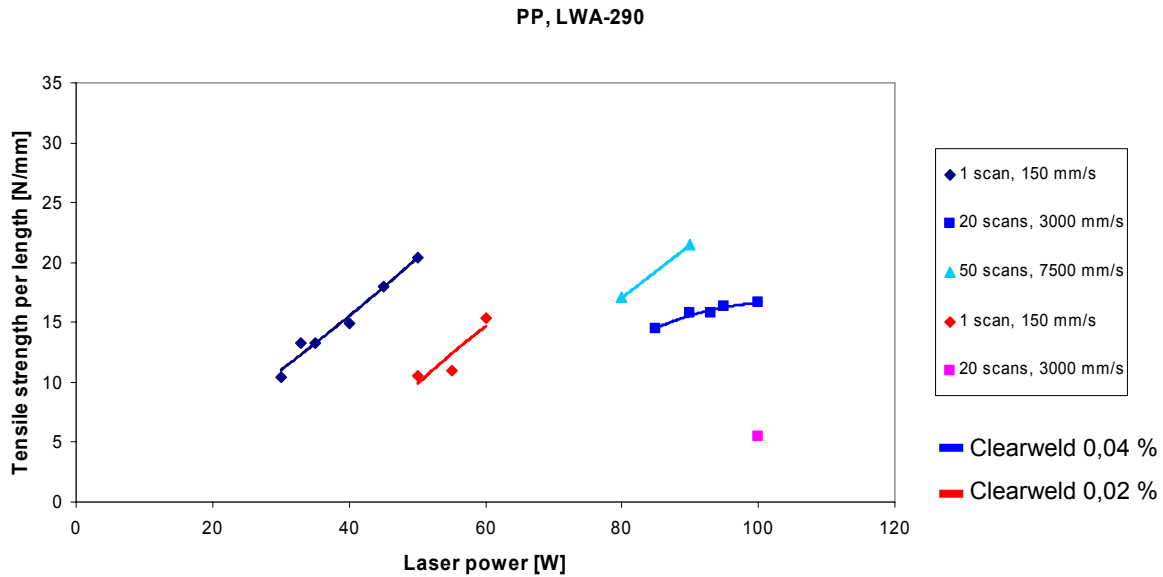


Figure 104. The effect of the Clearweld concentration and the effect of the number of scans to the weld strength per length for PP + LWA-290 (fiber laser).

Nd:YAG laser tests were done also to PC and the dye used in the tests was LWA-290. In these tests also the Nd:YAG laser was misaligned so that could effect to the results. In the Nd:YAG tests the Clearweld concentration was 0,04 %. The effect of number of scans can be seen in Figure 105. Number of scans 50 needs more laser power than the used 100 W. That's why the maximum weld strength with 50 scans can not be specified.

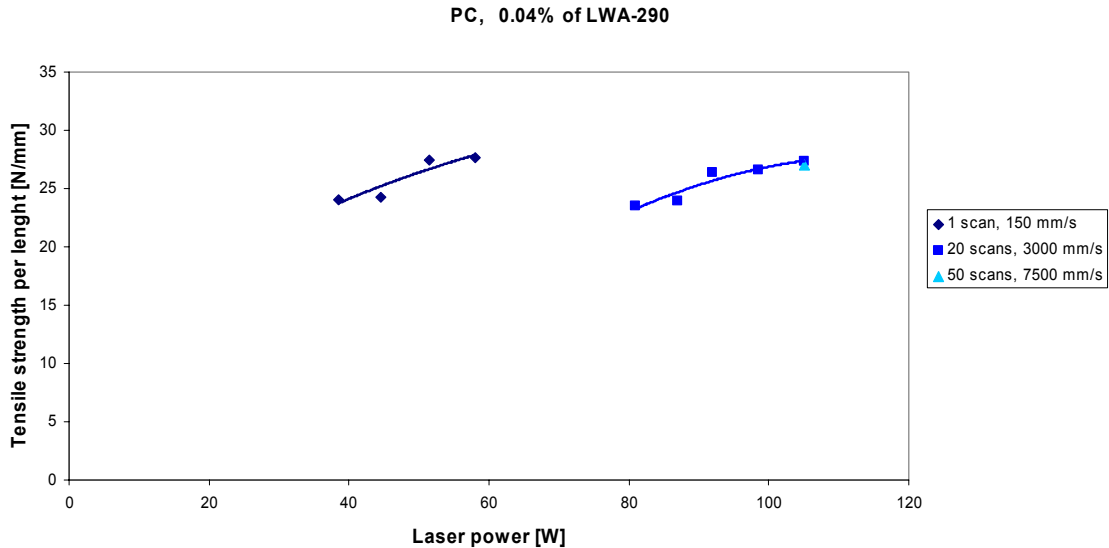


Figure 105. The effect of the number of scans to the weld strength per length for PC + 0,04 % of LWA-290 (Nd:YAG laser).

PP + 30 % GF and PC+ABS materials were tested with fiber laser. With PP + GF tests three different Clearweld concentrations were used, 0,01 %, 0,02 % and 0,04 %. When top plastic was fiber glass blended the welding was possible only with highest Clearweld concentration and contour welding technique. Low transmission of top plastic needs more laser power (than 100 W) to form a weld. Natural PP was used as the top plastics in the tests. Concentration of 0,01 % was not weldable with any of used parameters. Concentration of 0,02 % was weldable only with one scan. The tensile strength results from these tests are in

Figure 106. Used maximum laser power (100 W) was not high enough to weld these materials with higher number of scans and lower Clearweld concentrations.

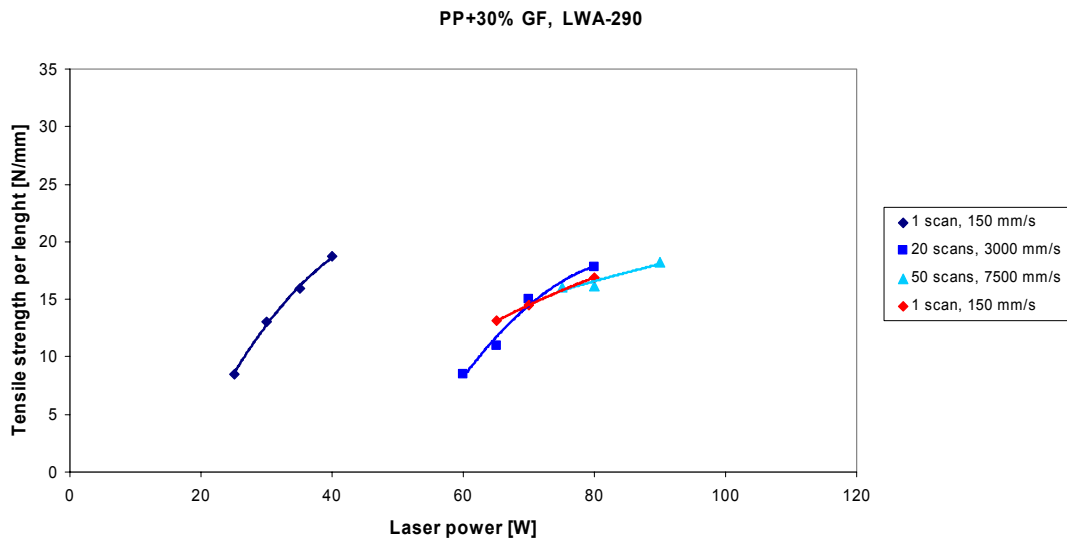


Figure 106. The effect of the number of scans and the effect of Clearweld concentration to the weld strength per length for PC + 30% GF and LWA-290 (fiber laser).

In PC+ABS tests with fiber laser the absorbing material used was PC+ABS blended with Clearweld LWA-290 dye, transmissive plastic used was PMMA. In these tests three different Clearweld concentrations were used, 0,01 %, 0,02 % and 0,04 %. The effect of number of scans can be seen in Figure 107. In these tests highest tensile strength per length was achieved with number of scans 20 and 50. Tensile strengths are near the same with 20 and 50 scans. The effect of the LWA-290 concentration can be seen in Figure 108. Highest tensile strength was achieved with the highest Clearweld concentration (0,04 w%).

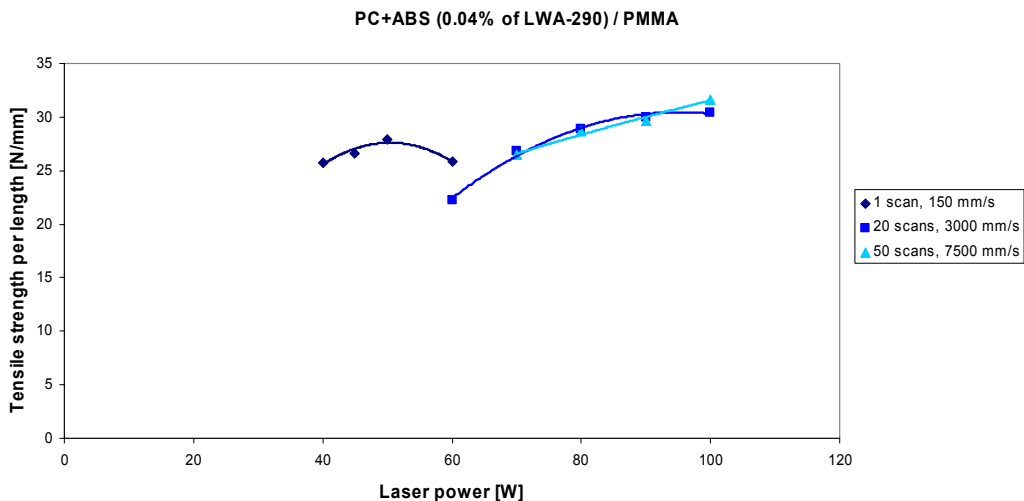


Figure 107. The effect of the number of scans to the weld strength per length for PC + ABS and LWA-290 (fiber laser).

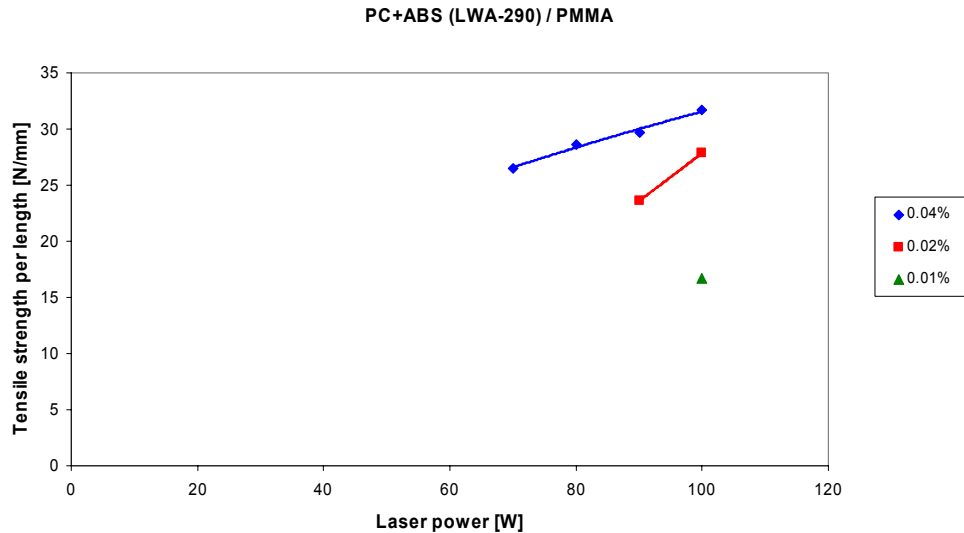


Figure 108. The effect of the Clearweld concentration to the weld strength per length for PC + ABS and LWA-290. Number of scans was 50 and the welding speed was 7,5 m/s (fiber laser).

4.5. T-joint welding tests

Two kinds of t-joint welding test were done. In the first tests flat surfaces were welded and in the second tests groove were machined in to the flange. Welding time was kept constant 1 s and the number of scans used was 5, 10, 15, 20, 30 and 50 scans. Welding speed was adjusted according to the number of scans so that the welding time was 1 s.

In the first test it was found out that the positioning of the laser beam was difficult because the web wasn't even (Figure 109). The problem of positioning can be seen in the welding results (Figure 110). In these tests the weld flash was formed. Used pressure was 1 bar.

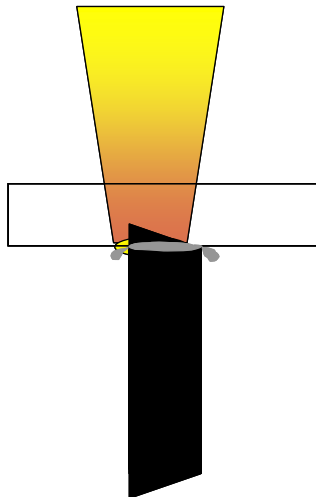


Figure 109. Problems in the first t-joint welding tests.

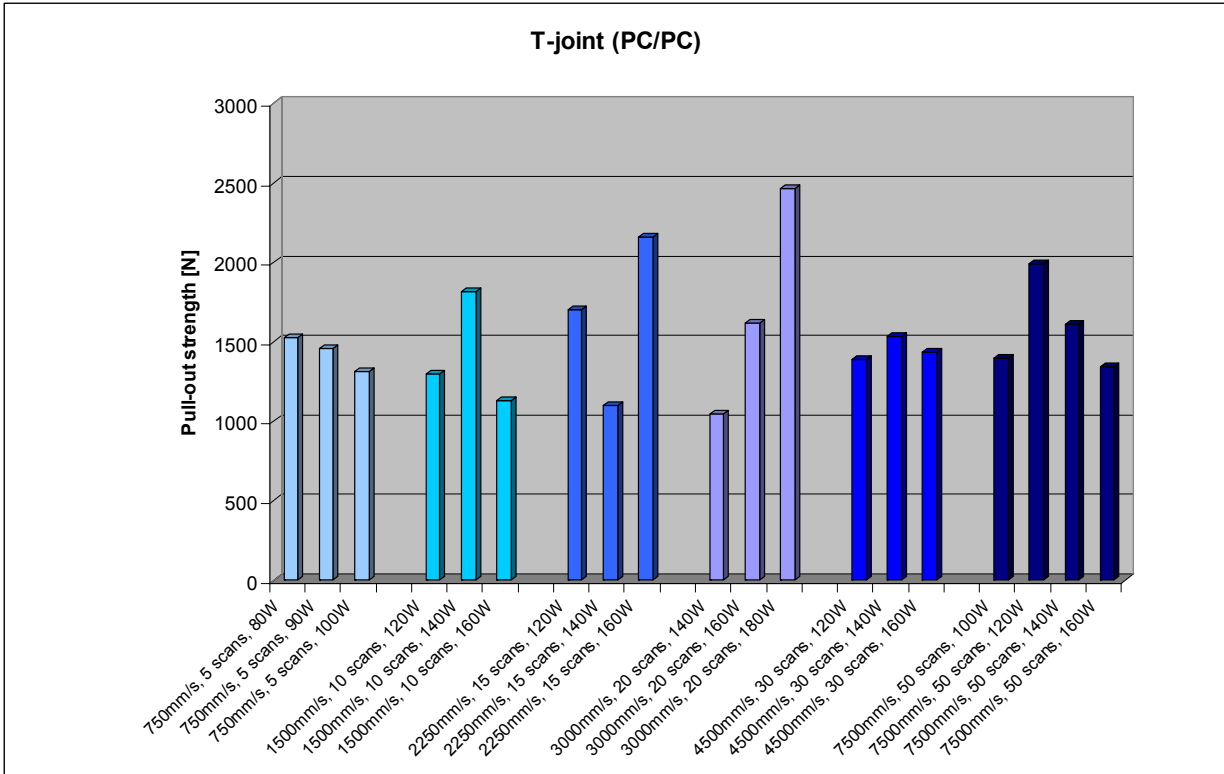


Figure 110. Pull-out strength of the t-joint welds. Welded with different welding speeds and number of scans (welding time 1 s).

In the second tests groove was machined in to the flange to prevent problems appeared in the first tests. Also in these tests welding time was kept constant 1 s and the number of scans used was 5, 10, 15, 20, 30 and 50 scans. Welding speed was adjusted according to the number of scans so that the welding time was 1 s. Used pressures were 4 bar and 5 bar to found out the effect of the welding pressure. Some samples were welded also with no groove in the flange to found out the effect of the machined groove.

It was found out that too much a power cause a weak weld if there was no groove in the flange (Figure 111). With higher pressure and groove the achieved weld strengths were same as the strength of the base material. An extra pressure may probably cause an enhanced diffusion phenomenon and a larger weld, because the weld flash can't get out of the weld. Number of scans effected also to the strength of the weld. With higher number of scans the pull-out strength of the weld was higher (Figure 112 and Figure 113).

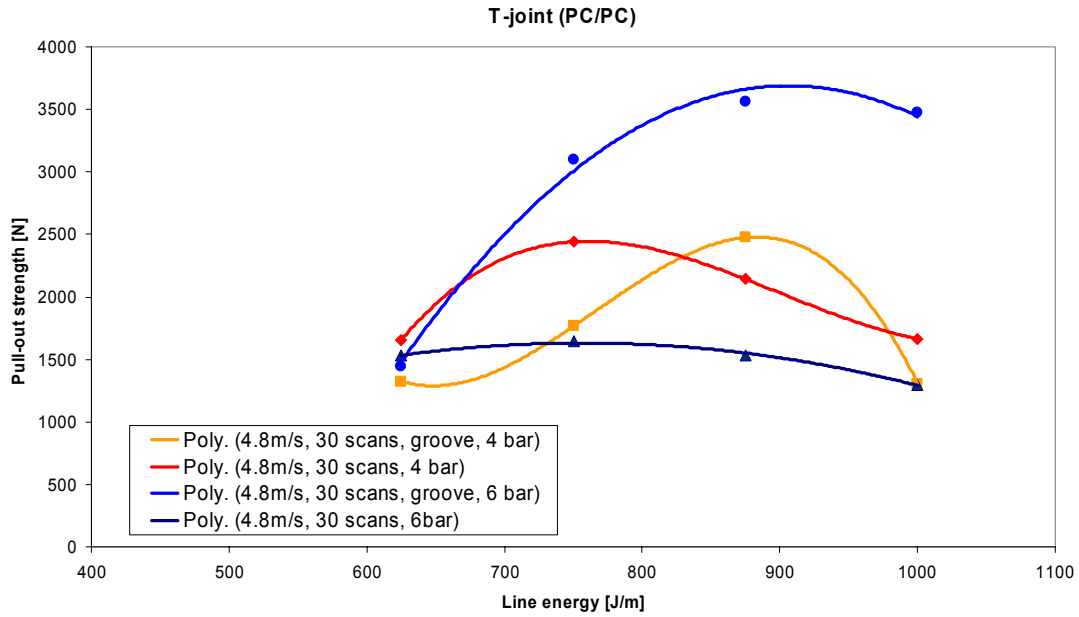


Figure 111. The effect of the line energy to the pull-out strength of the t-joint welds with different pressures, welding speeds and number of scans (welding time 1 s).

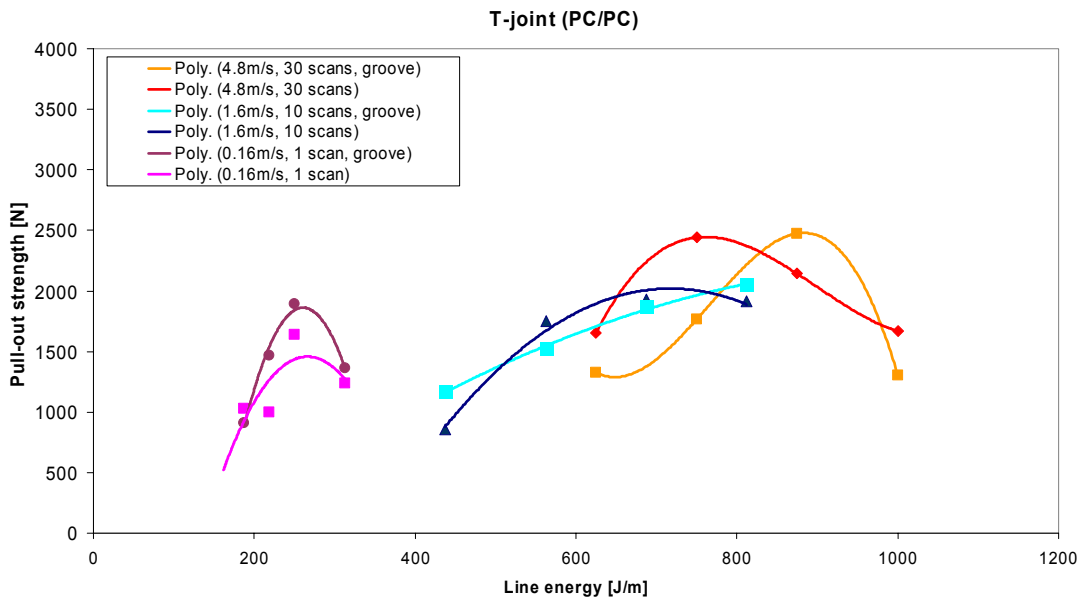


Figure 112. The effect of the number of scans to the pull-out strength of the t-joint welds with different welding speeds and number of scans (welding time 1 s). Pressure used was 4 bar.

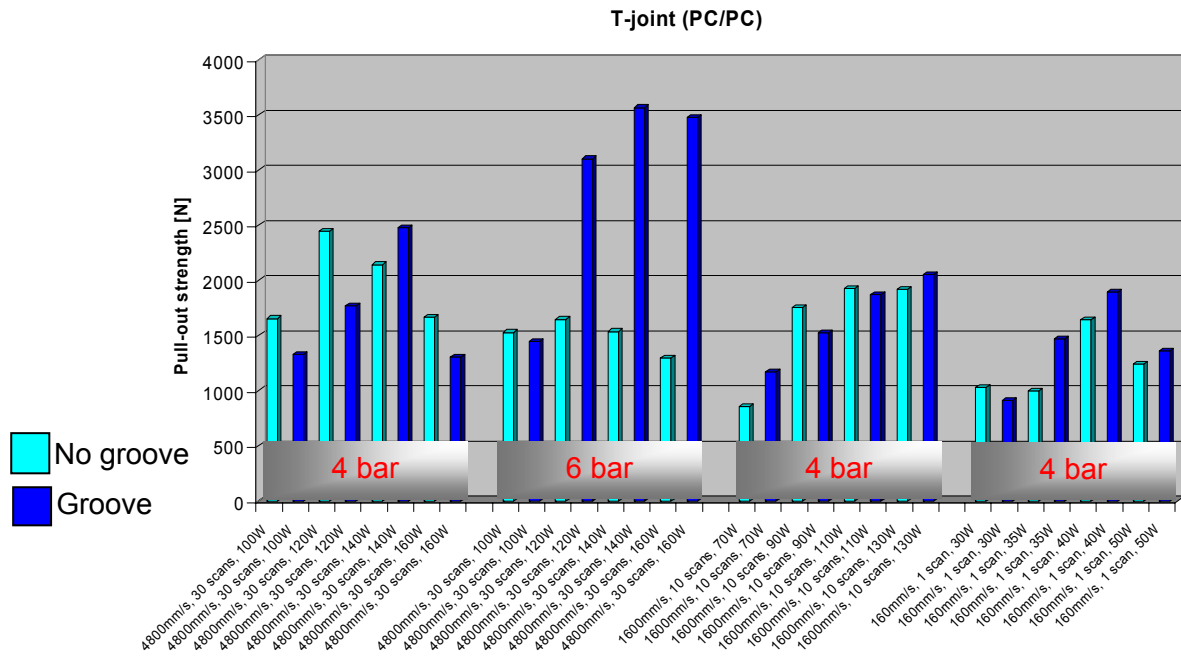


Figure 113. The effect of the different welding parameters to the pull-out strength of the t-joint welds.

4.6. 3D-welding tests

In the project two different types of 3D quasi-simultaneous welding techniques have tested and developed, multiple scanners and scanners + mirrors techniques (Figure 114). Material of tested sample box (Figure 115) was polypropylene and polycarbonate. Tensile tests weren't done for the sample box only the visual inspection for the weld was done. In the tests was noted that quasi-simultaneous welding of 3D sample box was possible with both used techniques.

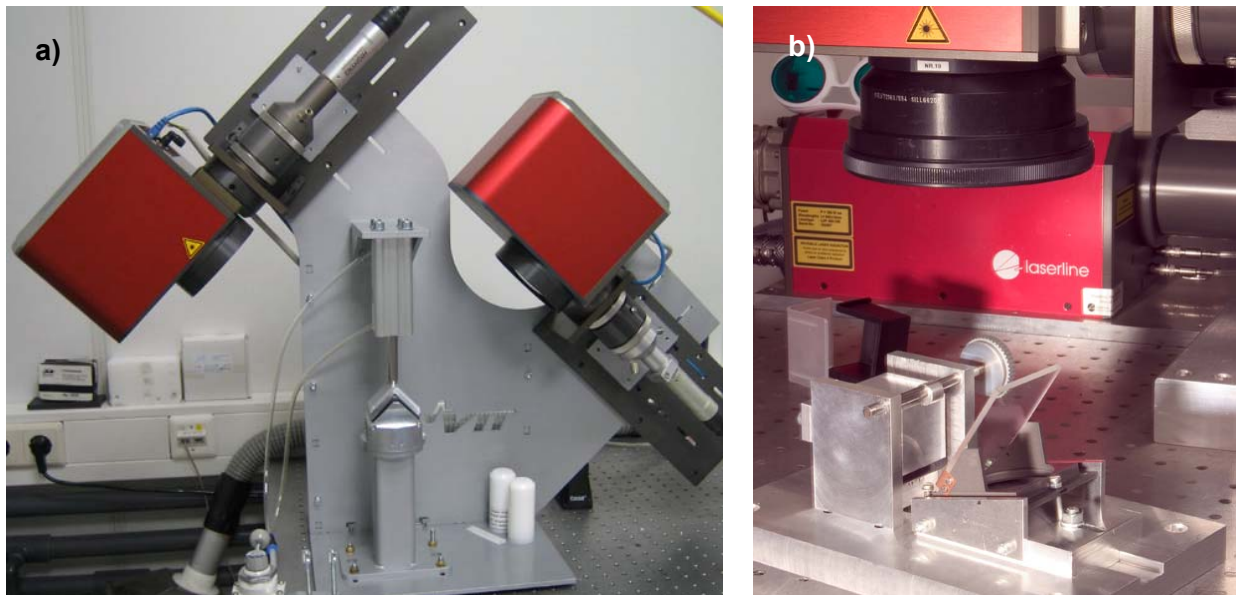


Figure 114. The setup of quasi-simultaneous 3D welding with a) two scanner system and b) mirror + scanner system.

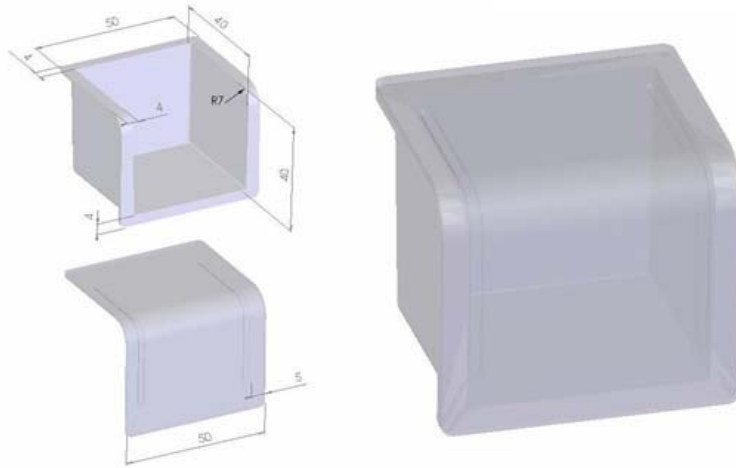


Figure 115. Sample box used in the 3D welding tests.

4.7. Thermodynamic modelling

In all simulations the total welding time was set to one second and the laser power was selected so that to total applied energy was about the same in all cases. The main idea was to compare how the number of scans effects to the melt area size and its distribution. The distribution of the melted area between the welded plates is important, because the melted volume must be large enough in both plates for a good weld.

The calculated cases and corresponding input parameters are shown in Table 18. The first column gives the nominal laser power for each case. Because of the internal losses in the laser, the effective laser power (the beam power at the upper surface of the upper plate) is less than the nominal power. Some measurements were done to get this figure for different level of the nominal power, but these results were not very consistent. The finally applied efficiency is thus only partly based on measurements and partly on good guesses as can be seen from fourth and fifth columns in the table.

Table 18. Calculated cases.

Power (W)	Speed (m/s)	Scans	Measured efficiency (%)	Applied efficiency (%)	Optical path length (μm)
16	0.15	1	66.8	80	25
27	0.45	3		83	25
42	3.00	20		85	25
45	7.50	50	84.7	85	25

Modelled temperatures were also compared to measured temperatures. Calculated and measured temperature curves for 3, 20 and 50 scans are shown in Figure 116 and Figure 117.

The general impression is that the calculated values match reasonably well with the measured values, but the model seems to give far larger temperature variations. The average calculated values seem also to be too high for 3 scans and too low for 20 scans and especially for 50 scans.

These differences can be partly related to the measurement method. Temperatures were measured with an IR-camera above the plates and through the upper plate. It is possible that the camera could not detect fast local temperature changes, but tended to average the temperature values spatially and in time. However, this cannot explain why the measured temperatures were lower for the 3-scan case.

It should be noted that calculated curves are not actually as unsmooth as they appear to be in Figure 116 and Figure 117. The visible effect is due to sparse time sampling for the drawn values.

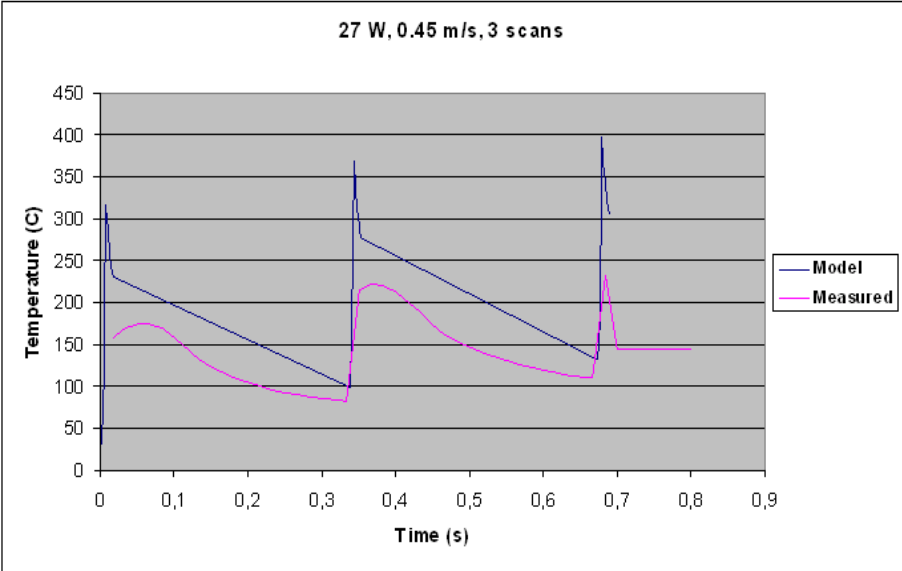


Figure 116. Modelled and measured temperature curve, 3 scans.

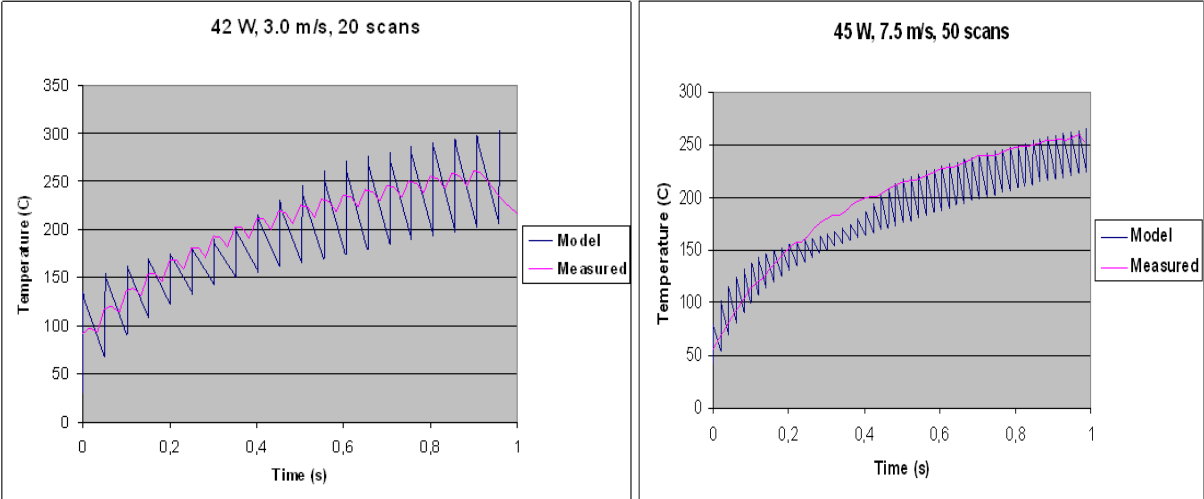


Figure 117. Modelled and measured temperature curve, 20 and 50 scans.

The temperature field near the end of the welding time at the middle cross section of the modelled weld path is shown in Figure 118. The vertical line is drawn between the plates and the vertical lines are at the middle and at the edges of the laser beam. The point of view is along the weld path and the laser beam is coming from above. The grey area is the melted area, i.e. the area where temperature is above 160 °C.

The picture shows clearly how the melt area is thickest at the middle of the laser beam, where the material is covered by the beam for the longest period (ref. Figure 35). This effect becomes more pronounced when the number of scans is increased, because the beam centre region gets relatively larger and larger share of the total energy. The averaging effect of heat

conduction becomes visible only at some distance from the melt when temperature curves become more spherical.

Both plates are melted and the width of the melted area is nearly the same as the width of the laser beam. However, most of the melted volume is in the lower plate, but the melted volume in the upper plate still seems to be large enough for a good weld.

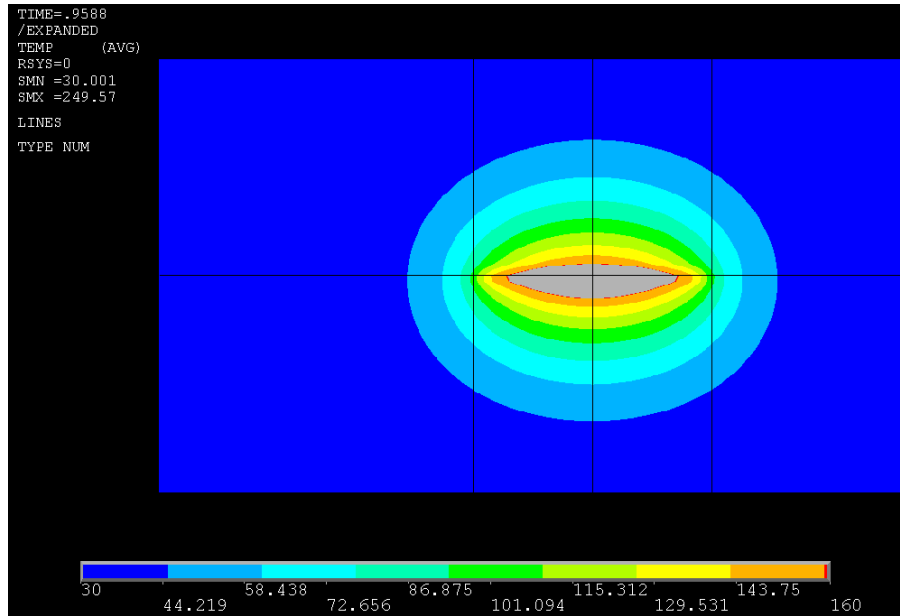


Figure 118. Temperature field at the cross section along the weld direction, 20 scans.

The calculated and measured melt area sizes are shown in Table 19. The relative value of the calculated value compared to the measured value is also given. It is evident that the width of the weld is modelled quite well, but the calculated depth values differ quite much from the measured values. The melt depth is overestimated for smaller number of scans and underestimated for larger number of scans. This is consistent with the temperature curves in Figure 116 and Figure 117 where the calculated values were too high for low number of scans and too low for larger number of scans.

It is possible that the laser efficiency value used in the modelling for low nominal laser power values was too high (ref. Table 18). At least this could explain the too high modelled temperatures and too large weld depth values for low number of scans.

Table 19. Measured and calculated melt area width and depth.

Power (W)	Scans	Measured width (mm)	Modelled width (mm)	Measured depth (mm)	Modelled depth (mm)
16	1	0.97	1.00 (103%)	0.11	0.14 (127%)
27	3	0.97	1.00 (103%)	0.12	0.14 (117%)
42	20	0.87	0.91 (105%)	0.25	0.21 (84%)
45	50	0.81	0.83 (102%)	0.28	0.26 (93%)

5. Conclusions

Quasi-simultaneous laser welding of plastics is a fast and flexible welding method to join plastics. It can be also used in mass-production applications where short welding times around 1 second are required. Parameters used (welding speed, number of scans, laser power) effects to the quality of the weld and to the welding time. Material properties effect also to the quality of the weld.

The strength of the weld and the size of the weld (width and height) decreases when the welding speed increases with polypropylene and polycarbonate. Increasing of the number of scans increases the strength and the size of the weld when the polypropylene and polycarbonate is used.

Material properties like pigment concentration and fiber glass concentration effects to the quality of the weld. Higher weld strengths can be achieved with higher carbon black concentration. And with lower carbon black concentration the laser power needed is higher. When the carbon black content is higher laser beam is absorbed near to the surface of the plastic and the weld is more symmetrical. When the fiber glass content is increased the strength of the weld is increased. Tested 30 % of fiber glass in transparent and in absorber polypropylene was weldable. Higher laser power is needed when the fiber glass content is increased.

Quasi-simultaneous welding technique showed great potential in bridging air gaps. Larger air gaps could be bridged with the quasi-simultaneous technique compared to the contour welding (PP and PC). With quasi-simultaneous welding air gaps 0,30 mm (PP) and 0,18 mm (PC) and with contour welding 0,06 mm (PP+PC) could be bridged without any critical decrease in the weld strengths.

Nearly the same strengths and sizes of the weld can be achieved with different parameter combinations used if the welding time is same. Very slight increase was found when the number of scans increased (time 1 sec.) with PP and PC.

With Clearweld materials the strength and the width of the weld is increased when the Clearweld concentration is increased. Higher laser power is needed when the Clearweld concentration is lower. With Clearweld additives the welding of white PC+ABS to PMMA and natural materials like PMMA, PC, PP, PP+30% FG, PC+ABS is possible. Welding is possible with diode laser, Nd:YAG laser and fiber laser, although different Clearweld dyes has to be used.

With T-joint too much laser power causes weak weld if there is no groove in the flange. Welds where is the groove in the flange same weld strengths as the base material (polycarbonate) has could be achieved. With higher number of scans (same welding time 1 sec.) the pull-out strength of the weld is higher.

3D welding of mass-produced components is possible with different welding techniques. With tested quasi-simultaneous 3D welding techniques two scanner system and mirror with scanner system the welding of sample box was possible.

By using thermodynamic modelling it is possible to estimate weld area size and its distribution between the welded plates reasonably well. In the modelling the effect of increasing the number of scans is consistent with the test results and shows that this tends to increase only the depth of the weld. This is explained by the fact that a relatively larger share of the total energy is accumulated at the centre of the weld and the thermal gradients in the material tend to direct the heat flow to increase the weld's depth more than its width.

6. References

- [1] Silvers, H. Jr., Wachtell, S. Perforating, welding and cutting plastic films with a continuous CO₂ laser, PA State University, Eng. Proc, pp. 88-97, August 1970.
- [2] Toyota Jidosha KK. Laser beam welding of plastic plates. Patent application JP85213304, 26 September 1985.
- [3] New Advances in Polymer Laser Welding, 2001, Brochure of the BriteEuram project – Polyweld. 22 pp.
- [4] Abed, S. et al. Diode Laser Welding of Polymers: Microstructures of the Welded Zones for Polypropylene. In: 20th International Congress on Applications of Lasers & Electro-optics: Proceeding of the Conference ICALEO 2001, Jacksonville, USA 15-18 October, 2001. Orlando, USA: Laser Institute of America, 2001. 9 pp.
- [5] Bachmann, F.G., Russek, U.A. Laser Welding of Polymers Using High Power Diode Lasers. Photonics West 2002 Conference, San Jose, USA 21-25 Jan, 2002. Proc. SPIE Vol. 4637B.
- [6] Kouvo, S., Jansson, A., Salminen, A. Laser Welding of Polymers – New Innovations for Joining 3D geometries. In: 24th International Congress on Applications of Lasers & Electro-optics: Proceeding of the Conference ICALEO 2005, Miami USA, 31 October - 3 November. Vol. 98. ISBN 0-912035-82-X.
- [7] Jones, I.A. Laser welding for plastic components. Assembly Automation, 2002. Vol. 22: 2. 7 pp.
- [8] Rofin-Sinar (2002) The Polymer-Connection, Product news, Press Release Euromold, December 2002.
- [9] Kouvo, S., Jansson, A., Kujanpää, V. Laser Welding of Plastics in Mass Production. Proceedings of The 10th Nordic Laser Materials Processing Conference, NOLAMP 2005, Luleå Sweden, 17-19 August 2005, s. 139-149, ISBN 91-631-7228-3.
- [10] Laserline (2002). Laserline brochure
- [11] Kagan, V.A., Bray, R. Chambers, A. Forward to Better Understanding of Optical Characterization and Development of Colored Polyamides for the Infra-Red/Laser Welding. PartI/II. ANTEC 2001, Annual Technical Conference: Conference
- [12] Kagan, VA., Bray, RG., Kuhn, WP. Laser Transmission Welding of Semi-Crystalline Thermoplastics-Part I: Optical Characterization on Nylon Based Plastics. Journal of Reinforced Plastics and Composites. 2002, vol. 21: 12. S. 1101-1122.
- [13] Hänsch, D., Haaf, D., Pütz, H. Treusch, H.G. Gillner, A., Poprawe, R. Welding of Plastics with Diode Lasers. Proceedings of the 17th International Congress on Applications of Laser & Electro Optics, ICALEO 1998, Orlando, USA 16-19 November, 1998. Vol. 85. pp G131-140.
- [14] Püts, H., Hänsch, D., Treusch, H. Verbindung mit Zukunft. Plasverarbeiter, vol 48, no 5. May 1997, pp. 28-30.
- [15] Haberstroh, E., Lutzeler, R. Influence of Carbon Black Pigmentation of the Laser Beam Welding of Plastics Micro Parts. Journal of Polymer Engineering, 2001, vol. 21: 2-3. S. 119-130.
- [16] Pashby, I.R., Bryden, B., Barnes, S. The Influence of Glass Reinforcement on the Diode Laser Transmission Welding of Nylon. Laser Materials Processing Conference: Proceeding of the Conference ICALEO 2000, Dearborn, USA. S. A 34-39.
- [17] Kagan, V., Bray, R.G. Advantages and Limitations of Laser Welding Technology for Semi-Crystalline Reinforced Plastics. 20th International Congress on Applications of

Lasers & Electro-optics: Proceeding of the Conference ICALEO 2001, Jacksonville, USA 15-18 October.

- [18] Haferkamp, H., Von Busse, A., Barcikowski, S., Bunte, J. Welding of Polymer and Wood Composites Using Laser Radiation. 22nd International Congress on Applications of Lasers & Electro-optics: Proceeding of the Conference ICALEO 2003, Jacksonville, USA 13-16 October. pp A 108-117.
- [19] Klein, R. Bearbeitung von Polymerwerkstoffen mit Infraroter Laserstrahlung. Technischen Hochschule Aachen. 1990. 161 s.
- [20] Kagan, VA. Forward to Better Understanding of Optimized Performance of Welded Joints: Local Reinforcement and Memory Effects for Polyamides. Society of Automotive Engineers, SAE Transactions: Journal of Materials & Manufacturing, 2001. Vol. 110. S. 514-530.
- [21] Russek, U.-A., Staub, H., Palmén, A., Kind, H. Simultaneous Laser Beam Welding of Thermoplastics – Innovations and Challenges. Proceedings of the 22nd International Congress on Applications of Lasers & Electro-Optics 2003.
- [22] Russek, U.-A., Aden, M., Poehler, J., Palmén, A., Staub, H. Laser Beam Welding Of Thermoplastics Parameter Influence on Weld Seam Quality - Experiments and Modeling. Proceedings of the 23rd International Congress on Applications of Lasers & Electro-Optics 2004.